ANALYSIS   OF   FUNICULAR

SUSPENSION   SYSTEMS

Thesis presented for the degree of Ph.D. (Engineering)

in the University of London

by

Prem Krishna, M.E.

Department of Civil Engineering

Imperial College of Science and Technology

London

November, 1964.

ABSTRACT

A study on a single cable, and on plane and three-dimensional prestressed funicular suspension systems, is described in this thesis.

The problem of a single cable with a uniformly distributed dead weight and an applied point load has been studied and good agreement is obtained between theoretical and experimental values.

The problem of interaction of two cables in a plane system has been studied by using two theoretical methods:

(i) The influence coefficient method,   and

(ii) A more general method.

Generalised computer programmes were written for both the methods of solution to solve problems on the plane system (symmetrical about the Y-axis) under any kind of loading. The values obtained by using the influence coefficient method showed reasonable agreement in smaller ranges of applied load. The agreement shown by the more general method was good for all ranges of loading tried.

The applicability of the general method to determine the initial geometry of three-dimensional systems and solving them under applied loading, has been illustrated by applying it to a three-cable structure. A generalised computer programme has also been written for the solution of the three-cable system.

CONTENTS

INTRODUCTION

GENERAL

A single cable is one of the most efficient tension-carrying structures, and is one, which is free of bending and buckling stresses. This capacity of the single cable has been utilised for hundreds of years in the form of both unstiffened and stiffened suspension bridges. In the very early days natural cables were used until cables made out of steel were used in a suspension bridge in Tibet in about 1630. Recently suspension bridges of spans up to 4200 feet have been constructed.

The idea of using cables as elements in a roofing system (perhaps first inspired by the suspension bridge), however, is comparatively very recent. Roof systems consisting partly or fully of cables as the supporting structure can be termed as "Suspension Roof Systems". This thesis concerns itself mainly with the study of these systems.

CHARACTERISTICS AND ADVANTAGES

All suspension systems use a single cable as their basic element and so the properties of a single cable under load are essentially applicable to suspension systems.

(1) In a cable the whole section is uniformly stressed, besides, in cables of small dip to span ratio tension is almost constant throughout the span and thus the material used is utilised to nearly 100 per cent efficiency. For this reason a cable has much larger average strain as compared to a member in flexure for the same maximum stress.

(2)   Cables have no bending stiffness and can carry loads only through a change in the funicular shape.

(3)   For reasons given in (1) and (2) above, a cable is a very flexible structure, and hence the need to stiffen cable structures.

(4)   The stiffness of a cable increases with the tension to which it is subjected and therefore the relationship between loads and deflections is non-linear. This property of a cable to get stiffer with loads, though statically advantageous, makes theoretical analysis complicated.

(5)   A suspension system can be so designed that most parts of the structure carry pure tension. Since cables can carry tension with great efficiency, quite a light and economic structure may result, especially if high tensile steels are used. This affects further economy in foundations.

(6)   The ease with which suspension roofs can be constructed and their attractive appearance make them a useful proposition both to the architect and the structural engineer. Suspension roofs are more advantageously used to cover large areas.

CLASSIFICATION

Suspension roof systems can be broadly placed into two categories:

(a)   Singly-curved roofs,

(b)   Doubly-curved roofs.

The singly-curved roof will consist mainly of a series of cables placed parallel to each other, supported at their ends and firmly anchored.   The covering material is carried by the cables and may also perform the function of imparting stiffness to the cables. The sketch in Figure 1(a)[x] represents a typical roof of this type. If necessary the cables can be prestressed and stiffened. For example, each one of the cables in the structure in Figure 1(a) can be prestressed by another cable of reverse curvature in any one

───────────────

× Page 5

of the ways shown in Figures 1(b),(c) **or** (d).

The photograph in Figure 2(a) and (b)[x] shows a wire model of a doubly-curved suspension roof system. The model was made in order to get a general idea of the problems involved with such systems and their behaviour.

The chief elements in the structure are:

(1)   The load-carrying cables, which are sagging,

(2)   Reverse-curvature prestressing cables,

(3)   Arches, which support the carrying-cables at the boundary and are the only part of the structure not in pure tension,

(4)   Cables at the boundary to support the prestressing cables,

(5)   Anchorages.

Several structural variations are possible in the way the boundary supports may be provided. In certain cases supports and anchorages may be merged. Carrying and prestressing cables, can if necessary be replaced by one of the units shown in Figures 1(b),(c) or (d), depending upon the requirements in a particular structure. In cases where the cable network has sufficient stiffness due to prestress, it is not necessary for the covering material to provide any gravity stiffness and a thin layer of the material is adequate enough to cover the network.

PROBLEM AND THE PURPOSE OF INVESTIGATION

During the past two to three decades some structures of the types described have been constructed, but any real attempts towards a study of their behaviour have been recorded only during the last few years. In the literature published so far, there does not appear any proven method for analysis of suspension systems. The work contained in this thesis is an attempt in that direction.

It will be clear from the study of the examples given that in order to understand the behaviour of suspension systems it is necessary to make

---

x Page 6

a fundamental study of:

(a)   A single cable

(b)   Two or more cables interacting with each other.

     With this requirement in view, the work listed below, was carried out.

(1)   Experimental study of three single wires of different span, size and geometry, under load.

(2)   Experimental study of the interaction between two single cables of opposite curvature prestressed by means of vertical, uniformly spaced members, was done on a wire model of the type of structure shown in Figure 1(b).

(3)   Theoretical study of 1 and 2.

     The above study is limited to plane-structures under vertical in-plane loading.

(4)   Theoretical study of a three-dimensional structure consisting of three cables interacting with each other through uniformly spaced prestressing members.

     The work is presented in the following order:

Chapter 1   :   Theory

Chapter 2   :   Experiments

Chapter 3   :   Discussion on results

Chapter 4   :   Conclusions
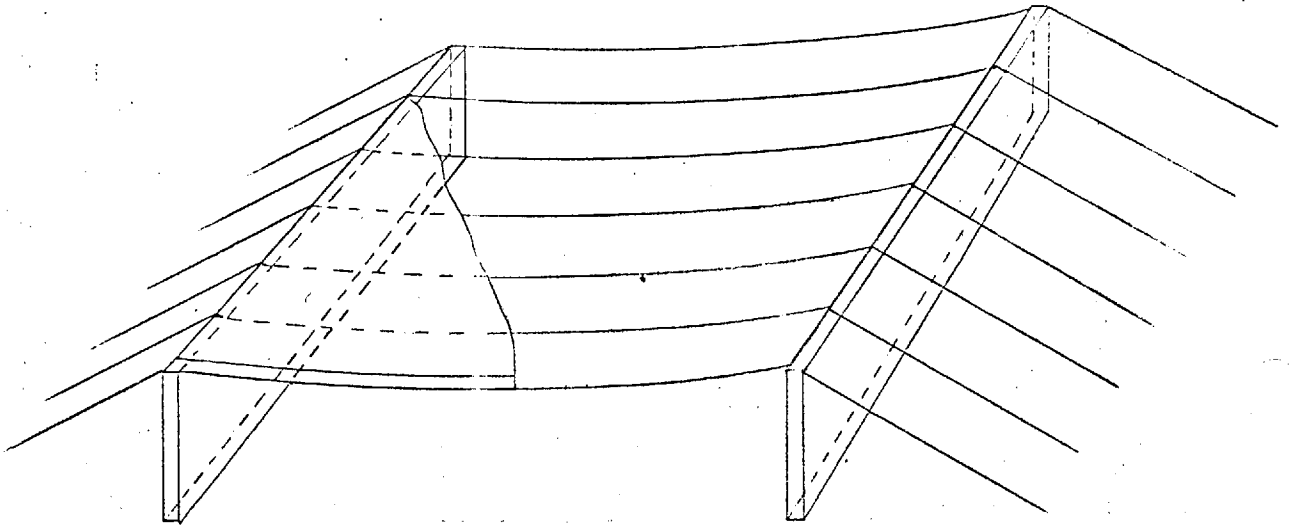
FIGURE 1a.
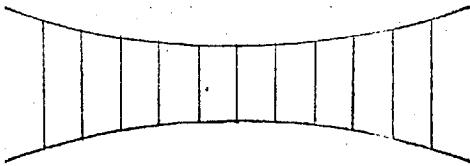
FIGURE 1b.
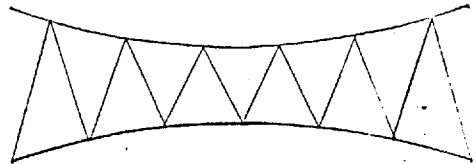
FIGURE 1c.
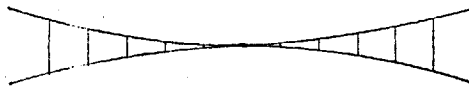
FIGURE 1d.

SOME EXAMPLES OF SUSPENSION SYSTEMS
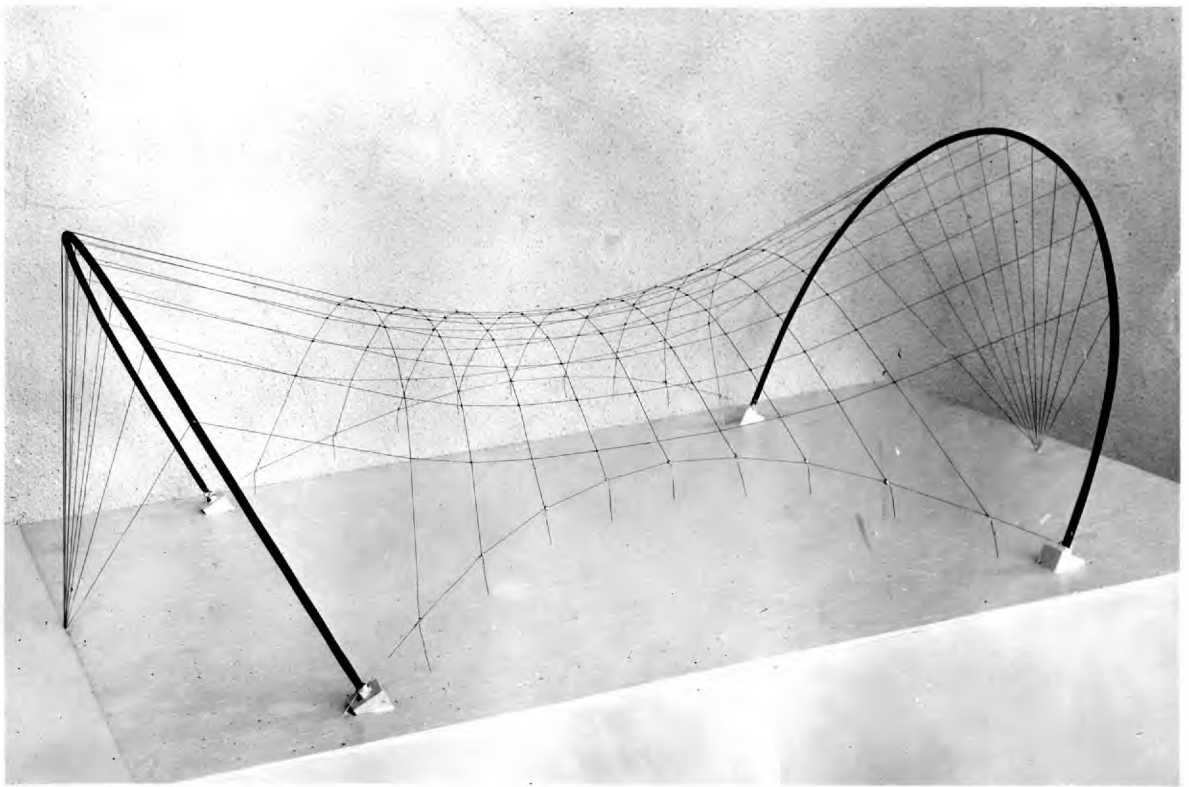
FIGURE 2a   MODEL OF A DOUBLY CURVED ROOF SUSPENSION SYSTEM
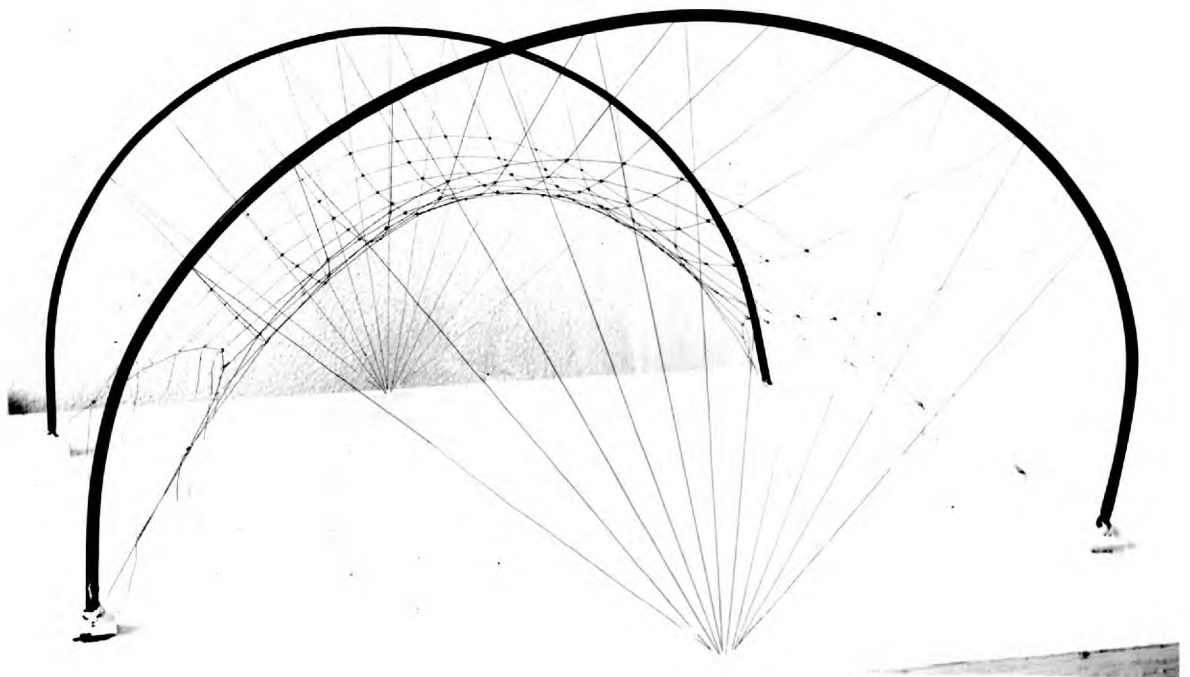
FIGURE 2b   END ELEVATION OF THE MODEL SHOWN ABOVE

CHAPTER I

THEORY

1.01 Review of existing theoretical work

This section deals with a brief survey of the existing theo-
retical work on plane and three-dimensional cable structures. The
work on plane-systems is mainly limited to the treatment of a single
cable and is described in Section 1.02. The term "single cable" is
here applied to a cable hanging under its own weight, the distributed
load from the hangers, and an applied point load. The weight is
considered uniformly distributed across the span.

The work on three-dimensional structures falls into two main
categories:

    (i)   Determination of their geometry under initial pre-
           stressing forces, and

   (ii)   Solution of a structure of known shape under applied
           loads,

and is described in Sections 1.04 and 1.05 respectively.

Some of the work reviewed here has been used later, with
necessary modifications, to solve the problems being studied in this
chapter.

1.02 The single cable

Treatment of a single cable under applied loads, as given by
Pugsley[1], is described in the following paragraphs. The cable is
assumed to hang initially in a continuous arc, which is parabolic in
shape. Behaviour of the cable under three types of vertical applied

loading has been considered.

     (i)   Single concentrated load applied anywhere along the span,

    (ii)   A short uniformly distributed load placed centrally in the span, and

   (iii)   A short uniformly distributed load placed at one end of the span.

The cable subjected to a single concentrated load is shown in Figure 3.[x] The cable is simply supported at A and B which are at the same level. The lowest point on the curve, C, is taken as the origin. It is assumed that the weight of the cable is w/unit length of span and uniform throughout.

The cable hangs in a parabolic arc whose equation is

$$y = \frac{wx^2}{2H} \tag{1}$$

where $H = \dfrac{wL^2}{8d}$ is the horizontal component of cable tension.

Let a point load P (P/wL is small) be applied at point Q as a result of which the horizontal component of tension changes to, say, H + h. The new arc AQ' can be described by the equation

$$y_1 = \frac{wx_1^2}{2(H+h)} \tag{2}$$

where x_1 and y_1 refer to a new origin C', the lowest point on AQ'. Since the cable is discontinuous at Q', another expression like (2) will be required to express the geometry of Q'B. The

---

x Page 9
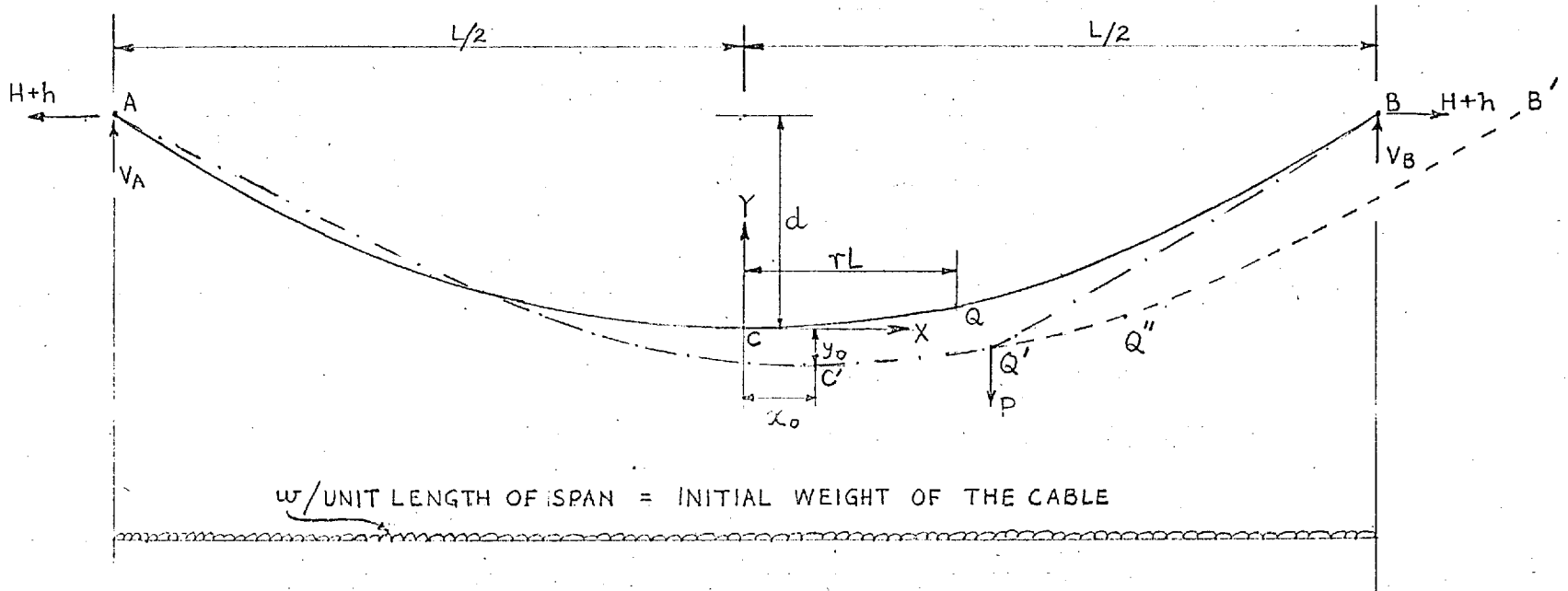
FIG. 3 : LOAD 'P' APPLIED TO A SINGLE CABLE.

arc AQ' would, if continued, carry on through the points Q", B'. Here Q" is such that w times this projected length is equal to P. The arc Q"B' will then be identical in form with the arc Q'B.

Now, from considerations of static equilibrium, V_A, V_B, x_o and y_o are evaluated as

$$V_A = \frac{1}{2} wL + P(\frac{1}{2} - r) \tag{3a}$$

$$V_B = \frac{1}{2} wL + P(\frac{1}{2} + r) \tag{3b}$$

$$x_o = \frac{P}{w}(\frac{1}{2} - r) \tag{4a}$$

$$y_o = d - \frac{wL^2}{8(H+h)} \cdot \left\{ 1 + \frac{P}{wL}(1 - 2r) \right\}^2 \tag{4b}$$

y_o is measured positive upwards from C.

The geometry of arcs AQ' and Q'B can now be expressed with the help of the property of arc Q'Q" and equations (2) to (4).

Taking C as origin the expressions for v are

$$v = y_o + \frac{w}{2(H+h)} \cdot \left\{ x - \frac{P}{w} \cdot (\frac{1}{2} - r) \right\}^2 - \frac{wx^2}{2H} \tag{5a}$$

for $-L/2 < x < rL$

$$v = y_o + \frac{w}{2(H+h)} \cdot \left\{ x + \frac{P}{w} \cdot (\frac{1}{2} + r) \right\}^2 - \frac{wx^2}{2H} \tag{5b}$$

for $rL < x < L/2$

The only unknown is h.

The force h is now evaluated by equating the change in length of the cable due to deformation to the extension of the cable due to increase in tension, i.e.,

Extension of the cable due to increase in tension =
length of the deformed cable AQ'B - length of the cable ACB .

Let v be the deflection, measured positive upwards. Length 1
of the arc ACB is given by,

$$1 = \int_{-L/2}^{+L/2} \left\{ 1 + \left(\frac{dy}{dx}\right)^2 \right\}^{1/2} dx \tag{6}$$

Putting (y + v) for y and expanding in Taylor series, we
have

$$\Delta 1 = \int_{-L/2}^{+L/2} \frac{\left(\frac{dy}{dx}\right)\left(\frac{dv}{dx}\right)}{\left\{ 1 + \left(\frac{dy}{dx}\right)^2 \right\}^{1/2}} dx \tag{7}$$

if higher order terms in v [x] are neglected.

Assuming the cable to be inextensible[I] and ignoring the term
$(\frac{dy}{dx})^2$ in comparison to unity[+], we have

$$\int_{-L/2}^{+L/2} \left(\frac{dy}{dx}\right)\left(\frac{dv}{dx}\right) dx = 0 \tag{8}$$

From the use of the equations (1) and (5) in equation (8) and
neglecting $(\frac{h}{H})^2$ in comparison to $(\frac{h}{H})$ we have

$$\frac{h}{H} = \frac{3}{2} \frac{P}{wL} (1 - 4r^2) \tag{9}$$

Knowing h , the deflected shape can be determined from

---

[x] [I] [+] The effect of neglecting these factors can be seen from a more
accurate analysis in section 1.11.

equation (5)

The horizontal movements can be evaluated by the consideration that the change in length of the cable between the support A and any point x due to deformation v is the horizontal movement at x because the cable is considered inextensible (it also means, indirectly, that the cable is very flat). This change in length is given by

$$\Delta l \; = \; \int_{x=-L/2}^{x=x} \left(\frac{dy}{dx}\right)\left(\frac{dv}{dx}\right) dx \tag{10}$$

Measuring u , the horizontal deflection, positive in the direction of x , we have

$$u \; = - \int_{x=-L/2}^{x=x} \frac{dy}{dx} \, dv \tag{11}$$

The value of horizontal deflection u_Q [*] at load point Q is obtained by using expression (5a) or (5b) in equation (11) as

$$u_Q \; = \; 8 \cdot \frac{P}{w} \cdot \frac{d^2}{L^2} \cdot \frac{r(1-16r^4)}{1+1\cdot5\frac{P}{wL}(1-4r^2)} \tag{12}$$

The above analysis is only recommended for use in cables of small dip to span ratio and for values of P small as compared to wL .

Values of maximum deflections under short uniformly distributed loads for a single cable have also been worked out by Pugsley[1]. Similar results have been obtained before by Johnson, Bryan and Turneaure[6] and Steinman[11]

---

[*] Expressions for horizontal movement anywhere under a point load at Q are given in section 1.11.

A numerical method for the determination of the deflected shape of a suspended cable subject to gradually applied, concentrated or uniformly distributed loads, is given by W. T. O'Brien and A. J. Francis[13]. The method consists in setting up equations of static equilibrium and solving them for geometric compatibility requirements by successive approximation. The effect of change in temperature, slip at the anchorage or movement at the support can be included. The paper deals with two classes of problems.

1. Rolling loads, which include moving loads and static loads whose final horizontal position along the cable, Q' in Figure 3, is specified, and the original position of application along the cable, Q in Figure 3, is unknown.

2. Fixed loads, which is the usual problem of loads with known position of application.

The basic approach to both problems is the same and differs only in the method of applying successive corrections to the initially assumed displacements.

The cable is divided into a number of segments depending on the loading. Two conditions must be satisfied at each node point,

(a) cable segments and load points must be in equilibrium,

(b) deformations and elastic extensions of the cable segments must be compatible with the overall deformations and elastic extensions of the cable.

Formulae and equations are set down to satisfy these requirement and solved by a process of iteration. Expressions for assuming initial values and correction terms are given. The method shows good convergence.

1.03 Influence coefficient method for solving suspension bridge problems

It is of some relevance here to state Pugsley's[1], [4] "Influence coefficient" approach to solve suspension bridge problems. Using the method of analysing a cable under an applied point load, its behaviour can be completely expressed in the form of tables of flexibility coefficients. These coefficients correspond to the effects of a small unit load placedsuccessively at various points along the cable span. Table 1 shows one of the 4 tables required (2 tables for vertical and horizontal movements under vertical load and 2 tables for vertical and horizontal movements under horizontal load). The cable is divided into segments by a number of equally spaced stations.

Loaded Station No.	Deflection at Station No.						
	1	2	3	- -	j	--	
1	v_{11}	v_{12}	v_{13}	--	--	- --	- -
2	v_{21}	v_{22}	v_{23}	--- ---	-	-	---
3							
i					v_{ij}		

v_{ij} = the deflection at station j due to unit load placed at station i .

Importance is, however, given only to vertical deflections under vertical loads, thus reducing the work to the preparation of one table only. A similar table can be prepared for the stiffening girder. Let the corresponding notation for stiffening girder deflections be V_{ij} .

Now, suppose a load P is placed on the girder at station 2 and causes changes in hanger tensions T_1 , T_2 , etc. The cable deflection at station 1 is given as

$$C_1 = T_1 v_{11} + T_2 v_{12} + \ldots \ldots \tag{13}$$

Similarly, the girder deflection at station 1 is given as

$$G_1 = T_1 V_{11} + (T_2 - P)V_{12} + \ldots \ldots \tag{14}$$

For continuity of deflections at station 1

$$G_1 - C_1 = \alpha_1 T_1 \tag{15}$$

where α_1 = extensibility of the hanger at station 1.

Equations such as (15) can now be written for all the stations and solved simultaneously to give the values of T_1 , T_2 , etc.

Once these forces are known, cable and girder deflections are calculable from equations (13) and (14) respectively. Girder moments and shears and cable forces can also be readily evaluated.

The approach is essentially based on the assumption that the principle of superposition is applicable. The assumption is stated to be justifiable for small applied loads.

1.04 Determination of the geometry of a suspension-structure under initial prestressing forces

Siev and Eidelman[8] give a method of determining the shape of a cable structure bounded by a non-planar boundary of known geometry. The cables are assumed to be suspended in an orthogonal family of parallel vertical planes. The dead weight, if considered, is taken to be concentrated at the nodes. The only unknowns in such a problem are the vertical ordinates. Equations of equilibrium of vertical forces are written for each node and solved simultaneously to give the unknown ordinates. The initial force in each wire is assumed to be known at any point along its length. The equations are of the form,

$$H_m (Z_{m;n+1} - 2Z_{m;n} + Z_{m;n-1}) +$$
$$H_n (Z_{m+1;n} - 2Z_{m;n} + Z_{m-1;n}) = 0 \qquad (16)$$

where H_m and H_n are the horizontal components of forces in cables intersecting at the node (m;n), numbers n and m being counted along X and Y axes respectively, and $Z_{m;n}$ is the ordinate at the same point. Simultaneous solution of these equations will give the shape of the network.

Equation (16) may be written as

$$H_m \left(\frac{\Delta^2 z}{\Delta x^2}\right)_{m;n} + H_n \left(\frac{\Delta^2 z}{\Delta y^2}\right)_{m;n} = 0 \qquad (17)$$

If the cables are closely spaced the finite difference expressions may be replaced by continuous functions and equation (17) becomes

$$H_Y \frac{\partial^2 z}{\partial x^2} + H_X \frac{\partial^2 z}{\partial y^2} = 0 \qquad (18)$$

where H_y = horizontal component of tension in x-direction per unit width of strip and H_x = horizontal component of tension in y-direction per unit width of strip.

Since the equations (17) and (18) are homogenous the shape of the surface depends only on the ratio of H_x and H_y and the surface will be hyperbolic.

It will be observed that the method is limited on application to roofs of very flat shapes only, on account of the assumption that cables lie in vertical parallel planes. The method is, in a way, limited to finding the geometry for hyperbolic or near hyperbolic shapes only.

A more general method is given by Eras and Elze[10] for determining the initial geometry. It is assumed that the forces in the different members of the structure under the initial prestress conditions are known[x]. Equations of force-compatibility are now set up at each node for a suitably assumed geometry. Consider a node k linked to i through members k - i (see Figure 4a)[+]. Initial force in the member is F_i and its length is l'_i. Let the co-ordinates of the nodes k and i be $(x_k$, y_k , $z_k)$ and $(x_i$, y_i , $z_i)$ respectively. For the equlibrium of node k the following equations must be satisfied:

---

[x] As shown later in Section 1.33, the initial forces may not necessarily be known and have to be assumed too.

+ Page 18
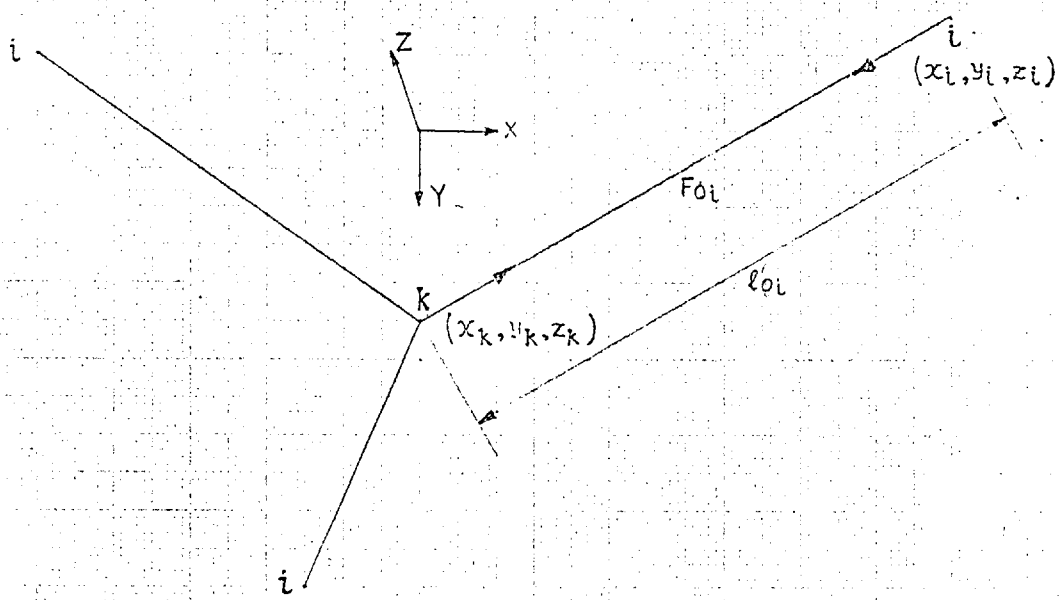
FIG.4a : GENERAL NODE 'k' IN A STRUCTURE LINKED TO NODES 'i'
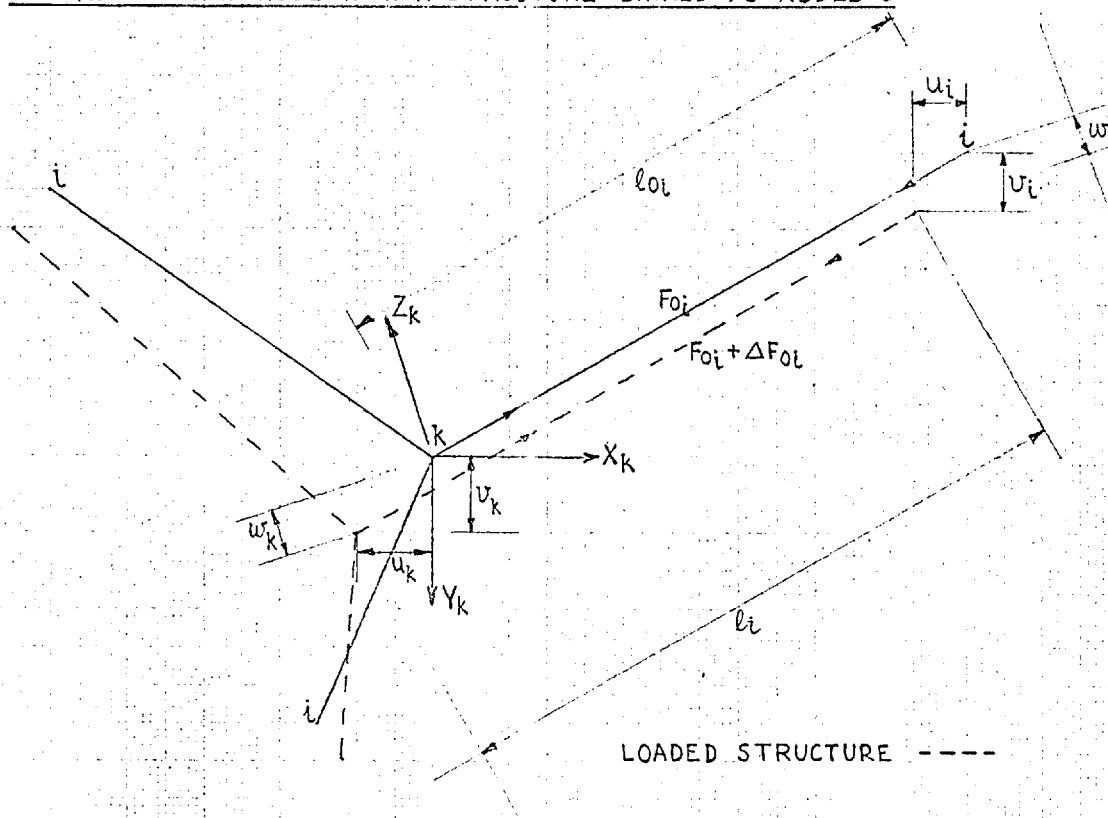
FIG.4b : LOADS X_k, Y_k, Z_k APPLIED AT 'k'

LOADED STRUCTURE - - - -

$$\sum_i \frac{F_i}{l_i'}(x_i - x_k) = 0 \tag{19a}$$

$$\sum_i \frac{F_i}{l_i'}(y_i - y_k) = 0 \tag{19b}$$

$$\sum_i \frac{F_i}{l_i'}(z_i - z_k) = 0 \tag{19c}$$

The values of the assumed coordinates may be such that equations (19a - c) are not satisfied. Corrections u', v' and w' are therefore applied to x, y and z respectively in order to obtain equilibrium and equations (19a - c) become

$$\sum_i \frac{F_i}{l_i'}(x_i + u_i' - x_k - u_k') = 0 \tag{20a}$$

$$\sum_i \frac{F_i}{l_i'}(y_i + v_i' - y_k - v_k') = 0 \tag{20b}$$

$$\sum_i \frac{F_i}{l_i'}(z_i + w_i' - z_k - w_k') = 0 \tag{20c}$$

or

$$\sum_i \frac{F_i}{l_i'}(\Delta x_i + \Delta u_i') = 0 \tag{21a}$$

$$\sum_i \frac{F_i}{l_i'}(\Delta y_i + \Delta v_i') = 0 \tag{21b}$$

$$\sum_i \frac{F_i}{l_i'}(\Delta z_i + \Delta w_i') = 0 \tag{21c}$$

where $\Delta x_i = x_i - x_k$, $\Delta u_i' = u_i' - u_k'$, $\cdots$etc.

Solutions of equations (21a - c) for all the nodes simultaneously gives the value of the correction terms. Change in the values of x , y and z alters the value of l' too, and the process of correcting the values may have to go through several cycles of iteration before the desired accuracy is obtained in the results.

The following equations are derived for the ν-th cycle of iteration for x-direction only and suffix i has been dropped for simplification.

In the ν-th cycle of iteration

$$x^{(\nu+1)} = x^{(\nu)} + u'^{(\nu)} \tag{22}$$

and

$$l'^{(\nu+1)} = \left\{ \left(\Delta x^{(\nu)} + \Delta u'^{(\nu)}\right)^2 + \left(\Delta y^{(\nu)} + \Delta v'^{(\nu)}\right)^2 + \left(\Delta z^{(\nu)} + \Delta w'^{(\nu)}\right)^2 \right\}^{1/2} \tag{23a}$$

From equation (23a) we have

$$\frac{1}{l'^{(\nu+1)}} = \left\{ \left(\Delta x^{(\nu)} + \Delta u'^{(\nu)}\right)^2 + \left(\Delta y^{(\nu)} + \Delta v'^{(\nu)}\right)^2 + \left(\Delta z^{(\nu)} + \Delta w'^{(\nu)}\right)^2 \right\}^{-1/2} \cdots \cdots \cdots \tag{23b}$$

and on expanding it and neglecting higher order terms, we have

$$\frac{1}{l'^{(\nu+1)}} = \frac{1}{l'^{(\nu)}} \left\{ 1 - \frac{1}{l'^{(\nu)2}} \left(\Delta x^{(\nu)} \Delta u'^{(\nu)} + \Delta y^{(\nu)} \Delta v'^{(\nu)} + \Delta z^{(\nu)} \Delta w'^{(\nu)} \right) \right\} \tag{24}$$

Using the value of $\frac{1}{1'^{(\nu+1)}}$ in equation (21a) and on rearranging terms, we obtain

$$\sum \frac{F_0}{1'^{(\nu)}} \left\{ \Delta u'^{(\nu)} - \frac{\Delta x^{(\nu)}}{1'^{(\nu)\,2}} \left(\Delta x^{(\nu)} \Delta u'^{(\nu)} + \Delta y^{(\nu)} \Delta v'^{(\nu)} + \Delta z^{(\nu)} \Delta w'^{(\nu)} \right) \right\}$$

$$\sum \frac{F_0}{1'^{(\nu)}} \Delta x^{(\nu)} \qquad (25a)$$

Equations in y- and z-directions (25b) and (25c) can be derived similarly. Equations (25a - c) have to be set up for all the nodes and solved simultaneously for a sufficient number of cycles to give the desired accuracy.

1.05 Solution of a prestressed suspension structure with known initial geometry under applied loading

Eras and Elze[9], [10] have suggested two methods of treating this problem. The first method is approximate and is described in detail in reference (9) (and briefly mentioned in reference (10)). The method considered only vertical loading to structures whose shape is defined by surfaces of negative Gaussian curvature. It is assumed that

(i)   The dip to span ratio is small,

(ii)   Cables lie in a family of parallel vertical planes cutting each other orthogonally; the first condition is necessary for this,

(iii)   Only vertical deflections occur and cables remain in parallel vertical planes after loading,

(iv)   Deflections are very much smaller than the dip, and

(v)   Cables are supported by unyielding boundaries.

The deflected shape of the structure is assumed in terms of trigonometric or hyperbolic functions, depending on the loading pattern. The basic equations are set up by equating the stretch of cables due to change in tension to the change in length due to deformations (this is based on the assumed deflected shape). From these equations the loading pattern is computed. If there is a fair agreement between the actual and computed loading pattern, the assumed deflected shape is accepted; if not, another assumed shape is tried.

The method is simple in application but limited to very simple cases of loading, where the deflected shape will be easy to assume. The other limitations in the method are underlined by the assumptions themselves.

A much more general method is also given by Eras and Elze[10] ("exact method" in reference (10)). The method consists of setting up equations of force-compatibility and solving them by a process of successive iteration to obtain the deformations.

Consider a node k linked through members $k - i$ to nodes i (Figure 4b).[x] Initial length of the member $k - i$ is lo_i and the initial force in it is Fo_i. The coordinates of the nodes k and i are (x_k, y_k, z_k) and (x_i, y_i, z_i) respectively. Let loads X_k, Y_k and Z_k be applied at node k, causing deflections u_k, u_i, v_k, v_i and w_k, w_i along X, Y and Z axes respectively at nodes k and i. The change in force in the member $k - i$ is ΔFo_i and its length changes to l_i.

The equation of equilibrium in the X-direction only has been derived, the derivation in Y- and Z-direction being similar.

The equation of equilibrium at k is

$$\sum_i \frac{Fo_i + \Delta Fo_i}{l_i} (\Delta x_i + \Delta u_i) = X_k \tag{26}$$

$$lo_i = (\Delta x_i^2 + \Delta y_i^2 + \Delta z_i^2)^{1/2} \tag{27a}$$

and
$$l_i = \left\{ (\Delta x_i + \Delta u_i)^2 + (\Delta y_i + \Delta v_i)^2 + (\Delta z_i + \Delta w_i)^2 \right\}^{1/2} \tag{27b}$$

where $\Delta x_i = x_i - x_k$

and $\Delta u_i = u_i - u_k$ and so on.

---

x Page 18

The suffix i has been dropped in the following equations for simplification.

Say $\quad e_1 = \dfrac{1}{l_0^2}\left(\Delta x.\Delta u + \Delta y.\Delta v + \Delta z.\Delta w\right)$ (28a)

and $\quad e_2 = \dfrac{1}{l_0^2}\left(\Delta u^2 + \Delta v^2 + \Delta w^2\right)$ (28b)

Substituting values from equations (27a), (28a) and (28b) in equation (27b) we have

$$1 = l_0\left(1 + 2e_1 + e_2\right)^{1/2}$$ (29)

Expanding the expression on the right hand side in equation (29) and neglecting terms containing 4th or higher powers of deflections, we have

$$1 = l_0\left(1 + e_1 + \tfrac{1}{2}e_2 - \tfrac{1}{2}e_1^2 - \tfrac{1}{2}e_1.e_2 + \tfrac{1}{2}e_1^3 + \cdots\cdots\right)$$ (30a)

and $\quad \dfrac{1}{1} = \dfrac{1}{l_0}\left(1 - e_1 - \tfrac{1}{2}e_2 + \tfrac{3}{2}e_1^2 + \tfrac{3}{2}e_1.e_2 - \tfrac{5}{2}e_1^3 + \cdots\cdots\right)$ (30b)

The change in the force in member $k - i$, ΔF_0 can be expressed as

$$\Delta F_0 = EA\left(\dfrac{1 - l_0}{l_0}\right) = EA\left(\dfrac{1}{l_0} - 1\right)$$ (31a)

Using the value of $\dfrac{1}{l_0}$ from equation (30a) we get

$$\Delta F_0 = EA\left(e_1 + \tfrac{1}{2}e_2 - \tfrac{1}{2}e_1^2 - \tfrac{1}{2}e_1.e_2 + \tfrac{1}{2}e_1^3\right)$$ (31b)

Putting the values of $\frac{1}{l}$ and ΔF_o from equations (30b) and (31b) respectively in equation (26) we obtain

$$\sum \left\{ F_0 + EA \left(e_1 + \frac{1}{2} e_2 - \frac{1}{2} e_1^2 - \frac{1}{2} e_1 e_2 + \frac{1}{2} e_1^3 \right) \right\} \cdot \left\{ \frac{1}{l_0} \left(1 - e_1 - \frac{1}{2} e_2 \right. \right.$$

$$\left. \left. + \frac{3}{2} e_1^2 + \frac{3}{2} e_1 e_2 - \frac{5}{2} e_1^3 \right) \right\} \cdot (\Delta x + \Delta u) \qquad = X_k \qquad (32)$$

Equation (32) is now expanded and rearranged so that co-efficients of terms u, v and w are on the left hand side and all other terms are on the right hand side.

$$\frac{F_0}{l_0} \Delta u + \frac{EA - F_0}{l_0} \Delta x \cdot e_1 \qquad = X_k - K_{x_k} \qquad (33)$$

where $\qquad K_{x_k} = (EA - F_0) \left\{ \frac{\Delta u \cdot e_1}{l_0} + \frac{\Delta x + \Delta u}{2 l_0} \left[e_2 - 3 e_1^2 \cdot \left(1 + \frac{e_2}{e_1} - \frac{5}{3} e_1 \right) \right] \right\}$

It will be noted that terms containing 4th or higher powers of u, v and w have been neglected and $\sum \frac{F_0}{l_0} \Delta x$ has been taken equal to zero (this is a necessary condition for initial equilibrium) in deriving equation (33). Two more equations like (33) can be similarly derived for Y- and Z-directions.

Equations like (33) have to be set up at each node in the structure and solved simultaneously by successive iterations to give the value of deflections at each point. Forces can be computed by using equation (31a) or (31b).

1.10 Study of a single cable under a concentrated load

Pugsley's method of analysing a single cable under a concentrated load has already been described in Section 1.02. The method is meant for point loads small in comparison to the total weight of the cable and various factors have been neglected in evaluating the force h . An attempt to get a more accurate solution by including the terms neglected and to study the effect of neglecting them now follows. This study was thought to be particularly necessary, because the single cable behaviour has been used, as described later in Section 1.20, to solve a plane prestressed cable system.

A more accurate value of the change in the cable length as compared to the one given in equation (7) is

$$\Delta l^* = \int_{-L/2}^{+L/2} \frac{\left(\frac{dy}{dx}\right)\left(\frac{dv}{dx}\right)}{\left\{1 + \left(\frac{dy}{dx}\right)^2\right\}^{1/2}} \, dx \; + \; \frac{1}{2} \int_{-L/2}^{+L/2} \frac{\left(\frac{dv}{dx}\right)^2}{\left\{1 + \left(\frac{dy}{dx}\right)^2\right\}^{3/2}} \, dx \tag{34}$$

Equating Δl to the cable extension, we have, instead of equation (8)

$$\int_{-L/2}^{+L/2} \frac{\left(\frac{dy}{dx}\right)\left(\frac{dv}{dx}\right)}{\left\{1 + \left(\frac{dy}{dx}\right)^2\right\}^{1/2}} \, dx \; + \; \frac{1}{2} \int_{-L/2}^{+L/2} \frac{\left(\frac{dv}{dx}\right)^2}{\left\{1 + \left(\frac{dy}{dx}\right)^2\right\}^{3/2}} \, dx \; = \; \frac{ShL}{AE} \tag{35}$$

where S^* is an empirical constant $= (1 + 4.8 \frac{d^2}{L^2})$

---

* Details are given in Appendix "A"

Using values from equation (1) and (5) in equation (35), we obtain instead of equation (9)[*]

$$\frac{12U}{FL}\cdot\bar{h}^3 + \left(\cdot15G +1 - \frac{12U}{FL}\right)\cdot\bar{h}^2 + G\left(12\bar{W}r^4 - 0\cdot75\bar{W} - 0\cdot6\right)\cdot\bar{h}$$

$$+ 12\left(1 - 1\cdot5G r^2\right)\bar{W}r^2 + 24\left(1 - Gr^2\right)\bar{W}^2 r^2 - \left\{1 + 3\bar{W} + 3\left(1 + 4r^2\right)\bar{W}^2\right\}$$

$$+ G\left\{0\cdot75\left(1 + 4r^2\right)\bar{W}^2 + 1\cdot125\,\bar{W} + 0\cdot45\right\} = 0 \qquad (36)$$

where, $\quad \bar{h} = 1 + \dfrac{h}{H} \quad$ is the unknown ,

$$\bar{W} = \frac{P}{wL} \quad , \qquad U = \frac{SHL}{AE} \quad ,$$

$$F = G = 32\,\frac{d^2}{L^2} \quad .$$

The effect of neglecting various factors in equation (36) is shown in the following cases:

<u>Case 1</u> If the cable is assumed to be flat, $\left(\dfrac{dy}{dx}\right)^2$ can be neglected in comparison to unity and also the tension along the cable can be assumed to be constant and equal to H . This is obtained by putting $G = 0$ and $S = 1$ in equation (36) and we have

$$\frac{12U'}{FL}\cdot\bar{h}^3 + \left(1 - \frac{12U'}{FL}\right)\cdot\bar{h}^2 + 12\,\bar{W}r^2 + 24\bar{W}^2 r^2 - \left\{1 + 3\bar{W} + 3\left(1 + 4r^2\right)\bar{W}^2\right\} = 0 \qquad (37a)$$

where $\quad U' = \dfrac{HL}{AE}$

<u>Case 2</u> If the cable is assumed inextensible, i.e. $\dfrac{1}{AE} = 0$

---

[*] Details are given in Appendix "A"

equation (36) becomes

$$\left(0.15\,G+1\right)\bar{h}^2 + G\left(12\,\bar{W}r^4-0.75\,\bar{W}-0.6\right)\cdot\bar{h} + 12\left(1-1.5\,Gr^2\right)\bar{W}r^2$$

$$+24\left(1-Gr^2\right)\bar{W}^2r^2 - \left\{1+3\bar{W}+3\left(1+4r^2\right)\bar{W}^2\right\} + G\left\{0.75\left(1+4r^2\right)\bar{W}^2\right.$$

$$\left.+1.125\,\bar{W}+0.45\right\} \quad = 0 \tag{37b}$$

<u>Case 3</u>   If the second term in the left hand side of equation (35) is assumed negligible as in equation (7), we obtain, by putting $\bar{W}^2 = 0$ in equation (36),

$$\frac{12\,U}{F\,L}\cdot\bar{h}^3 + \left(0.15\,G+1-\frac{12\,U}{F\,L}\right)\cdot\bar{h}^2 + G\left(12\,\bar{W}r^4-0.75\,\bar{W}-0.6\right)\cdot\bar{h}$$

$$+12\left(1-1.5\,Gr^2\right)\bar{W}r^2 -\left(1+3\bar{W}\right) + G\left(1.125\,\bar{W}+0.45\right) \;=0 \tag{37c}$$

<u>Case 4</u>   If all factors neglected in cases 1, 2 and 3 are neglected together, we have

$$\bar{h}^2 + 12\,\bar{W}r^2 - \left(1+3\bar{W}\right) \quad = \; 0 \tag{37d}$$

<u>Case 5</u>   Pugsley's expression can be obtained from equation (37d) as follows:

Putting $1+\dfrac{h}{H} = \bar{h}$ in equation (37d) we have

$$\left(1+\frac{h}{H}\right)^2 + 12\,\bar{W}r^2 - \left(1+3\bar{W}\right) \quad = 0$$

or $\quad 1 +2\left(\dfrac{h}{H}\right) + \left(\dfrac{h}{H}\right)^2 +12\,\bar{W}r^2 -1 -3\bar{W} \quad = \; 0$

or $\quad 2\left(\dfrac{h}{H}\right) \quad = \quad 3\bar{W} - 12\,\bar{W}r^2$

on neglecting $(\frac{h}{H})^2$ in comparison to $(\frac{h}{H})$, we get

$$h = \frac{3}{2} H \bar{W} (1 + 4r^2) \tag{37e}$$

Equation (37e) is identical to equation (9).

Now equations (5a) and (5b) can be stated in dimensionless form as

$$\frac{v_{\rho}}{d} = (1-4\rho^2) - \frac{1}{\bar{h}}\left\{(1-4\rho^2) + 2\bar{W}\cdot(1+2\rho)\cdot(1-2r)\right\} \tag{38a}$$

for $-0.5 \leqslant \rho < r$ where $\rho = \frac{x}{L}$

and $\frac{v_{\rho}}{d} = (1-4\rho^2) - \frac{1}{\bar{h}}\left[(1-4\rho^2) + 2\bar{W}(1-2\rho)\cdot(1+2r)\right] \tag{38b}$

for $r \leqslant \rho \leqslant 0.5$

Deflection under the load can be obtained by putting $\rho = r$ in either equation (38a) or (38b).

$$\frac{v_r}{d} = (1-4r^2)\cdot(1 - \frac{1+2\bar{W}}{\bar{h}}) \tag{39}$$

Expressions for the horizontal deflection anywhere under a point load at r can be obtained from equation (11) and are given below,

$$\frac{u_{\rho}}{d} = -64\frac{d}{L}\left\{-\frac{1}{24}\cdot(1+8\rho^3)\frac{\bar{h}-1}{\bar{h}} + \frac{1}{16}\cdot\frac{\bar{W}}{\bar{h}}(1-4\rho^3)(1-2r)\right\} \tag{40a}$$

for $-0.5 \leqslant \rho < r$

and $\frac{u_{\rho}}{d} = -64\frac{d}{L}\left\{-\frac{1}{24}(1+8\rho^3)\frac{\bar{h}-1}{\bar{h}} + \frac{1}{4}\cdot\frac{\bar{W}}{\bar{h}}\left[-2r^2-3r(1+\rho^2)+(4+\rho^2)\right]\right\} \tag{40b}$

for $r \leqslant \rho \leqslant 0.5$

Figure 5 shows the values of $(\overline{h} - 1)$ obtained from equations (36) and (37a - e) for various values of $\overline{W}$. Figure 6 shows the values of deflections v_r obtained by using the above values of $\overline{h}$ in equation (39). Data used for these calculations is,

L = 40 in. d = 2.5 in. r = 0

wL = 25 lb. H = 50 lb. AE = 91000 lb. (wire diameter = .064 in. modulus of elasticity = 28.3×10^6 lb./in.^{2})

Figure 7 shows the effect of varying the dip to span ratio on v_r for

$\overline{W}$ = 0.1 r = 0 and H = 50 lb.

Only cases 1, 2 and 5 are compared with the accurate solution.

It will be seen from Figures 5 and 6 that for a small value of $\overline{W}$ equal to 0.1 or less, the effect of neglecting the various factors is very small, but as the value of $\overline{W}$ increases, this effect increases. Errors in cases 3 and 4 are comparatively much larger than in other cases, and the predominating factor seems to be the neglecting of $\overline{W}^2$. If, however, $(\frac{h}{H})^2$ is also neglected, as in case 5, the values come much nearer to the values from the accurate solution. Therefore, neglecting either $\overline{W}^2$ or $(\frac{h}{H})^2$ causes serious errors, which are compensating if both these terms are neglected together.

Figures 8 and 9 show the values of vertical deflection of a cable under a concentrated load applied successively at centre and quarter point. The values are for .0164 in. and .064 in. diameter wires, with wL equal to 2 lb. and 25 lb. respectively. The rest of the data used for these calculations is

L = 40 in., d = 2.5 in. E = 28.3 x 10^6 p.s.i. $\overline{W}$ = 0.1, 0.2 and 0.3.

It will be seen that the value of deflection v_y is non-linearly related to the value of load $\overline{W}$. There is not much difference in the deflections for the two sizes of wires and the values for the thinner wire are comparatively closer to those obtained by using Pugsley's expression than for the thicker wire. These values have been obtained by using equations (36), (37c), (38a) and (38b).

Figure 10 shows the values of the horizontal deflection of a cable under a vertical concentrated load applied successively at quarter point and centre point. The values have been calculated by using equations (9), (40a) and (40b) and the data used is

$$d = 2.5 \text{ in.} \quad L = 40 \text{ in.} \quad \overline{W} = 0.1, 0.2, \text{ and } 0.3$$

It will be seen that the relation between the deflection u_A and $\overline{W}$ is non-linear just as for the vertical deflections. A load applied unsymmetrically on the cable (quarter point in this case) causes much larger horizontal movements than a central load.

1.20 The influence coefficient approach as applied to a plane prestressed system

A brief mention of this method as applied to the solution of a suspension bridge has been made in Section 1.03. Its application to a cable system of the type shown in Figure 11a[x] is illustrated here. The plane system could be seen as a suspension bridge without any bending stiffness and with the stiffening girder replaced by a prestressing cable of reverse curvature.

The structure consists of two cables prestressed together by means of vertical uniformly spaced hangers, each carrying equal tension T with an average value of 'w' per unit length of span.

[x] Page 32
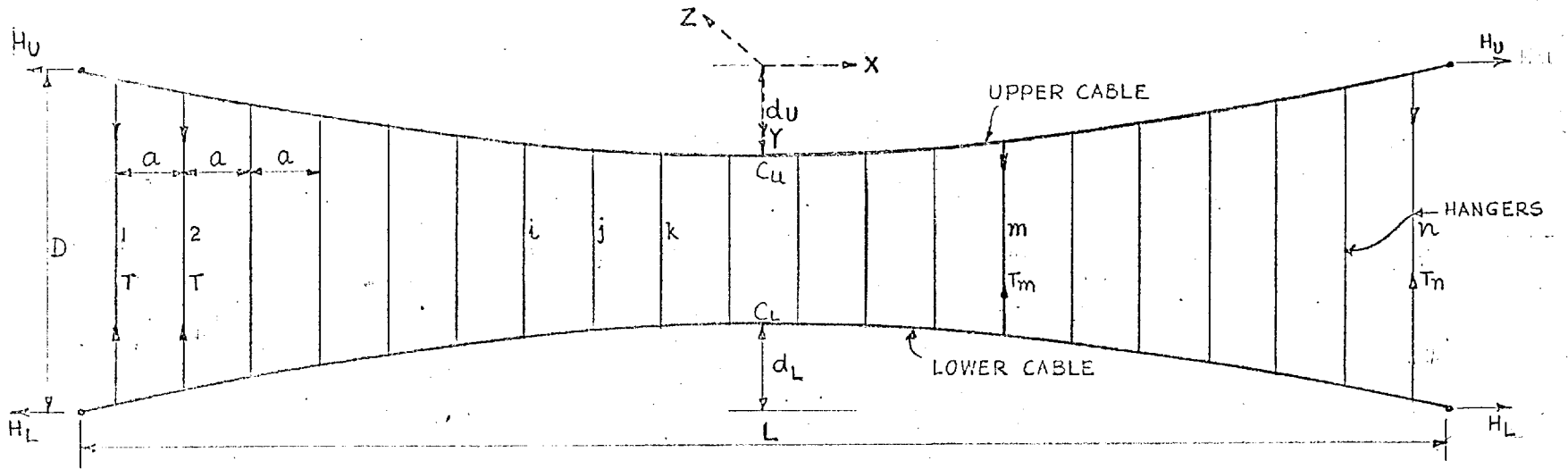
FIG. 11a : PLANE SYSTEM AT PRESTRESS
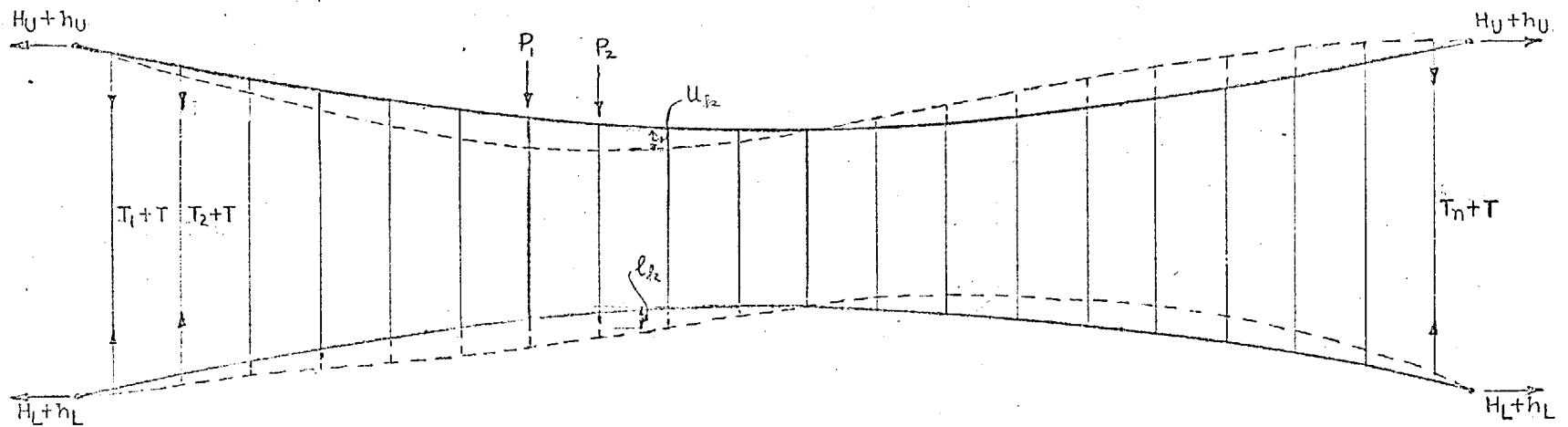
FIG. 11b. : LOADS APPLIED TO PLANE SYSTEM

The cables are anchored at level supports. The shape of each cable is parabolic and the structure is symmetrical about the y-axis. H_U and H_L are the horizontal components of tension in the upper and lower cable respectively.

Due to application of vertical loads P_1, P_2, etc. it is assumed that internal tensile reactions T_1, T_2, ..., T_n occur in the hangers and the values of H_U and H_L change by h_U and h_L respectively (see Figure 11b). The vertical deflection at any hanger k in terms of the applied loads and reactions can be written down as

$$u_k = T_1 u_{1k} + T_2 u_{2k} + ... + T_m u_{mk} ..... + T_n u_{nk} + u'_k \qquad (41a)$$

and $l_k = T_1 l_{1k} + T_2 l_{2k} + ... + T_m l_{mk} ..... + T_n l_{nk} + l'_k \qquad (41b)$

where u_k = the upper cable vertical deflection at k due to applied loads and reactions, measured positive downwards,

l_k = the lower cable vertical deflection at k due to applied loads and reactions, measured positive upwards,

u'_k = the upper cable deflection at k due to applied loads only, measured positive downwards,

l'_k = the lower cable deflection at k due to applied loads only, measured positive upwards,

u_{mk} = the upper cable deflection at k due to a unit load applied at m , measured positive downwards,

l_{mk} = the lower cable deflection at k due to a unit load applied at m , measured positive upwards.

Loads are positive when applied in the direction of positive deflections.

The extension in the hanger at k ,

$$\alpha_k = \frac{T_k \, L_k}{(AE)_h}$$

where L_k = length of the hanger at k

and $\dfrac{1}{(AE)_h}$ = the hanger extensibility, which is assumed uniform throughout.

For displacement - compatibility at k

$$u_k + 1_k = -\alpha_k \tag{42}$$

Equation (42) can be written on rearranging terms as

$$\sum_{m=n}^{m=i} T_m \left(u_{mk} + 1_{mk} \right) = -\alpha_k - u'_k - 1'_k \tag{43}$$

n simultaneous equations like (43) can now be set up and solved to give the unknowns, T_1 , T_2 , etc. Once these values are known, deflections of cables can be determined from equations (41a) and (41b), and forces h_U and h_L can be worked from equation (36).

Setting up equations (41a) and (41b) requires the knowledge of deflections of a sinlge cable under concentrated applied loads, so that u_{mk} , 1_{mk} , u'_k and $1'_k$ may be evaluated. This is possible with the help of equations (36), (40a) and (40b).

It is possible to consider the effect of

(1)   temperature change, and

(2)   slip at the anchorage

by a suitable modification of equation (35), and the values of α_k .

For a change in temperature of t^o , α_k becomes

$$= \frac{T_k \, L_k}{(AE)_h} + \omega t L_k$$

and the right hand side in equation (35) becomes

$$= S \, \frac{h \, L}{(AE)_c} + \omega t L \left(1 + \frac{8}{3} \frac{d^2}{L^2}\right)$$

where ω = the coefficient of linear expansion /degree of temperature change.

For a slip at the anchorage equal to, say, ε, the right hand side in equation (35) becomes

$$= S \, \frac{h \, L}{(AE)_c} + \varepsilon$$

α_k remaining unchanged.

1.21   Basic assumptions in the method

1.   The basic assumption that the law of superposition is applicable will now be studied. The relation between applied load and deflection for a cable is non-linear, because as the magnitude of the applied load increases, the cable gets relatively stiffer. The summation of the terms $T_m \, u_{mk}$ and $T_m \, l_{mk}$ and the evaluation of terms u'_k and l'_k (which may or may not involve summation depending upon the number of loads applied) is erroneous. The inaccuracy in the term

$T_m \, u_{mk}$ will, however, be small if the value of the unit load is kept fairly small. It has been found that the value of the unit load if taken as 0.01 of wL or less does not affect the results (Figure 28). This is reasonable as the relationship between deflection and loads for the cable does tend to be linear for small loads. However, it will not be correct to choose a small value of unit load if the actual values of T_1, T_2, etc. are going to be far bigger, and if, to avoid this error, a larger value of unit load is chosen, inaccuracy is inevitably introduced, because larger values are being superimposed. In order to evaluate u'_k and l'_k , summation will be necessary if several loads are applied; in such a case errors will again be introduced if loads are large. Therefore, the assumption, though justifiable if the loads and reactions remain small, introduces errors for larger loads.

2.   Horizontal movements have been neglected, assuming thereby, that the hangers remain vertical after loading and the force in the hangers has, therefore, no horizontal component. The assumption is justifiable because, although horizontal movements do occur, they are too small to incline the hangers appreciably.

3.   The dead weight of the structure is neglected in comparison to the prestressing forces. The assumption may not be quite correct for large spans. The necessary modification can be readily made by adding the dead weight to the prestress for the upper cable and subtracting it from the prestress for the lower cable.

4.   The structure is incapable of taking compression. This is justifiable as the buckling strength of the members is negligible in comparison to the tensile strength.

1.22 Solution of a plane system by the influence coefficient method

The following paragraph describes the use of the "influence coefficient" method to solve a plane system, shown in Figure 11a. A computer programme has been written to analyse the system for any general case of loading. Any of the parameters in the system can be varied except for the limitation that the structure should be symmetrical about the centre line of the span and have the two cables identical in geometry and size. The steps involved in the computation are

(1)   The left had side matrix in equation (43) is set up for a chosen value of the unit load.

(2)   The right hand side matrix in equation (43) is set up for any number of point loads applied anywhere on the structure. For setting up both these matrices equations (36), (38a) and (38b) are used.

(3)   On solving the matrices set up in steps (1) and (2) above we get the values of the unknowns T_1, T_2, etc.

(4)   Using equations (36), (38a), (38b), (41a) and (41b) the deflected shape and change in main cable forces are computed.

A flow diagram for the computer programme is given in Appendix "B".

The data used for the numerical problem solved is given below.

n = 20   L = 40 in.   a = 2 in. (the first hanger is at a distance a/2 from the left support)   D = 10 in.

$d_U = d_L$ = 2.5 in.

T = 1.25 lb. each, total vertical pretension   L = 25 lb.

Unit load = .01 of   L

Main wires diameter = .064 in.

Hangers wire diameter = .010 in.

$(AE)_c$ = 91000 lb., $(AE)_h$ = 2225 lb.

There is no change in temperature.

The various cases for which the structure is solved are enumerated here.

1. Concentrated applied vertical load equal to
   (a) 2.5 lb. at quarter point on top cable
   (b) 2.5 lb. at hanger no. 10 on top cable
   (c) 5.0 lb. at quarter point on top cable
   (d) 5.0 lb. applied to the top cable at hanger no. 10. In this case $T_{10} < - T$, which is inadmissible as the hangers cannot take compression. The solution is obtained by taking T_{10} as a known value equal to $- T$ while setting up and solving equations.

   Various results for 1(a) to 1(d) are given in Figures 12 to 18.

   It may be observed from these results that

   (i) Under a point load on the top cable there is a sharp decrease in tension in the hanger just below the load. All other hangers show an almost equal increase of tension, the average value of this increase is, say, λ .

   (ii) The value of λ increases and the deflections decrease non-linearly with the magnitude of applied load.

   (iii) There is comparatively little change in the lower cable tension, most of the load being carried by the upper cable.

   (iv) Only top cable deflections are plotted, as there is negligible difference between the deflections for the two cables.

(v)   In all the figures for changes in hanger tension, the
change per hanger is shown, and not the change per unit
length of span.

2.   Influence lines for h_U and h_L for a unit load of 2.5 lb. applied
to the top cable are given in Figure 19, and influence line for λ and values
of deflection under the load are given in Figure 20. The maximum
value of λ and the deflection occurs near the quarter point.

3.   Concentrated vertical loads at hanger nos. 2, 3, 4, 5, 6, 7, 8 and 9
equal to
(a)   0.5 lb. each on the upper cable;   p = 0.25 lb./in.
(b)   1.0 lb. each on the upper cable;   p = 0.50 lb./in.
(c)   1.5 lb. each on the upper cable;   p = 0.75 lb./in.
(d)   0.5 lb. each on the bottom cable;   p = 0.25 lb./in.
(e)   1.0 lb. each on the bottom cable;   p = 0.50 lb./in.

This loading is meant to represent a uniformly distributed
load p over part of the left half of the span and the various
results are given in Figures 21, 22 and 23.

The non-linearty of deflections and changes in hanger tension
with increase in the magnitude of load can be readily observed. Most
of the load is carried by the upper cable and the lower cable tension
starts increasing beyond a certain magnitude of load. The overall
stiffness of the system thus increases with applied load, just as in
a single cable. There is small difference in deflections for load on
the upper or the lower cable.

4.   Effect of reducing the number of hangers from 20 to 9 is shown by
results in Figures 24 and 25. It will be seen that the effect on
h_U , h_L and the deflections is negligible.

5. Figures 26 and 27 show the effect of distributing an applied point
load of 2.5 lb. at quarter point on the upper cable, over a length of
2 in. (exactly between hanger nos 5 and 6). Similar results are
obtained if an applied point load of 2.5 lb. at hanger no. 6 is
distributed over a length of 1 in. either side of the hanger.

6. Effect of neglecting hanger extensibility $1/(AE)_h$ is less than 2% .

7. If $1/(AE)_c$, the cable extensibility, is neglected, the value of
the reactions T_1 , T_2 , etc. increases manyfold making the results
valueless. This emphasizes the fact that much care is necessary
before neglecting any factors while evaluating the value of the
"influence coefficients".

8. Effect of varying the unit load on the values of λ and h_U and h_L
for a vertical load of 2.5 lb. applied at centre point on the upper
cable is shown in Figure 28.

1.23 Some important features in the influence coefficient method

1. This is a numerical method in which equations of displacement-
compatibility are set up at each hanger and solved to give the unknown
hanger forces, from which the structure can be solved completely.

2. The method requires the cables to be subject to a uniform prestress
and each cable lies on a continuous parabolic arc.

3. Expressions for evaluating the "influence coefficients" should be
as accurate as possible.

4. Value of the unit load does not affect the results to any appreciable
degree if taken as .01 or less, times the total vertical pretension.

5. The value of applied loads has to be kept small to ensure reasonable
accuracy, because the law of superposition is used to solve a
structure which is basically non-linear.

6. The method is in this case limited to solving the system for vertical loads only.

7. Effect of change in temperature and slip at the anchorage can be easily considered.

8. Loads can be applied anywhere on the cable and not necessarily at the nodes.

9. The method is straightforward from the point of view of computation. Coefficients are easily calculable. Use of digital computers has to be resorted to because of the number of simultaneous equations (n) to be solved and the accuracy required to solve them.

1.30 Application of a general method of solution to plane and three-dimensional structures

The basis of this method ("exact method" by Eras and Elze[10]) along with the equations in general has been given in Sections 1.04 and 1.05. The application of the method to the solution of plane and three-dimensional structures is now given.

1.31 Plane system

The plane system solved here has already been described in Section 1.20. The initial geometry of the structure is already known, the cables having a parabolic shape and the structure is to be solved for applied loads only.

It is aimed to solve the structure for in-plane vertical or horizontal loading only and as such it will have no movements out of the plane. The axes are shown dotted in Figure 11a.^{x} Therefore, 4n equations like equation (33) will have to be set up for n hangers, and solved simultaneously to give the values of u and v.

---

^{x} Page 32

The solution consists of the following steps.

1. Set up the matrix for the unknowns u and v from the left hand side of equation (33), say "A".

2. Assume the values of u and v (they are assumed to be zero in this case) to evaluate K_{xk} and K_{yk} in equation (33), and knowing X_k and Y_k , set up the right hand side matrix, say "B".

3. Now, if the unknown matrix is denoted by $\bar{U}$,

$$A \bar{U} = B$$

or $\qquad \bar{U} = A^{-1} B$

This gives the values of u and v . It will be noted that the "A" matrix will be the same for the same structure, and so the matrix inversion has to be done only once. This is very beneficial from the point of view of computation, as the multiplication of the inverted matrix A^{-1} and B is much less time consuming than the inversion itself.

4. From the values of $u^{(1)}$ and $v^{(1)}$ thus obtained, evaluate the "B" matrix again and multiplying by A^{-1} get the values of $u^{(2)}$ and $v^{(2)}$ etc.

The next cycle of iteration can be carried out in two ways.

5. (a) Use the values of $u^{(2)}$ and $v^{(2)}$ to compute the next value of the "B" matrix, or

   (b) Put $u^{(2)} = 0.5 u^{(2)} + 0.5 u^{(1)}$

   and $v^{(2)} = 0.5 v^{(2)} + 0.5 v^{(1)}$

and use the new values of $u^{(2)}$ and $v^{(2)}$ to evaluate the "B" matrix and get the values of $u^{(3)}$ and $v^{(3)}$ and so on. Table 2 (page 54) shows the more rapid convergence obtained by using the step 5(b).

6. The value of ΔF_o can now be evaluated by using equations (31a) or (31b).

Steps (5) and (6) can be repeated as many times as necessary for the accuracy desired.

It will be noted that equations are not set up for u and v at the support since they are considered as knowns. The values are, however, used in evaluating the "B" matrix. For a rigid support these values are zero and a movement at the support can be readily considered by assigning the proper values to u and v at the support.

Consideration of changes in temperature involves the alteration of equations (29),(30a), (30b), (32) and (33) as given below.

Equation (29) becomes

$$1 = l_0 \cdot \left(1 + 2e_1 + e_2\right)^{1/2} + \frac{l_0}{1 + \frac{F_0}{EA}} \cdot \omega t$$

or
$$1 = l_0 \cdot \left\{ \left(1 + 2e_1 + e_2\right)^{1/2} + C \right\} \tag{44}$$

where $C = \frac{EA}{EA + F_0} \cdot \omega t$ and $C.l_0 =$ the change in length due to rise in temperature of t^o.

Equation (30a) becomes

$$1 = l_0 \cdot \left\{ \left(1 + C\right) + e_1 + \frac{1}{2} e_2 - \frac{1}{2} e_1^2 - \frac{1}{2} e_1 \cdot e_2 + \frac{1}{2} e_1^3 \right\} \tag{45a}$$

and equation (30b) can be written as

$$\frac{1}{1} = \frac{1}{l_0} \cdot \left[(1+c)^{-1} - (e_1 + \frac{1}{2} e_2 - \frac{1}{2} e_1^2 - \frac{1}{2} e_1 \cdot e_2 + \frac{1}{2} e_1^3) \cdot (1+c)^{-2} + (e_1 + \frac{1}{2} e_2 - \frac{1}{2} e_1^2 \right.$$

$$\left. - \frac{1}{2} e_1 \cdot e_2 + \frac{1}{2} e_1^3)^2 \cdot (1+c)^{-3} - (e_1 + \frac{1}{2} e_2 - \frac{1}{2} e_1^2 - \frac{1}{2} e_1 \cdot e_2 + \frac{1}{2} e_1^3)^3 \cdot (1+c)^{-4} + \cdots \right\}$$

neglecting 4th or higher order terms, we get,

$$\frac{1}{1} = \frac{1}{l_0 (1+c)} \cdot \left\{ 1 - \frac{1}{1+c} \cdot (e_1 + \frac{1}{2} e_2 - \frac{1}{2} e_1^2 - \frac{1}{2} e_1 \cdot e_2 + \frac{1}{2} e_1^3) \right.$$

$$\left. + \frac{1}{(1+c)^2} \cdot (e_1^2 + e_1 \cdot e_2 - e_1^3) - \frac{1}{(1+c)^3} \cdot e_1^3 \right\} \qquad (45b)$$

Using equation (45b) and (31b) in equation (26), and on neglecting 4th or higher power terms, we get instead of equation (33)

$$\frac{F_0}{l_0 (1+c)} \cdot \Delta u + \frac{EA}{l_0 (1+c)} \cdot \Delta x \cdot e_1 - \frac{F_0}{l_0} \frac{\Delta x \cdot e_1}{(1+c)^2} = X_k - K x_k \qquad (46)$$

where

$$K x_k = \frac{EA}{l_0 (1+c)} \cdot \Delta u \cdot e_1 - \frac{F_0}{l_0 (1+c)^2} \cdot \Delta u \cdot e_1 + \left\{ \frac{EA}{l_0} \cdot \frac{\Delta x + \Delta u}{1+c} \right. -$$

$$\left. \frac{F_0}{l_0} \cdot \frac{\Delta x + \Delta u}{(1+c)^2} \right\} \cdot \left\{ (\frac{1}{2} e_2 - \frac{1}{2} e_1^2 - \frac{1}{2} e_1 \cdot e_2 + \frac{1}{2} e_1^3) - \right.$$

$$\left. \frac{1}{(1+c)} \cdot (e_1^2 + e_1 \cdot e_2 - e_1^3) + \frac{1}{(1+c)^2} \cdot e_1^3 \right\}$$

If we put $C = 0$ in equation (46), the original equation (33) will be obtained.

The procedure of studying the effect of changes in temperature and the support movements as described above, is applicable to three-dimensional structures as well as plane systems.

1.32 Numerical examples and results for plane system

The amount of computation involved in applying the general method described in the preceding article to a numerical example becomes considerable if the number of nodes n is large. A computer programme has been written to solve any case of loading applied to a plane structure of general dimensions, symmetrical about the y-axis. The programme forms the matrix A (sec. 1.31) for a structure and evaluates A^{-1}. The B matrix (sec. 1.31) is then formed and multiplied by A^{-1} to give the deflection values. This can be done for any number of cycles as necessary and for any number of loading cases without disturbing the values of A^{-1}, so that the evaluation of A and A^{-1} is to be done only once. Values of deflections and ΔF_o (calculated from step (6) of section 1.31) are printed for each cycle of iteration. A flow diagram for the programme is given in Appendix B. The numerical examples solved are given below.

Example 1. This has been solved to show the difference in using steps 5(a) and 5(b) for successive iteration in the preceding section.

Data: n = 5   L = 30 in.   a = 5 in. $d_U = d_L$ = 3 in.   T = 5 lb.

Applied vertical load = 2.5 lb. ($\frac{1}{10}$ of pretension) at hanger No. 3 on upper cable.

It will be seen from Table 2[x] that results obtained in the 5th cycle by using step 5(b) are nearly the same as those obtained in the 9th cycle by using step 5(a). A study of the values of u and v shows a steady and decreasing change in their values if step 5(b) is used but the values keep oscillating if step 5(a) is used. It will be seen that 5 - 6 cycles will give sufficiently accurate results for this magnitude of load. Step 5(b) has been used in solving all other examples.

---

x Page 54

Example 2. This has been solved to compare the convergence of the method for various intensities of load.

Data: n = 9   L = 40 in. $d_U = d_L = 2.5$ in.   a = 4 in.   T = 2.4 lb.

Load is applied at hanger no. 5 on upper cable.

Table 3[x] shows the value of vertical deflection under the load and ΔF_o value for the top cable segment adjacent to the loaded hanger. It will be seen that at the end of six cycles, fair results are obtained for up to a load of 7.5 lb. (nearly 0.4 of the total pretension). For a load of 12.5 lb. (nearly 0.6 of the total pretension) several more cycles will be needed before the final results are obtained. For a load equal to the total pretension the results show a definite and drastic divergence.

Example 3. The data used for this example is the same as for the structure already solved in section 1.22. The various cases of loading solved are enumerated below.

1. Concentrated vertical load equal to

    (a)   2.5 lb. at quarter point on upper cable [+]
    (b)   5.0 lb. at quarter point on upper cable [+]
    (c)   2.5 lb. at hanger No. 10 on upper cable
    (d)   5.0 lb. at hanger No. 10 on upper cable

Deflections and change in forces ΔF_o in various members are shown in Figures 12 - 18. ΔF_o for the main cables shows a

---

[+] It is not possible for the load to be placed at the quarter point as in this example the quarter point lies between hangers No.5 and 6. These results are therefore obtained by taking a mean of results for load applied at hangers No. 5 and 6.

[x] Page 55.

variation from segment to segment but since the variation is slight a mean value has been taken. This has been done for all the other cases too, unless otherwise mentioned.

2. Influence lines for h_U, l_L, λ and values of deflection under the load for a concentrated load of 2.5 lb. applied on the top cable are given in Figures 19 and 20.

3. Concentrated vertical loads at hangers No. 2, 3, 4, 5, 6, 7, 8 and 9 equal to

   (a)   0.5 lb. each on upper cable
   (b)   1.0 lb. each on upper cable
   (c)   1.5 lb. each on upper cable
   (d)   0.5 lb. each on lower cable
   (e)   1.0 lb. each on lower cable

   Various results are given in Figures 21, 22 and 23.

4. Concentrated horizontal load equal to 2.5 lb. applied at hanger No. 10 on upper cable for which results are shown in Figures 29 and 30.

5. Concentrated vertical load equal to

   (a)   2.5 lb. applied at centre point on lower cable
   (b)   5.0 lb. applied at centre point on lower cable

   Values of ΔF_o are shown in Figure 31. There is an increase of tension in all the hangers. Values of deflection are not plotted as there is no appreciable difference in deflection values whether the upper or the lower cable is loaded.

6. Concentrated vertical loads at hanger No. 6, 7, 8, 9, 10, 11, 12, 13, 14 and 15 of 1.0 lb. each on the upper cable. The results are shown in Figures 32 and 33.

7. For an approximate analysis the hangers may be grouped together to

reduce the number of equations. Values of ΔF_o for the cables and the vertical deflections under a point load of 2.5 lb. at centre point on the top cable have been compared if the number of hangers is reduced from 20 to 9 to 5. The hanger stiffness is changed accordingly from AE to $\frac{20}{9}$ AE to $\frac{20}{5}$ AE. Results in Figures 34 and 35 show the very little effect of the variation.

8. Effect of varying the hanger stiffness value has also been found to be very small. Comparison was made by using AE = 2225 lb. and AE = 8900 lb. in the 5 hanger case in (5) above. The difference in forces is under 2% and deflections under 1%.

1.33 Application to a three-dimensional system

This section describes how the method can be applied to a structure consisting of three cables prestressed together. The structure shown in Figure 36[x] is a special case of a general structure. Two of the three cables are sagging, completely similar and placed symmetrically in the structure; the third cable is hogging and placed below and centrally between the two top cables. The three cables are anchored at rigid and level supports and are prestressed by means of several sets of hangers which lie in parallel vertical planes at right angles to the x-axis. The horizontal hangers have an initial tension T_o each and the inclined hangers have an initial tension T_1 and T_2 each, respectively as shown in Figure 36. The value of the horizontal and vertical dip at the centre of each cable is specified as C_1, D_1, etc. The initial geometry of the structure under the specified boundary conditions is not known and its determination will consist of the following steps.

1. The forces in the cables are not known and have to be assumed (see footnote on p. 17). The forces can be assumed by considerations of

---

x Page 49

HANGER no. 1

HANGER no. 0

CABLE 1

T_0

T_1

T_2

A

B

C

A'

B'

CABLE 2

HANGER no. 2

C'

CABLE 3

ELEVATION

Z

$\mathcal{C}$

X

Y

A,B

A',B'

SECTION 1

2

3

4

n

T_1, T_2

T_1, T_2

a

a

a

D

C

C'

L

SIDE - ELEVATION

$\mathcal{C}$

C_0

CABLE 1

CABLE 2

T_0

D_1

T_0

D_2

C_1

C_2

T_1

T_1

T_2

T_2

CABLE 3

D_3 ; $C_3 = 0$

$\mathcal{C}$

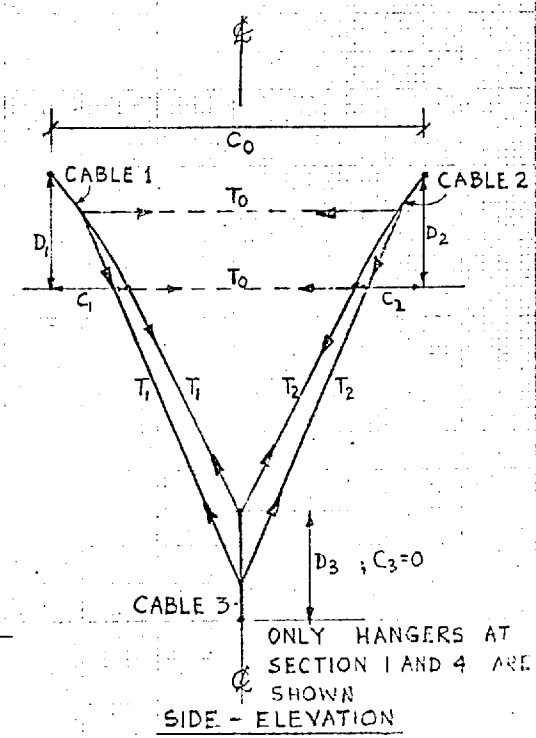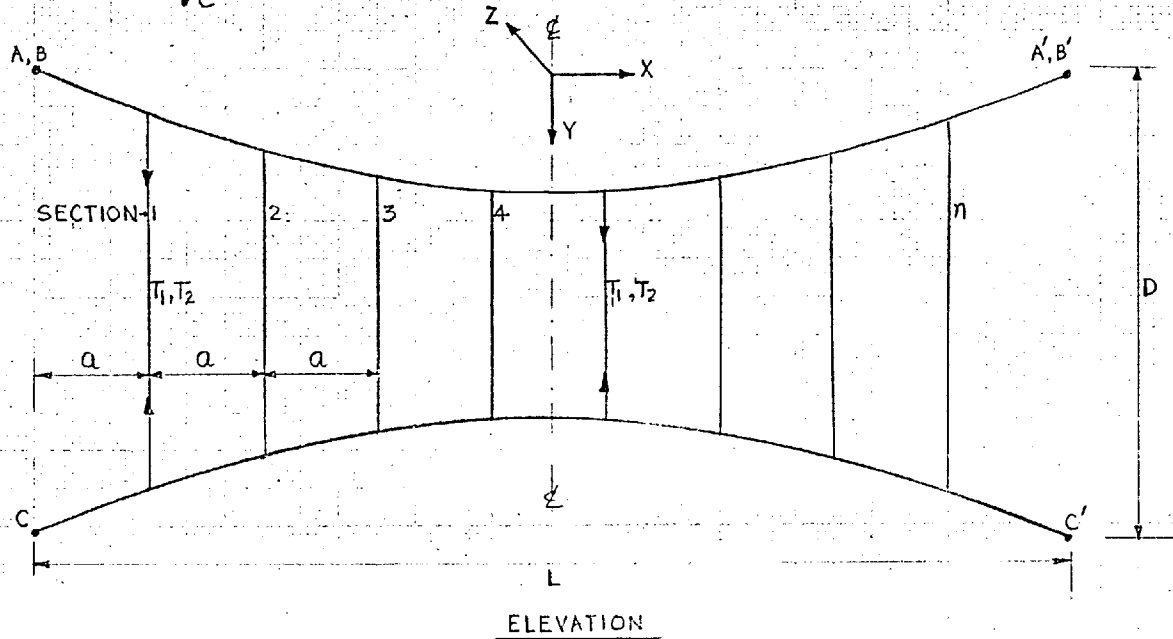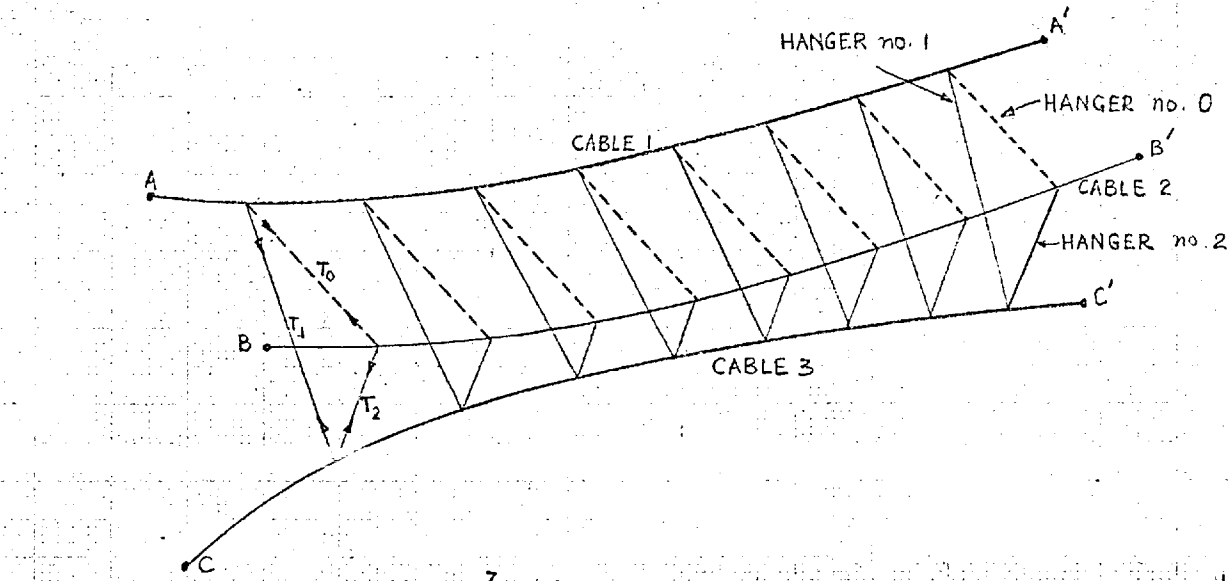ONLY HANGERS AT
SECTION 1 AND 4 ARE
SHOWN

FIG. 36 THREE - CABLE SYSTEM

simple statics if the inclination of the hangers is known, for which the geometry must be known. In order to establish an approximate initial geometry, it is assumed that the horizontal and vertical ordinates of each cable lie on parabolii with their dips equal to C_1 , C_2 , C_3 and D_1 , D_2 , D_3 respectively. The cable forces are then calculable.

2. For the assumed set of forces equations (25a) and (25b) are set up for each point and solved simultaneously to give the correction terms $v^{\prime(1)}$ and $w^{\prime(1)}$. (Position of hangers along the x-axis is fixed and hence the values of x are known in this problem.)

3. The assumed values of y and z are now corrected as

$$y^{(2)} = y^{(1)} + v^{\prime(1)}$$

$$\text{and} \quad z^{(2)} = z^{(1)} + w^{\prime(1)}$$

Steps (2) and (3) are repeated, say ν times, until $y^{(\nu)}$ and $z^{(\nu)}$ are very close to $y^{(\nu-1)}$ and $z^{(\nu-1)}$ respectively.

4. With this change in the geometry the inclination of the hangers has also changed and the forces are calculated again.

5. Steps (2) and (3) are repeated again for the new set of forces.

Steps (4) and (5) are repeated until the forces and ordinates obtained from subsequent cycles are close enough.

The method is rapidly convergent, which can be seen from the numerical example given here.

A computer programme has been written to use the procedure described above to solve numerical examples on a general three-cable structure symmetrical about the y-axis. The programme is extended further to solve the structure for applied loads. A flow diagram for the complete programme is given in Appendix B.

Example 1. A small number of hangers has been deliverately chosen because the initial shape will be farther from parabolic with a smaller number than with a larger number of hangers. The data is

C_o = 20 in.   D = 30 in.   L = 60 in.   a = 20 in.

number of set of hangers   n = 2

C_1 = C_2 = 2 in. C_3 = 0

D_1 = D_2 = D_3 = 5 in.

T_c = 0 T_1 = T_2 = 5 lb.

Cables AA' and BB' are symmetrically placed.

Table 4^x shows the values of the forces in the end segment of cables AA' and CC' and y and z ordinates at the first hanger section in AA' and CC' , for the subsequent cycles of iteration. It will be seen that the cycle of operations shown below will be sufficient.

2 to 3 times

Step (1) ⟶ Step (2) ⟶ Step (3) ⟶ Step (4) ⟶ Step (5)

2 to 3 times
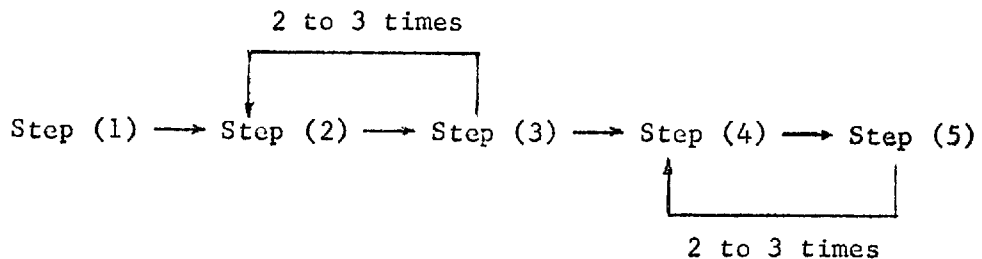
Note: Step (5) is equivalent to steps (2) and (3).

The unstretched length of each member can be calculated from the knowledge of the structure thus obtained and it can now be solved for applied loads.

The method of solving the three-cable structure for applied loads is exactly the same as for the plane-system except for the following differences:

(i) Equations have to be set up for deflections u, v, and w for loading along either of the three axes.

(ii) The total number of equations for n hanger sections is $9n$.

Data used for the numerical problem solved is,

$n = 9$ $1 = 40$ in. $a = 4$ in. $C = .025$ in. $D = 10$ in.

$C_1 = C_2 = .01$ in. $C_3 = 0$

$D_1 = D_2 = D_3 = 2.5$ in.

$T = 1.20$ lb.

EA for top cables $= 45000$ lb.   EA for bottom cable $= 90000$ lb.
EA for inclined hangers $= 2225$ lb.   EA for horizontal hangers $= 0$
Load $= 1.25$ lb. applied to each of the top cables at the centre point.

This structure can be approximated to the plane system solved in example 2 (section 1.32). The top cable and each hanger have been replaced by two cables and two hangers of half the area respectively. The top cables are placed a small distance of .025 in. apart and have a small horizontal dip of .01 in. each, thus converting the plane system into a three cable one. The two systems are, however, so close to each other that the deflections obtained for the same magnitude of applied load to the two systems should be comparable. If the ΔF_o values for the two cables and each pair of inclined hangers are added these should also be comparable to the ΔF_o values for the plane system. Table 5[x] shows the results for the two structures. The values of ΔF_o in one of the upper cables and each one of the two inclined hangers are doubled instead of summed, since the system is symmetrical.

1.34 Some important features of the general method of solution

Some of the main points of the method are enumerated below:

1. Equations of force-compatibility are set up at each node and solved simultaneously to give the value of displacements.

2. The structure consists of straight weightless links between the nodes.

3. The computational work involved with this method is considerable. The number of equations required for each node are 3 and the coefficients are more cumbersome to evaluate. The use of digital computers has to be resorted to. The number of equations can be cut down, however, for preliminary work by reducing the number of hangers.

4. Loads can be applied at the nodes only.

5. The effect of the movement of the support can be studied and the effect of temperature change can be considered by modifying the original equations.

6. The method is very general and can be applied to plane or three-dimensional prestressed structures and can give solutions for an kind of static loading.

7. For applied point loads of up to 0.3 times the total pretension, fair results can be obtained from 6 cycles of iteration; a load of 0.6 times the total pretension needs more cycles than 6, but for higher loads of say equal to the total pretension the method shows drastic divergence.

TABLE 2

Cycle No.	u in the upper cable at hanger no. 2 ins. x 10^6		v in the upper cable at hanger no. 3 ins. x 10^6		$\triangle F_0$ in upper cable in the segment between hangers no. 2 and 3 lbs.		$\triangle F_0$ in hanger no. 1 lbs.		$\triangle F_0$ in hanger no. 3 lbs.	
Step No.	5(a)	5(b)	5(a)	5(b)	5(a)	5(b)	5(a)	5(b)	5(a)	5(b)
1	4042	4042	59176	59176	-	-	-	-	-	-
2	3554	3554	49494	49494	-	6.142822	-	.171043	-	-1.00553
3	4217	3925	58145	54303	6.612061	5.369873	.210854	.207634	-.944740	- .951332
4	3889	3993	53226	55029	-	5.063721	-	.226311	-	- .924797
5	4170	4023	57073	55280	-	4.896729	-	.237282	-	- .909981
6	3992	4040	54516	55411	-	4.791748	-	.244087	-	- .901237
7	4126	4052	56401	55494	-	4.724854	-	.248436	-	- .895851
8	4034	4059	55093	55545	-	4.680420	-	.251244	-	- .892448
9	4102	4064	56037	55580	4.825928	4.650635	.252312	.253105	-.891792	- .890312

TABLE 3

Cycle No.	2.5 lb. v_r ins. $\times 10^6$	2.5 lb. ΔF_o lb.	5.0 lb. v_r ins. $\times 10^6$	5.0 lb. ΔF_o lb.	7.5 lb. v_r ins. $\times 10^6$	7.5 lb. ΔF_o lb.	12.5 lb. v_r ins. $\times 10^6$	12.5 lb. ΔF_o lb.	22.5 lb.
1	68400	-	136800	-	205200	--	342000	-	
2	62829	6.893	93370	13.126	59905	5.174	-325912	-5.956	Results for this load show a definite and rapid divergence.
3	65046	6.130	123714	15.372	196791	29.956	287008	-8.957	
4	65623	5.827	120870	14.537	159196	23.104	319699	64.484	
5	65837	5.675	121725	14.172	170437	25.106	202010	30.816	
6	65936	5.588	122015	13.890	165902	23.172	273587	62.545	

v_r is the upper cable vertical deflection under the load

ΔF_o is the change in the upper cable tension between hangers no. 4 and 5

TABLE 4

Step and cycle no.	Force in AA' end segment lb.	Force in CC' end segment lb.	Y-Ordinate in AA' ins.	Z-Ordinate in AA' ins.	Z-Ordinate in CC' ins.	Remarks
1	19.29549	38.41994	-8.22222	4.44444	25.55556	
2 and 3 $\nu = 1$	"	"	-8.01246	4.97808	25.02224	
2 and 3 $\nu = 2$	"	"	-8.00845	4.98257	25.01852	
2 and 3 $\nu = 3$	"	"	-8.00845	4.98257	25.01852	not necessary
4	19.23273	38.28598	-8.00845	4.98257	25.01852	
5 $\nu = 1$	"	"	-8.00025	4.99950	25.00053	
5 $\nu = 2$	"	"	-8.00024	4.99950	25.00053	not necessary
4	19.23095	38.28219	-8.00024	4.99950	25.00053	
5 $\nu = 1$	"	"	-8.00001	4.99999	25.00001	
5 $\nu = 2$	"	"	-8.00001	4.99999	25.00001	not necessary

TABLE 5

Hanger No.	THREE CABLE SYSTEM			PLANE SYSTEM		
	u for one of the top cables ins. x 10^6	v for one of the top cables ins. x 10^6	$2 \times \Delta F_o$ for one of the inclined hangers lbs.	u for top cable ins x 10^6	v for top cable ins x 10^6	ΔF_o for hangers lbs.
1	3674	-15363	.05967	3825	-16031	.06717
2	4212	-17047	.06026	4391	-17853	.06778
3	2879	- 4624	.06032	3010	- 5027	.06785
4	1017	22144	.05240	1072	22730	.06043
5	0	63737	-1.08898	0	65936	-1.07619
6	-1017	22144	.05240	-1072	22730	.06043
7	-2879	- 4624	.06032	-3010	- 5027	.06785
8	-4212	-17047	.06026	-4391	-17853	.06778
9	-3674	-15363	.05967	-3825	-16031	.06707

$2 \Delta F_o$ for one of the top cables in the three cable system = 5.313682 lb.

ΔF_o for the top cable in the plane system = 5.454204 lb.

ΔF_o for the bottom cable in the three cable system = 2.174884 lb.

ΔF_o for the bottom cable in the plane system = 2.044376 lb.

CHAPTER 2

EXPERIMENTS

2.01 Experiments on single wires

Experiments on three wires of different dimensions and
span, suspended between rigid supports, under their own weight
(including the initial uniformly distributed superimposed weight
over the whole span) are described in Sections 2.02 and 2.03.
All three wires were tested under applied vertical concentrated loads
placed successively at various points along the span. The
main purpose of these tests was the verification of theoretical
values obtained in Chapter 1.

2.02 Experiment on a wire of .032" diameter

The wire* was suspended between two rigid towers under its
own weight and the dead weight of the uniformly spaced steel
blocks fixed to the wire. Details about the wire are given below.

The wire was drawn from high tensile steel.
Span, $l = 33$ ft.,   Central-dip, $d = 3$ ft.
Spacing of steel blocks 4.5",
Dead weight of the wire and blocks $w = 0.85$ lb/ft span,
Total dead weight 28.15 lb.
Weight of the hanger used for loading $= 0.156$ lb.

---

* The wire was part of a one hundredth full size model of the cables
and towers of the Forth Road Bridge, set up for a study of its
vibration characteristics.

The span was divided into ten equal segments by means of nine equally spaced stations, and both vertical and horizontal deflections were measured at each station, for concentrated loads of varying magnitude, applied successively at station nos. 1, 2, 3, 4, and 5. The value of applied load P (including the weight of the hanger) varied from 2.156 lb. to 5.156 lb., with increments of 1 lb., i.e. $\bar{w}$ varied from 0.0765 to 0.1835.

A typical set of curves for vertical and horizontal deflections are given in Figures 37 and 38. The figures show values of deflection for load applied at station no. 2. Theoretical values of vertical deflections for $\bar{w}$ equal to .0765 and .1835 are also given in Figure 37. It will be noted that agreement between theoretical and experimental values under the loaded point is good but the differences become considerable away from the loaded point. Figure 39 gives the vertical and horizontal deflections at the loaded point, for the two extreme values of point load. Horizontal deflection to the right and vertical deflection downwards is taken as positive. The relation between $\bar{w}$ and the deflections will be seen to be non-linear. It will also be observed that the maximum values of deflection under the load occur near the quarter points of the span.

2.03 Experiments on .064" and .0164" diameter wires

The knowledge of a single cable behaviour has been used in obtaining theoretical results for a plane system (see 1.20) and it is desired to check these against experimental values. It was, therefore, thought necessary to check the single cable theory against experimental results obtained from the same size

of wire (.064" diameter) as used in the experimental model of a plane system. Another reason for doing these experiments was that, although the values from the tests on the .032" diameter wire showed good agreement with the theory under the loaded point the discrepancy was rather large away from this point. A study of the results obtained for the .064" diameter wire led to the experiment on the thinner wire.

The set-up for both the wires is shown in Figure 40. Figure 41 shows the .064" diameter wire loaded at the quarter point. Both wires were set up in the manner described below.

(i)   The wire was clamped at one end on a rigidly fixed support.

(ii)   The other end was stretched over a pulley with a load equal to the desired horizontal component of wire tension.

(iii)   Vertical loads were then applied to the wire by means of uniformly spaced hangers over the whole span.

(iv)   The wire was then clamped at the pulley end and the pulley removed.

Data for the .064" diameter wire and results

Span 40".

Central sag (measured from a horizontal wire stretched between the supports) 2.52".

Spacing of hangers, each carrying 1.25 lb., 2".

Average uniformly distributed weight w = .625 lb/in.

Horizontal component of wire tension (computed) = 50 lb.

Horizontal component of wire tension (measured) = 49.8 lb.

Measurements were taken at an average temperature = $70^\circ \pm 1.5^\circ$ F.

The wire was intercepted by two load cells each 1/2" away from

the central hanger. The load cells were calibrated by direct loading
and then used for measuring forces. (The load cells are described
in detail later in Section 2.13).

1/8" diameter nylon balls were cemented on the wire at each hanger
position and measurements for vertical and horizontal movements for
applied loads were taken by sighting these balls through a cathetometer.

Figure 42 shows the vertical deflections for values of P equal to
2.54 lb., 5.04 lb., and 7.54 lb., applied vertically at centre and
quarter points respectively. Figure 44 shows the horizontal deflections
for the same applied loads *. The results for the change in wire
tension (mean value from the two load cells) are given below.

$\bar{w}$	Change in tension for load at centre point (lbs)	Change in tension for load at quarter point (lbs)
0.1	5.50	7.57
0.2	11.15	15.00
0.3	16.94	22.65

It will be observed in Figure 42 that the experimental deflection

* The horizontal deflections have been calculated by using equations
40a and 40b which are derived from equations given by Pugsley
(Section 1.02).

curves do not have a sharp discontinuity under the load point but have a smooth cusp instead. This is contrary to the results obtained from the tests on the .032" diameter wire ($_{Sec.}$2.02) and it appears that the .064" diameter wire suspended over 40" span has some bending stiffness. It was decided to confirm this by testing a .0164" wire, whose moment of inertia is approximately 230 times smaller than the thicker wire.

Data for the .0164" diameter wire and results

Span, L = 40".
Measured central sag 2.48".
Spacing of hangers, each carrying 0.1 lb., 2".
Average uniformly distributed weight, w = 0.05 lb/in.
Total weight of the wire 2 lb.
Horizontal component of tension (computed) 4 lb.

The results obtained for applied load P equal to 0.2 lb. and 0.4 lb. ($\bar{w}$ = 0.1 and 0.2 respectively) are shown in Figures 43 and 44. It will be observed that the curves for experimental vertical deflections show a very sharp cusp under the loaded point, unlike a smooth cusp for the .064" diameter wire, which can now be justifiably attributed to the bending stiffness.

Correlation between theoretical and experimental results is discussed in Chapter 1.

2.10   Experiments on the model of a plane system

Sections 2.11, 2.12, 2.13, 2.14 and 2.15 describe the experiments carried out on a structural model of a plane prestressed system. The main purpose of the experiment was the verification of the theories, applied to solve a plane system in Chapter 1, and to get a better physical appreciation of the practical problems involved. The experiment was just a fundamental study and the model did not represent any full scale structure. The model consisted of two main wires, anchored firmly at their ends, within a rigid frame, and prestressed by means of uniformly spaced vertical wires. The wires used were of stainless steel.

The letters used to mark the photographs (Figures 47, 48, 49, 51 and 52) are applicable only in the section of the text where the particular part of the experimental set-up is described and have no connection with the general notation being used in the thesis.

2.11   A note on the size of the model and the material used

The choice of the size of the model, wires and the material used was governed by the following factors.

(1)   It was required to have rigid supports for the two main wires. Whereas massive supports would have been needed for a large size model, a welded frame, made out of 3" x 1-1/2" channel sections (welded together to form a 3" x 3" box section) was sufficient to provide a rigid self-contained support.

(2)   In terms of sheer labour involved it is much easier to deal with a small size model than with a bigger one.

(3)   In order to get any real advantages of a bigger model (even disregarding some problems created by its size) it was thought that a

50 ft. to 60 ft. long model would be required. It might have been possible to get a more accurate model and also better measurements on a bigger scale. This size was not easily possible because of limitations of space and facilities at the time the experiment was planned.

(4) It is necessary for this kind of experiment to have reasonable temperature control. Considerable difficulty was experienced in obtaining proper temperature conditions for the model tested. It was found that small changes in temperature and drafts of wind affected the results appreciably, until finally the model was moved into a small room with strict temperature control. Similar control on a bigger size model would be extremely difficult.

(5) Normally roof structures of this kind have a dip to span ratio of 1/15 to 1/20. Main wires in this model have a dip to span ratio of 1/16 and their spacing was governed by the method of measurement of forces in the hangers.

(6) It was decided to join the wires at their junctions by means of fusion-welding, as it was preferred to mechanical joints from the point of view of slip. Also, on this scale mechanical joints would have been difficult to make and too big.

(7) Stainless steel wires were chosen for the model with a particular consideration of their welding properties. Although wires of magnetic stainless steel would have been preferable from the point of view of measuring forces in the hangers, they had to be rejected because of the brittle welded joints obtained from them.

(8) Once the size of the model was decided upon it governed the size of the wires. The smallest possible size of the wires was chosen. The .010" diameter wire used for the hangers was about the smallest practicable size that could be used. Each hanger was to carry an initial tension of 1.25 lb. (stress = 7.12 t.s.i.). The main wire

size was .064" diameter, and initial maximum tension in either wire
was expected to be 51.5 lb. (stress = 7.15 t.s.i.).

2.12   General description of the model and the procedure used for its assembly

The erection of the model consisted of the steps described in
this section.

(1)   The frame, made by welding 3" x 3" box sections, and having inside
dimensions 41" x 24", was placed on level supports. The frame had two
1/4" diameter holes spaced at 10" centres vertically in each of its
short sides. Four anchor blocks 1-1/2" x 1-1/2" x 1/2" were screwed
to the frame, with their anchoring surfaces level with the centre of
each hole. The frame also had a 2" x 1/2" flat bar fixed to it at
the top and carried hooks above each hanger position.

(2)   The top wire, with load cells in the right position, was anchored
at one end and loaded over a pulley at the other to calibrate the load
cells. (For details see 2.13).

(3)   The wire was then stretched over a template to give it the correct
profile. The template consisted of 3/8" diameter copper tubes,
screwed vertical on to a 1" thick wooden board. The tubes were
uniformly spaced and placed such that a tangent to the outside surface
of the tubes would be a parabolic curve with a central sag of 2.5".

In order to provide more welding surface and a more uniform heat
of fusion small stubs of stainless steel approximately .025" thick
were welded to the wire at hanger points.

(4) The wire was loaded over a pulley with a weight of 50 lb. (the desired value of H_u). Hangers were suspended from the hooks in the top bar and loaded with 1.25 lb. each; alternate hangers were placed on opposite sides of the wire, in order to reduce overall torsion. It was confirmed that the torsion caused had little effect on the results.   The hangers were welded to the stubs on the main wire and the template pulley removed. A check on the load cell readings showed negligible change when the wire was clamped and the pulley removed.

(5) Mild steel wire of .004" diameter was now coiled round and affixed at its ends to the hangers, over a length of about half an inch, to make the hanger magnetic locally, so that it could be excited magnetically and the force measured acoustically. The mild steel coil was so positioned that it would be central in each hanger when the structure was fully assembled. The hangers were then calibrated for 'Frequency of vibration against tension' by direct loading. (For details see Section 2.13).   The hangers were then unloaded.

(6) Steps (2) and (3) were then repeated for the lower wire and it was loaded with 50 lb. over the pulley. An extra set of hangers loaded with 1.25 lb. each was now suspended from springs, which were fixed to the hooks on top. The hangers were welded to the lower main wire on the side opposite to the first set of hangers and slightly away from the stubs. The load on the hangers and the template was then removed and the wire was just spring loaded. Loads of 1.25 lb. each were replaced on the original set of hangers. Figures 45 and 46 show the two wires loaded with loads and springs respectively and by means of separate sets of hangers.

The idea of using springs was that, if the profile of the template was slightly wrong, the geometry of the wire would be corrected by a readjustment in the large extension of the springs (1.5" average extension for 1.25 lb. load). Measurements showed small readjustments, all within .01".

(7) The original set of hangers, loading the upper wire, were then welded to the lower wire springs, loads and extra set of hangers were removed. Measurement on load cells still showed only very small changes.

(8) The pulley end of the lower wire was clamped and the pulley was removed. Figure 47 shows the completed model. The numbers on top of the frame refer to the hangers.

Welding

It is important to note that if the wires were welded, with the thinner wire under tension, it was broken due to the high heat of fusion. Therefore, the wires were first held in position between the tongs of the welding tweezer head, the load was removed from the thin wires and the fusion was affected. The load was then replaced on the hanger.

2.13   Methods for measurement

The choice of suitable devices of measuring forces in the model was governed by the following requirements.

(1)   It was important to know the absolute pretension in the structure and to keep a record of any variations in it. It was therefore necessary that the measuring instrument would not show a drift in reading unless the pretension itself changed.

(2)   The measuring device should not affect the stiffness properties of the elements of the structure.

The use of thin single wire electrical strain gauges, directly cemented to the wire, was first envisaged but rejected due to the above-mentioned reasons.

Optical and mechanical methods of measuring strain in the hangers were thought of and rejected for want of too much precision and elaboration. The methods of measurement finally decided upon and used are described in the following paragraphs.

Measurement of forces in the main wires (.064" diameter)

Load cells of the type shown in Figures 48[x] and 49[x] were used for measuring forces in the main wires. A load cell consisted of the following components (see Figure 48).

(1)   Two aluminium strips, 1" x 5/16", marked 'A'. The thinner part of the strips is 3/8" long and 5/16" x .0145" in cross-section.   One electrical strain gauge on each strip was cemented longitudinally along the axis of the wire on the outside of the strip, marked 'O', and one strain gauge each was cemented on the inside, marked 'I'.

(2)   Anchoring blocks marked 'B', were cut out of 3/8" diameter stainless steel rounds and are 3/16" high. 1/8" diameter pins protrude on either side of the block and the pins are hollow and threaded to fit 10 BA screws. The wire 'W' is threaded at its end and has two nuts fitted to it (each nut locking the other). The nuts bear on block 'B' within a cylindrical hollow space provided in the block. The anchor block was so designed that the wire and nuts could rotate freely, thus avoiding any kind of fixity.
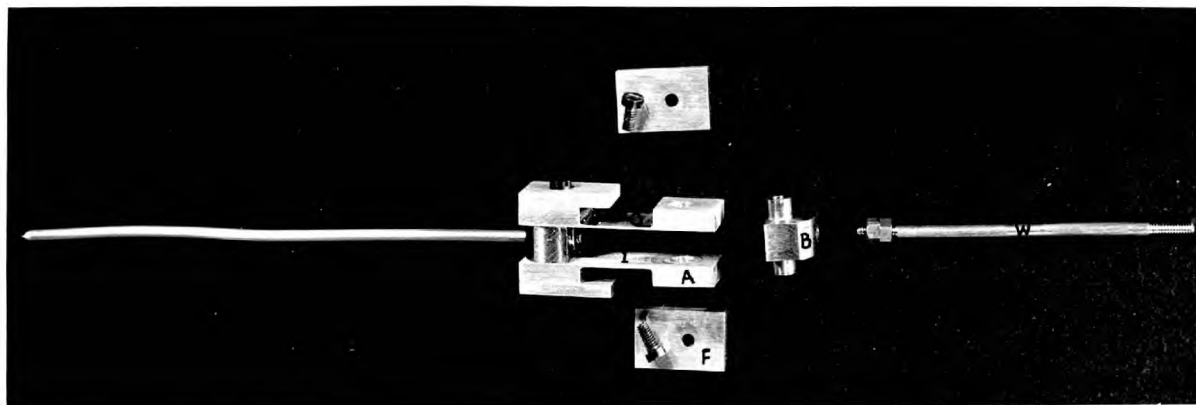
FIGURE 48   A LOAD-CELL BEFORE STRAIN GAUGES HAVE BEEN
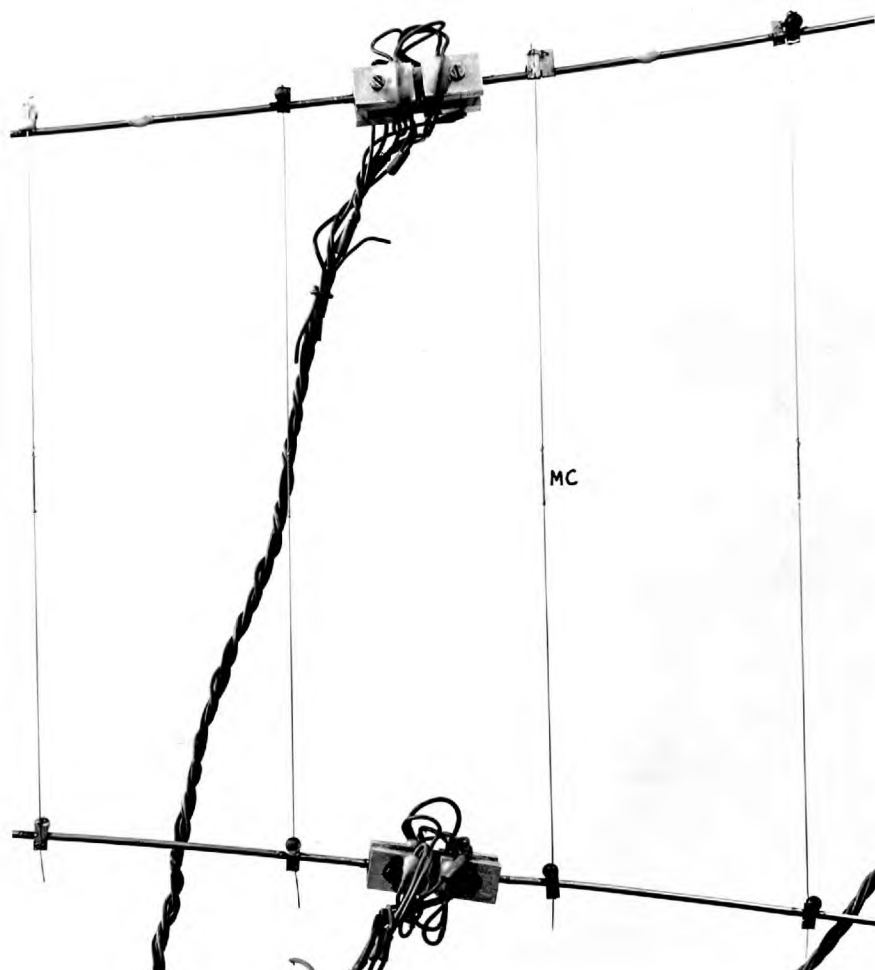PUT ON THE ALUMINIUM STRIPS

FIGURE 49   A CLOSE UP VIEW OF THE MODEL

(3)   Small stainless steel flats, 'F', fitted as shown. The
purpose of these flats was to protect the outside gauges and provide
a place for securing the lead wires from the gauges. Figure 49
shows the load cells after gauges have been cemented and they have
been placed within the structure. The way the lead wires are
cemented to the flats 'F' can be seen.

The four gauges on each load cell formed part of a wheatstone
bridge circuit in such a way that

(i)   for a direct pull on the load cell, the tensile strain in
the longitudinal gauges and the compressive strain in the
transverse gauges all adds up, thus giving increased
sensitivity to the device

(ii)   for a change in temperature all gauges have the same sign
of strain which cancels out, thus making the load cell self
compensating for temperature

(iii)   any strains caused by bending about the horizontal plane
of symmetry, passing through the wires, would cancel out.

Each gauge had a gauge length of 1/8" and a gauge factor of 2.14.
The cross section of the aluminium strips was so designed that the
gauge will have the same extensibility as the wire. Average strain
per pound of load was found to be 30.66×10^{-6}, measured on an
instrument designed for a gauge factor of 2.

$$\text{The actual strain} = 30.66 \times 10^{-6} \times \frac{2}{2.14}$$

$$= 28.65 \times 10^{-6}$$

If Poisson's ratio for aluminium is assumed to be 0.3,

$$\text{longitudinal strain per gauge} = \frac{28.65}{2(1+0.3)} \times 10^{-6}$$

$$= 11.03 \times 10^{-6}/\text{lb.}$$

Area of the wire is 3220×10^{-6} sq. ins.

'E' for the wire (determined experimentally) is 28.3×10^{6} p.s.i.

Strain per pound on the wire = $\dfrac{1}{3220 \times 10^{-6} \times 28.3 \times 10^{6}}$

$$= \frac{1}{91000} = 11.1 \times 10^{-6}$$

On an average the load cell is 0.6% stiffer.

While calibrating the load cells it was found that the reading in the cell altered appreciably if its orientation was altered with respect to the axis of the wire (it is presumed this imposed some sort of eccentricity in loading or altered the eccentricity if already present). The load-strain relationship, however, did not alter by more than 2-3%. In order to avoid errors on this account the load cells were calibrated within the model frame. The wire was anchored at one end and loaded over a pulley at the other end to calibrate the load cells. The orientation of the load cells was also fixed, and in order that the absolute reading could be relied upon, was maintained the same throughout the experiment as far as possible.

Four load cells of the type described were placed in each wire at 2", 20", 30" and 38" away respectively from the left hand support (Figure 47). A typical load-strain curve, for load cell number 1 on Figure 47, is given in Figure 50. The curve shows very slight non-linearity but departure from a straight line is so small that the mean values were used for calculating forces from strains. Mean values of strain per pound are given here.

Load cell	1	2	3	4	5	6	7	8
Strain $\times 10^{6}$	30.86	32.05	29.31	27.84	33.28	32.50	30.30	29.15

The load cells, however, did show a drift in reading with time and could not be relied upon to maintain a force-history of the main wires. It was justifiably hoped on the basis of previous readings that the load-strain relationship could still be relied upon to evaluate changes in tension.

Measurement of forces in the hangers (.010" diameter wire)

The type of load cells used for the main wires would have been difficult to manufacture for the hangers because it would be impractical to have load cells of the same extensibility as the hangers. It was decided to use the property that the frequency of vibration of a thin wire is a function of its tension. If the bending stiffness of the wire is neglected, its frequency of vibration is given by:

$$f = \frac{1}{2l} \cdot \sqrt{\frac{T}{m}} \qquad (47)$$

where, f = fundamental frequency of natural vibration

T = tension in the wire

m = mass per unit length of wire

and l = gauge length, i.e. the distance between the two nodes.

The principle used here is that the wire hanger forms part of a vibrating wire gauge. The wire is plucked by a magnet (connected to an oscillator) to initiate the vibrations and the frequency of vibration is measured on an oscilloscope. Since the hangers were of non-magnetic wire, the wire was made locally magnetic by coiling a .004" diameter mild steel wire around it (see 'MC' in Figure 49).

The gauge is shown in Figures 51[+] and 52[x] (the magnet is shown disconnected from the oscillator). The instrument was mounted on a telescope stand, so that it could be moved from hanger to hanger.

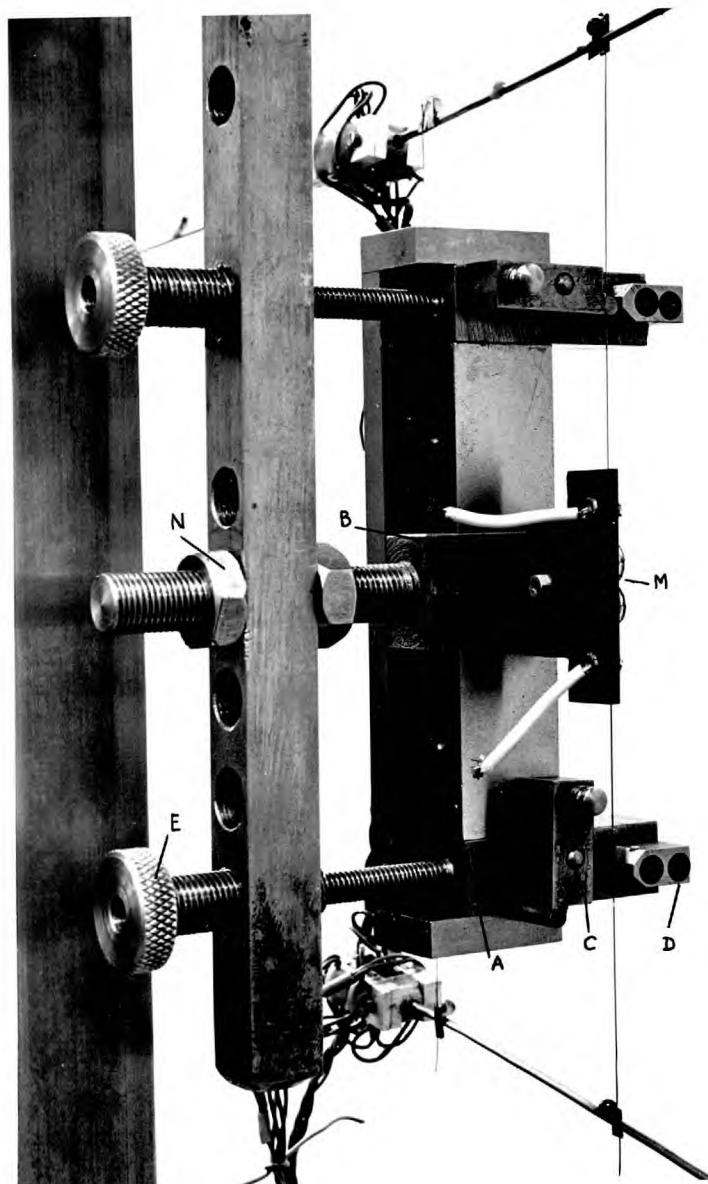[+] Page 73   [x] Page 74.

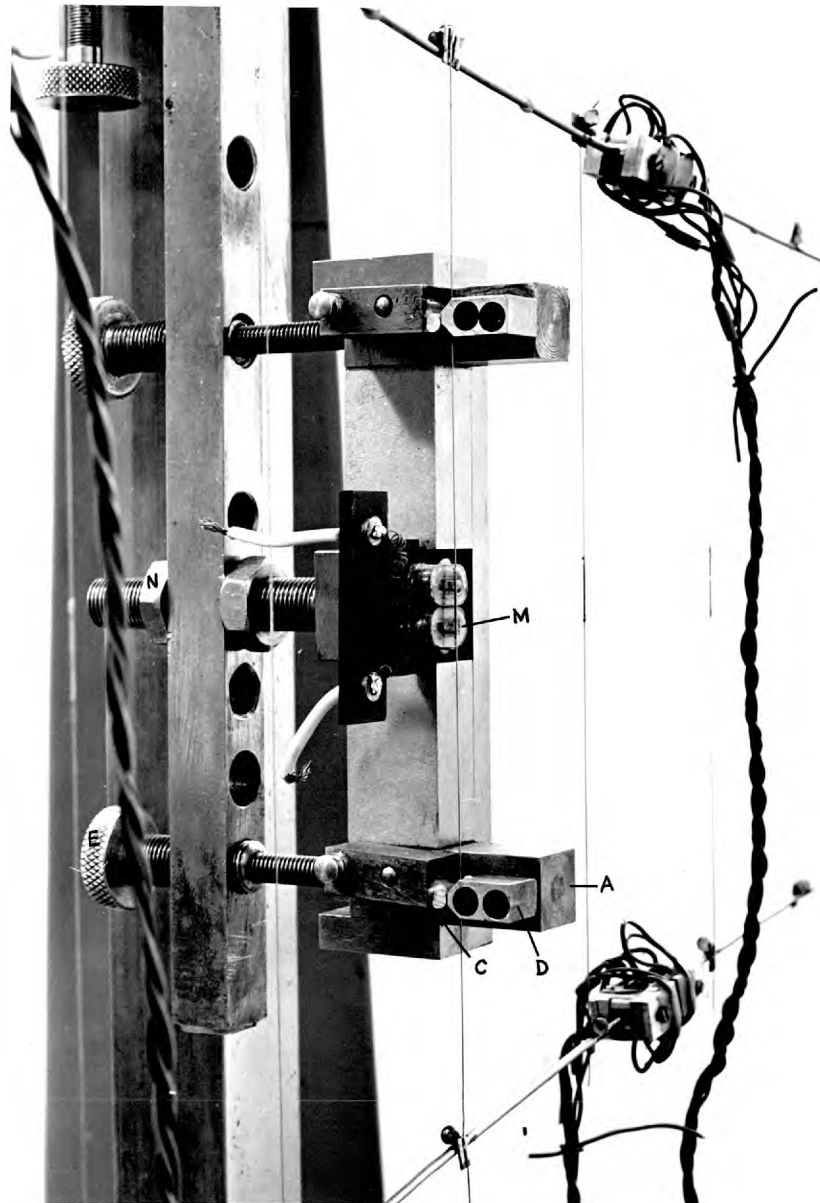FIGURE 51   THE VIBRATING WIRE GAUGE

FIGURE 52   THE VIBRATING WIRE GAUGE

THE HANGER IS SHOWN HELD BETWEEN BLOCKS C AND D

The telescope stand was provided with adjusting screws for fine vertical movement and rotation about the vertical axis to facilitate the positioning of the gauge. Major parts of the gauge, marked on Figures 51 and 52, are described below.

(1)　Block 'A', which could be moved nearer to or farther away from the wire by adjusting the nuts 'N', had the magnets 'M' fixed to it.

(2)　Block 'B' carrying the blocks 'C' and 'D' could be moved along its horizontal axis by a differential thread screw head 'E'.

(3)　Block 'C', weighing approximately 1/2 oz., pivots about a pin with an eccentricity of approximately 0.2". Block 'D' is fixed to 'B' and the flat portion against which the wire rests has a width of .05". The roller at the end of Block 'C' just holds the wire against the flat in block 'D'.

The gauge length (the distance between the two nodes produced by blocks 'C' and 'D') was measured to be 3-3/4". During the development stage of the gauge, which was extensive, the following important points were noted.

(i)　Gauge lengths of 1-1/4", 2", 3" and 3-3/4" were tried. At gauge lengths of 1-1/4" and 2" the wire was too stiff to be initiated by the pull of the magnet and at 3" the vibrations did not last long enough for being able to get a balance on the oscilloscope. At 3-3/4" the damping was not quite so high and the vibrations lasted a convenient period of time.

(ii)　It was required to have the magnet at a specific distance (approximately 1/32") from the wire to get a proper Lissajous figure on the oscilloscope screen.

(iii)　It was most important that the conditions at the support be repeated precisely in order to get consistent results. The points particularly noted with regard to the supports were:

(a)　the flat portion in block 'D' should just touch the wire,

so that the wire is not pushed out of its plane;

(b)   the pressure exerted by the roller should be kept the minimum possible, otherwise there is a tendency to drag the wire, which would affect the tension in the wire;

(c)   the blocks 'C' should rotate in the same direction so that the drag, if any, is compensating.

Figure 53 shows a long plate, which is fixed to the frame. A number of washers are glued down to the plate and two of the legs of the telescope stand are positioned by the washers. The position of the washers was fixed when the hangers were being calibrated, so that it would be possible to repeat the same position of the gauge whenever readings were taken.

Each hanger was calibrated separately. All hangers fell into three slightly different classes (the difference perhaps attributable to the slight difference in length of the mild steel coil), say A, B and C. The calibration curves are shown on Figure 54. Good consistency was obtained in the results. This can be seen from Tables 6 and 7, which show how accurately it was possible to measure loads and small differences in loads with the help of the calibration graphs.

Taking measurements with the vibrating wire gauge consisted of the following steps.

(i)   The telescope stand was brought into position for the particular wire on which measurement was to be made.

(ii)   The gauge was adjusted such that blocks 'D' were just touching the wire and the magnets were facing the mild steel wire coil.

x Page 82

(iii) The blocks 'C' were rotated about the pins to restrain the wire at two points.

(iv) The wire was placed by the magnets to give a Lissajous figure on the oscillator screen and reading was taken at resonance.

(v) The wire was released by rotating back the block 'C' and the structure was then loaded or unloaded and allowed to deflect, unobstructed by the gauge.

(vi) Steps (ii), (iii), (iv) and (v) were repeated to take the next readings.

Measurement of deflections

Nylon balls 1/8" diameter were cemented to the main wires, at each hanger position. Deflections were measured by sighting these balls through a cathetometer, reading to 1×10^{-3} in.

2.14 Main dimensions of the model and experimental results

The important details and dimensions of the model are given below (see Figure 11a for notation).

n = 20

L = 39-7/8" (measured between inner faces of the anchor blocks)

D = 10-1/16" (centre to centre distance of the main wires at the anchorage block)

$d_U = d_L$ = 2.54" (obtained by plotting a profile of the wire)

Average value of a = 2"; the first hanger is at 1" from the left support. Average value of T = 1.20 lb. There is a scatter of ±15%; the desired value was 1.25 lb. in each hanger. Hanger tensions were measured several times during the course of the experiment and the average value showed no appreciable change.

w = 0.600 lb/in.

H_U (measured at the time of assembly) = 47.8 lb.

H_L (measured at the time of assembly) = 49.0 lb.

Measurements were taken in a temperature-controlled room at an average value of $68^O \pm 1^O$ F.

Measurements at the supports showed no movement due to applied loading.

The value of the Young's Modulus of elasticity, E, for the wire was determined experimentally to be 28.3×10^6 p.s.i.

The method of loading can be seen from Figure 52. Load hangers are suspended from wires straddled over the main wire.

For both the 'load' and 'no load' condition three sets of readings were taken, unless the first two sets agreed very closely. Results were obtained by taking a mean value from the different sets of readings.

The various cases of loading and the results obtained are enumerated here.

(1) Concentrated applied vertical load equal to:

(a) 2.5 lb. at quarter point on upper wire

(b) 5.0 lb. at quarter point on upper wire

(c) 2.5 lb. " hanger no. 10 on upper wire

(d) 5.0 lb. at hanger no.10 on upper wire

The results are shown in Figures 12 to 18.

(2) Concentrated applied vertical loads at hanger nos. 2, 3, 4, 5, 6, 7, 8 and 9 equal to:

(a) 0.5 lb. each on upper wire , p = 0.25 lb/in.

(b) 1.0 lb. each on upper wire , p = 0.50 lb/in.

(c)   1.5 lb. each on upper wire , p = 0.75 lb/in.

(d)   0.5 lb. each on lower wire , p = 0.25 lb/in.

(e)   1.0 lb. each on lower wire , p = 0.50 lb/in.

The loading is meant to represent a uniformly distributed load, 'p' per unit length of span, over part of the left half of the span. The results are shown in Figures 21, 22 and 23.

(3) Concentrated applied vertical loads at 4", 8", 12", 16", 20", 24", 32" and 36" from the left support equal to:

(a)   1.0 lb. each on upper wire , p = 0.25 lb/in.

(b)   2.0 lb. each on upper wire , p = 0.50 lb/in.

(c)   3.0 lb. each on upper wire , p = 0.75 lb/in.

The load is meant to represent a uniformly distributed load, p, over the central 36" of the span. The results for the change in forces are given in Figure 55.

(4)   Influence lines for change in tension in hanger nos. 5 and 16 (which are symmetrically placed in the structure) are given for applied vertical loads of 2.5 lb. and 5 lb. in Figure 56.

(5)   Influence lines for h_U, h_L and values of deflection in the upper cable under the loaded point for vertical applied loads of 2.5 lb. and 5.0 lb. are given in Figure 57 and 58. Values of h_U and h_L, measured at centre point load cells only, are given. Measured values from other load cells show similar variation and very little difference in magnitude from the values given.

It will be noted from the above results that:

(i)   under an applied point load, there is a sharp decrease in tension in the hanger immediately under it and the two

hangers adjacent to it have a bigger increase in tension than the rest of the hangers;

(ii) the stiffness of the structure goes on increasing with applied load;

(iii) under a load uniformly distributed over the whole span, there is an almost equal sharing of load between the two main wires, unlike for any other kind of loading;

(iv) a maximum value of deflection under load occurs near the quarter point.

The correlation of experimental and theroetical results is discussed in Chapter 3.

2.15 Sources of error and points of difference from an 'ideal' model

(1) The main wires are broken up into several segments by the load cells causing some change in their stiffness value. This also gives a certain degree of undesirable freedom to the segments to rotate with respect to each other, despite the fact that this tendency is resisted at the load cells due to the friction between nuts and anchor blocks 'B' (Figure 47).

(2) The hangers have unequal pretension, which may have been caused by slight rotations at the joints while welding or some other steps of assembly.

(3) The hangers are eccentrically connected to the main wires and although alternate hangers are on the opposite side of the wire, this would cause a certain amount of torsion.

(4) There is the possibility of errors being caused by a slight error in the positioning of the vibrating wire gauge.

(5) If there is a certain degree of eccentricity in the loading, the wire segments can rotate with respect to each other, causing undesirable changes in the hanger tension. Measurements were taken for rotations in the wire due to applied loading. The rotations were noted to be greatest near the centre point load-cells.

TABLE 6

Load on the wire lb.	Load measured lb.	% error
0.64	0.655	2.33
0.84	0.860	2.33
1.04	1.050	0.96
1.24	1.255	1.21
1.44	1.440	Nil
1.64	1.640	Nil
1.84	1.855	0.80
2.04	2.040	Nil

TABLE 7

Initial load on the wire (1b)	Final load on the wire (1b)	Differences in the load measured (1b)	% Error
0.64	0.74	0.103	+3.00
1.04	1.14	0.099	-1.00
1.64	1.74	0.104	+4.00

CHAPTER 3

DISCUSSION ON RESULTS

3.01

The theoretical and experimental results obtained have already
been given in Chapters 1 and 2 respectively, along with comments about
the important features of the results. Most of the experimental results
are plotted on the same figures as the corresponding theoretical
results. This Chapter gives a summary of observations from the results
as well as a discussion on the comparison between the theoretical and
experimental values.

3.02

Results of point loads applied only at the quarter point and
the centre point (or very near the centre point) of the span are given,
because the maxima and the minima of the different parameters,
being studied, occurs when point loads are applied near these points.
(See Figures 19 and 20.)

3.10 Single Cable

The theory used for analysing the single cable is for flexible
cables only and it will be seen from Figures 42 and 43 that the agreement
between theoretical and experimental values for vertical deflections is
closer for the .0164" diameter wire than for the .064" wire, which has
considerably more bending stiffness than the thinner wire. The agreement
for the .0164" diameter wire is excellent. For small values of $\bar{W}$
there is little difference between the values obtained from Pugsley's
theory and the more accurate theory but for larger values of $\bar{W}$ the
values obtained from the more accurate theory show better correlation.

The correction terms included in the more accurate theory, which are neglected by Pugsley, are only material at high values of applied loads.

The agreement between experimental and theoretical results for horizontal deflections (Figure 44) is also reasonable, the agreement being better for the thinner wire. Theoretical values for horizontal deflections have been obtained by using Pugsley's theory, which does not consider the size of the wire.

The theory is extremely simple to use and the required computations can be easily done on a desk calculating machine.

3.20   The Plane-system

3.21   General Observations

(i)   The resistance of a single cable to deflections under applied loads is mainly due to its 'gravity stiffness'. A plane system, on the contrary, derives most of its stiffness from its prestress, and has very little 'gravity stiffness'. Indirectly, however, it can be seen as a structure with two single cables of reverse curvature interacting with each other.   Therefore, there is justification in expecting that the plane system will have greater stiffness than a single cable (provided 'w' is the same for both). It will be seen from the results that the ratio of the maximum experimental vertical and horizontal deflections for a single cable and a plane system is approximately 1.6 for the same value of w and $\overline{W}$.

(ii)   It has been shown that the .064" diameter wires used as the main cables in the experimental model, are not completely flexible at that scale. Both methods of theoretical solution are only meant for

structures with flexible elements and as such the model with the
.064" diameter wire does not comply entirely with theoretical requirements.
There are also some differences arising because of the difficulty of
representing all model conditions in a theoretical treatment.

(iii) The structure gets increasingly stiffer with applied loads and
has a basically non-linear behaviour, just like a single cable. It
will be seen for all cases of loading that the values of deflection,
λ, h_U and h_L vary non-linearly with the magnitude of applied loads.

(iv) For loads applied to the upper cable, the hangers immediately
under the load or within their immediate vicinity experience a decrease
in tension and all other hangers undergo an increase in tension.
If the magnitude of applied loads is increased to an extent such that
some of the hangers go slack and become inactive, the two cables
still continue to interact through the rest of the hangers (except
for a case of uniformly distributed load over the whole span). For
loads applied to the lower cable all the hangers undergo an increase
in tension.

(v) It will be seen for loads applied on either the upper or the
lower cable that values of h_U are much larger than $| h_L |$, which shows
that the upper cable is the load-carrying cable.

(vi) Results for the range of loads applied have shown that there
is negligible difference between the upper and the lower cable vertical
deflections; also there is negligible difference in vertical
deflections whether the upper or the lower cable is loaded. Therefore
only upper cable vertical deflections have been plotted for all
loading cases. Corresponding points on the two cables move in
opposite directions horizontally and the deflections are comparable.

(vii) The ratio between maximum horizontal and vertical deflections
calculated under a load, P = 2.5 lb. ($\bar{W}$ = 0.1) varies from

approximately 0.25 for a load near the end to approximately 0.075 for a load at the centre point.

The ratio of maximum calculated vertical deflections for a load P = 2.5 ($\bar{V}$ = 0.1), applied horizontally or vertically at the centre point is approximately 0.125.

3.22   Discussion on the comparison of results

(i)   Figures 12 to 23 show the experimental and theoretical results for the plane system, which are being compared here. It will be seen that there is better all-round agreement between experimental values and the values from the 'General method', than the values from the 'Influence Coefficient' method. The experimental results lie between the results from the two theories.

(ii)   Deflections

The agreement shown in Table 8[+] is reasonable. It will be seen that the errors from the 'Influence coefficient' method go on increasing with the values of load whereas they are almost unaffected in the case of values obtained from the 'General method'. Figure 23 shows that for uniformly distributed load, p, negative deflections obtained by the 'General method' show much better agreement than those obtained by the 'Influence coefficient' method.

(iii)   Values of h_U

Excellent agreement between the theroetical values obtained from the 'General method' and the experimental values can be seen in Table 9[x]. The values of the point load applied at the quarter point obtained by the 'Influence coefficient' method are particularly bad but the other values show reasonable agreement. Values of h_U have not been tabulated as they are small and unimportant; the values can be

+   Page 89   x   Page 90

seen in Figures 19, 21 and 22.

Errors given in Tables 8 and 9 are computed on the experimental values.

(iv)   Values of change in hanger tension

It can be seen from Figures 12 and 15 that reasonable agreement is obtained by the 'General method' for all values and positions of the applied point load. The values from the 'Influence coefficient' method are not so close to the experimental values, especially for $\bar{W}$ = 0.2. For a uniformly distributed load on the upper cable (see Figure 21) values from the 'General method' show fairly good agreement and the order of error is unaffected by the variation in p.

The 'Influence coefficient' values show fair agreement for p/w = 0.4 but start to diverge from the experimental values for larger values of p. Both methods show good agreement for the lower cable carrying load p (see Figure 22).

3.30   Three-dimensional system

A suspension system consisting of three cables has been solved in Section 1.33. It has been shown that the 'General method' gives satisfactory solutions for the initial geometry. A numerical example has also been solved for an applied point load. The different parameters in the structure are deliberately chosen such that it is very nearly the same as a plane-system.
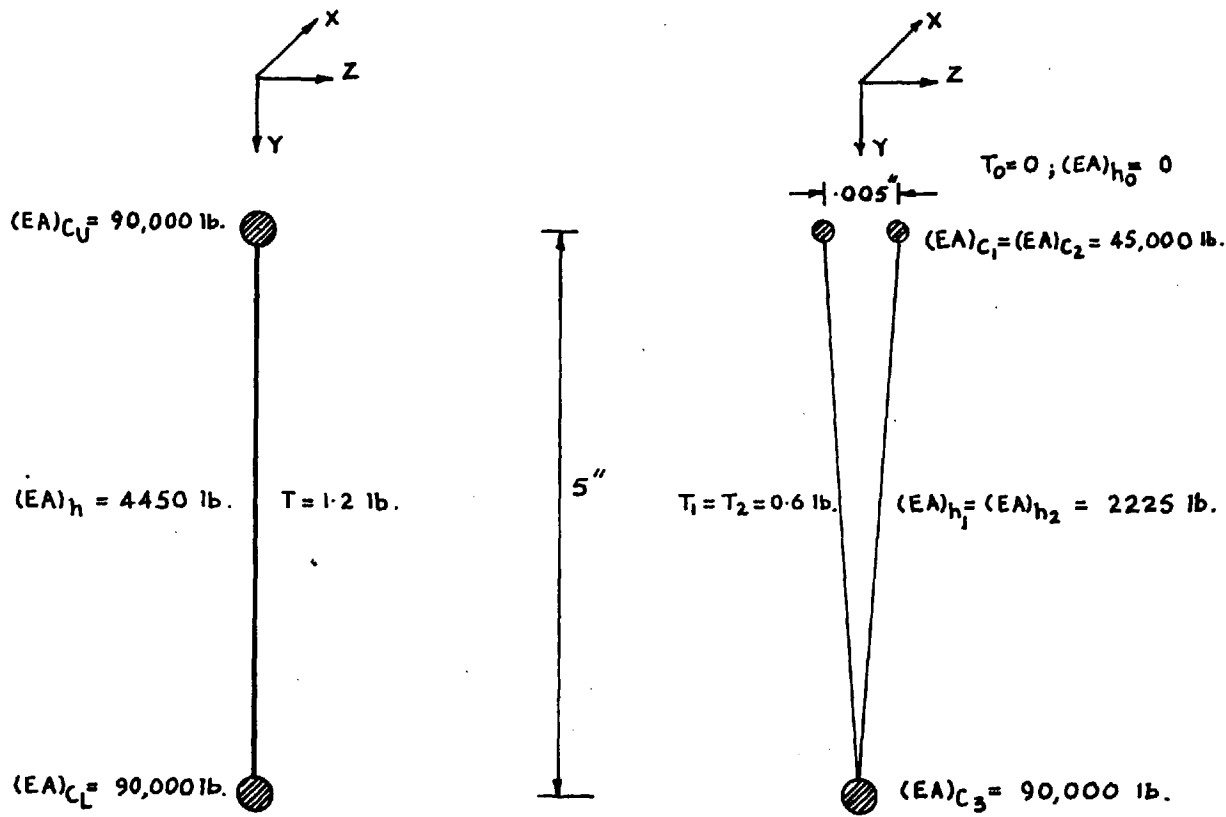
PLANE SYSTEM   3-CABLE SYSTEM

CROSS SECTION AT THE CENTRE

Table 5 shows that the results from the two solutions agree within about 2.5%, as expected.

TABLE 8

Load	Applied at	% Error in values of deflections	
		Influence Coefficient method	General method
$\bar{W} = 0.1$	Hanger no.10	- 4.3	+ 11.2
$\bar{W} = 0.2$	Hanger no.10	- 11.3	+ 13.8
$\bar{W} = 0.1$	Quarter point	- 6.5	+ 3.9
$\bar{W} = 0.2$	Quarter point	- 11.6	+ 4.0
p/w = 0.4)		+ 3.0	+ 5.0
p/w = 0.8)	Part of the left half of the span	+ 6.0	+ 6.0
p/w = 1.2)		+ 10.0	+ 3.7

TABLE 9

Load	Applied at	% Error in values of h_U	
		Influence Coefficient method	General method
$\bar{W} = 0.1$	Hanger no.10	+ 14.7	nil
$\bar{W} = 0.2$	Hanger no.10	+ 14.4	+ 1.5
$\bar{W} = 0.1$	Quarter point	+ 42.5	+ 2.1
$\bar{W} = 0.2$	Quarter point	+ 54.0	+ 2.6
$p/w = 0.4$)	Part of the left half of the span on upper cable	- 10.0	nil
$p/w = 0.8$)		- 7.5	nil
$p/w = 1.2$)		- 3.2	nil
$p/w = 0.4$)	Part of the left half of the span on lower cable	- 11.7	- 3.9
$p/w = 0.8$)		- 2.0	- 0.7

CHAPTER 4

CONCLUSIONS

4.01 Introduction

Chapters 1, 2 and 3 describe the fundamental study on a single cable, which is basically a gravity system, and plane and three cable structures, which are basic prestressed funicular suspension systems with little or no 'gravity stiffness'. Most suspension systems (except the type shown in Figure la) consist of two or more cables of reverse curvature, prestressing and thus stiffening each other. The study of two cables interacting with each other is, therefore, fundamental and the results obtained for the plane system are of application to general suspension systems. The study of the three-cable system is a step towards a more detailed study of space suspension structures.

All this study has been carried out for structures supported by rigid and unyielding supports and at constant temperature. A method for considering the effects of support movements, slip at the support and temperature changes has, however, also been suggested.

The main features of the 'influence coefficient' method and the 'General' method have been discussed in Sections 1.23 and 1.34 respectively. Observations on the theoretical results on a single cable and the plane system are made in Sections 1.10, 1.22 and 1.32. The possible sources of error in the experimental work are given in Section 2.15, and other important points about the experiments are discussed in general in Chapter 2. General observations about the behaviour of the plane system are made in Section 3.21, and those on the comparison of theoretical and experimental values follow in Section 3.22.

The main conclusions drawn from the above study are given in the following sections.

4.10   Single cable

An experimental and theoretical study has been made for single cables under applied point load. The theory, which is very simple in approach, is meant for flexible cables only. Excellent agreement has been obtained between the theoretical and experimental values. The theory has been used to obtain an approximate solution for a plane prestressed suspension system.

4.20   Plane-system

The plane system has been studied in great detail, experimentally as well as theoretically. Two methods of theoretical solution have been used, and keeping in view that the experimental model could not comply entirely with theoretical requirements, the agreement obtained is quite reasonable for most cases.

The 'influence coefficient' method is much simpler to apply but it is limited to considering vertical loads and deflections only. It gives reasonable results for deflections under applied loads; agreement for forces is also reasonable for small applied loads. Where a large discrepancy has occurred between theoretical and experimental values of forces, the theoretical values are the greater.   It has been shown that the value of unit load should be .01 or less times the value of wL, in order not to affect the results.

It will be seen from the comparison of results in Section 3.22 that the values from the 'Influence coefficient' method are in reasonable agreement for small values of load, but are in error for larger values. This shows that the law of superposition used in the method is justifiable for small loads but introduces errors for larger values of applied load.   The method is thought to be quite suitable for a preliminary analysis.

The 'General method' is very simple in principle but involves a considerable amount of computation. The agreement obtained with this method is very good for both concentrated and uniformly distributed applied loading and is hardly affected by the magnitude of loads.

It has been shown for both methods of solution that the number of nodes can be cut down, reducing the computation work considerably and at little sacrifice of accuracy.

4.30   Three-dimensional structures

The applicability of the 'General method' of solution to three-dimensional prestressed systems has been shown by using it to solve a three-cable structure. The generality of the method makes it a very useful tool for the analysis of prestressed suspension systems.

4.40   Experiments

The experiment on the plane system presented some difficulties in the measurement of forces, particularly as it was desired to maintain a force-history of the structure. The load cells used as links in the main wires and the vibrating wire gauge for the hangers proved to be a satisfactory means of measurement. The vibrating wire

gauge **was found** satisfactory for maintaining the force-history of the model, but the design of the load-cell needs further improvement before it is sufficiently dependable in this respect. The load cells and the vibrating wire gauge are described in detail in Section 2.13.

4.50   Computation

Both the theoretical approaches used to solve the plane system lead to the numerical solution of simultaneous equations sufficiently large in number to require the use of digital computers. Computer programmes were written in 'MERCURY AUTOCODE' and are suitable to be run on the 'ATLAS' computer using 'compiler EMA'. The programmes are most general in nature and a study of Section 1.31 and the flow diagrams in Appendix 'B' will show that it will be more economical if a large number of cases of loading are solved in the same run of the programme. The programmes require as data the geometry and stiffness of the structure and the loading.

A similar programme was written for the solution of the three-cable system. The programme can determine the geometry of the structure for initial force and then solve the structure for applied loads. It will be more economical to solve a large number of cases of loading in the same run of the programme.

REFERENCES

1. Theory of suspension bridges   A.G. Pugsley, 1957.

2. Some experimental work on model suspension bridges
   A.G. Pugsley. Journal of Institution of Civil Engineers,
   1949.

3. The gravity stiffness of a suspension bridge cable
   A.G. Pugsley. Quarterly Journal of Mechanics and Applied
   Mathematics, Vol. 5, Pt. 4, 1952.

4. A flexibility coefficient approach to suspension bridge
   theory   A.G. Pugsley.   Journal of the Institution of Civil
   Engineers, Vol. 32, April 1949.

5. A simple theory of suspension bridges   A.G. Pugsley.
   Journal of the Institution of Structural Engineers, Vol. XXXI,
   March 1953.

6. The theory and practice of modern framed structures, Vol. II.
   Johnson, J.B., Bryan, C.W., and Turneaune, F.E.   John Wiley, 1911.

7. Hung roofs and their structural solutions.
   Dr. Hanskarl Bandel.

8. Shapes of suspended roofs   A. Siev and J. Eeideman.

9. Berechnungserfahren für vorgespannte, doppelt gekrümmte
   seilnetzwerke. Eras and Elze.

10. Zur berechnung und statisch vorteilhaften formgebung von
    seilnetzwerken. Eras and Elze.

    (note: References 7-10 were presented at a "Colloquium on
    Hanging Roofs, Continuous Metallic Shell Roofs and Super-
    ficial Lattic Roofs" convened by the I.A.S.S. in Paris, in
    July, 1962)

11. A practical treatise on suspension bridges   D.B. Steinman,
    2nd Edition, John Wiley, 1929.

12. The collected papers of S.P. Timoshenko.   McGraw-Hill, 1952.

13. Cable movements under two-dimensional loads
    W.T. O'Brien and A.J. Francis. Journal of Structural
    Engineering, Proceedings A.S.C.E., June 1964.

14. Movements of a cable due to changes in loading. J. Michalos
    and C. Birnstiel. Transactions of A.S.C.E., Vol. 127, Pt. II,
    1962.

15. Mathematical handbook for scientists and engineers, Chapter 4,
    G.A. Korn and T.M. Korn.   McGraw-Hill, 1961.

Notation

The symbols and letters used have the following definition, unless otherwise mentioned. Cables No. 1, 2, and 3, and hangers No. 0, 1 and 2, refer to the three-cable system. Upper and lower cable refer to the plane system.

A	The area of the cables or the hangers
E	Young's modulus of elasticity
$(AE)_h$	The value of AE for the hangers
$(AE)_{h_0;\ h_1;\ h_2}$	The value of AE for hangers No. 0; 1; 2
$(AE)_C$	The value of AE for a cable
$(AE)_{C_U;\ C_L}$	The value of AE for upper cable; lower cable
$(AE)_{C_1;\ C_2;\ C_3}$	The value of AE for cables No. 1; 2; 3
w	A uniformly distributed vertical dead weight or the initial prestress per unit length of span
p	The uniformly distributed applied vertical load per unit length of span
P	An applied vertical point load
$\overline{W} = \dfrac{P}{w \times span}$	
T	The pretension in the hangers of plane system
T_k	The change in hanger tension at node k
F'_i	The initial assumed force in a member $k - i$ member $k - i$ is the member joining nodes k and i, k and i being any general nodes in a structure
Fo_i	The pretension in member $k - i$
ΔFo_i	The change in force in member $k - i$

X_k	An applied point load at node k along X-axis
Y_k	An applied point load at node k along Y-axis
Z_k	An applied point load at node k along Z-axis
$T_{o;\ 1;\ 2}$	The pretension in hangers No. 0; 1; 2
H	The horizontal component of the single cable tension
h	The horizontal component of the change in the single cable tension
$\bar{h}$ $\quad = \quad 1 + \dfrac{h}{H}$	
$\bar{T}$	The tension in a single cable at any point x
$H_{U;\ L}$	The horizontal component of tension in the upper cable; lower cable
$h_{U;\ L}$	The horizontal component of change in tension in the upper cable; lower cable
$R_{U;\ L}$	The vertical reaction at the supports (under pretension only) in the upper cable; lower cable
λ	The average value of the positive values of T_k
L	The span of the structure
l	The length of a single cable
Δl	The change in cable length
D	The vertical distance between supports
C_o	The distance between supports measured along the Z-axis
d	The central sag of a single cable
$d_{U;\ L}$	The central sag of the upper cable; lower cable
$D_{1;\ 2;\ 3}$	The vertical sag of cables No. 1; 2; 3

$C_{1;\ 2;\ 3}$	The horizontal sag of cables No. 1; 2; 3
$1'_i$	The assumed length of member $k - i$
lo_i	The length of member $k - i$ under pretension
L_k	The length of the hanger k
$r \quad = \quad \frac{x}{L}$	, where x is the distance from the origin of the point where the deflection is being calculated
a	The spacing of hangers
n	The total number of hangers, or the number of the sets of hangers in the three-cable system
$(x_k,\ y_k,\ z_k)$	The coordinates of a node k
$(u_k,\ v_k,\ z_k)$	The movements of the node k along the X, Y and Z axes respectively
$(u'_k,\ v'_k,\ z'_k)$	The values of correction applied to the initially assumed values of x_k, y_k and z_k respectively
u	The horizontal deflection of the single cable
v	The vertical deflection of the single cable
v_r	The vertical deflection at the loaded point in the single cable
v_{ij}	The vertical deflection of a single cable at station j for a vertical applied load at station i
V_{ij}	The vertical deflection in a suspension bridge stiffening girder at station j for a vertical unit load applied at i
u_{mk}	The vertical deflection of the upper cable at hanger k for a vertical unit load applied at hanger m
l_{mk}	The vertical deflection of the lower cable at hanger k for a vertical unit load applied at hanger m

$$K \quad = \quad \frac{\overline{W}}{2}(1 - 2r)$$

$$M \quad = \quad \frac{\overline{W}}{2}(1 + 2r)$$

$$F \quad = \quad G \quad = \quad 32\,\frac{d^2}{L^2}$$

$$U \quad = \quad \frac{SHL}{AE}$$

$$U' \quad = \quad \frac{HL}{AE}$$

$$\alpha_k \quad = \quad \frac{T_k\,L_k}{(AE)_k} \qquad \text{at hanger } k$$

ω The coefficient of linear expansion / degree change in temperature

t change in temperature

ε Slip at the support

$$C \quad = \quad \frac{EA}{EA + Fo} \cdot \omega.t$$

γ_{U_1} Vertical displacement of the upper cable support at $x = -L/2$

γ_{U_2} Vertical displacement of the upper cable support at $x = L/2$

γ_{L_1} Vertical displacement of the lower cable support at $x = -L/2$

γ_{L_2} Vertical displacement of the lower cable support at $x = L/2$

β_{U_1} Horizontal displacement of the upper cable support
at $x = -L/2$

β_{U_2} Horizontal displacement of the upper cable support
at $x = L/2$

β_{L_1} Horizontal displacement of the lower cable support
at $x = -L/2$

β_{L_2} Horizontal displacement of the lower cable support
at $x = L/2$

Appendix A

Derivation of equation (34)

Length of a small element in
the cable can be given as

$$dl = \left\{ 1 + \left(\frac{dy}{dx}\right)^2 \right\}^{1/2} \cdot dx \qquad (48a)$$

After deflection v has occurred
the changed length can be
obtained by replacing y by
(y + v), as

$$dl' = \left\{ 1 + \left(\frac{dy}{dx} + \frac{dv}{dx}\right)^2 \right\}^{1/2} \cdot dx \qquad (48b)$$
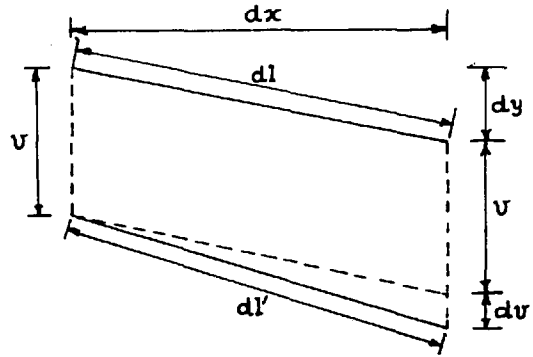
The change in length due to deflection v is, from equations
(48a) and (48b)

$$\frac{\delta(dl)}{dx} = dl' - dl = \left\{ 1 + (a+b)^2 \right\}^{1/2} - \left\{ 1 + a^2 \right\}^{1/2}$$

$$\text{or} \qquad \phi(a+b) - \phi(a) \qquad (49)$$

where $\qquad a = \dfrac{dy}{dx} \qquad$ and $\qquad b = \dfrac{dv}{dx}$

$\phi(a+b)$ can be expanded in Taylor's series [15] as

$$\phi(a+b) = \left[\phi(b)\right]_{b=a} + b\left[\frac{d}{db}\phi(b)\right]_{b=a} + \frac{b^2}{2}\left[\frac{d^2}{db^2}\phi(b)\right]_{b=a} + \cdots$$

$$\text{or} \qquad \phi(a) + b\left[\frac{b}{(1+b^2)^{1/2}}\right]_{b=a} + \frac{b^2}{2}\left[\frac{1}{(1+b^2)^{3/2}}\right]_{b=a} + \cdots \cdots \qquad (50)$$

Neglecting higher order terms and substituting this value of
$\phi(a+b)$ in equation (49) we have

$$\frac{\delta(dl)}{dx} = b \cdot \frac{a}{(1+a^2)^{1/2}} + \frac{b^2}{2} \cdot \frac{1}{(1+a^2)^{3/2}}$$

Substituting the original values of a and b and integrating to obtain the total change in length, we have

$$\Delta 1 = \int_{-L/2}^{L/2} \frac{dy}{dx} \cdot \frac{\frac{dv}{dx}}{\left\{1+\left(\frac{dy}{dx}\right)^2\right\}^{1/2}} \cdot dx + \frac{1}{2} \int_{-L/2}^{L/2} \left(\frac{dv}{dx}\right)^2 \cdot \frac{1}{\left[1+\left(\frac{dy}{dx}\right)^2\right]^{3/2}} \cdot dx \qquad (51)$$

Equating this change in length to the extension of the cable due to increase of cable tension, we can restate equation (35) as

$$\int_{-L/2}^{L/2} \frac{dy}{dx} \cdot \frac{\frac{dv}{dx}}{\left[1+\left(\frac{dy}{dx}\right)^2\right]^{1/2}} \cdot dx + \frac{1}{2} \int_{-L/2}^{L/2} \left(\frac{dv}{dx}\right)^2 \cdot \frac{1}{\left[1+\left(\frac{dy}{dx}\right)^2\right]^{3/2}} \cdot dx = S \cdot \frac{hL}{AE} \qquad (52)$$

(Note: Evaluation of S is given later in this appendix.)

Derivation of equation (36)

Equation (51) can be rewritten as

$$\Delta 1 = \int_{-L/2}^{L/2} \left(\frac{dy}{dx}\right) \cdot \left(\frac{dv}{dx}\right) \cdot \left\{1 - \frac{1}{2}\left(\frac{dy}{dx}\right)^2\right\} dx + \frac{1}{2} \int_{-L/2}^{L/2} \left(\frac{dv}{dx}\right)^2 \cdot \left\{1 - \frac{3}{2}\left(\frac{dy}{dx}\right)^2\right\} \cdot dx \qquad (53)$$

neglecting higher order terms of $\left(\frac{dy}{dx}\right)^2$

Change in length from x = - L/2 to x = rL , $\Delta 1$

Differentiating equation (1) with respect to x and substituting the value of H we have

$$\frac{dy}{dx} = \frac{8.d.x}{L^2} \tag{54}$$

Differentiating equation (5a) with respect to x we get

$$\frac{dv}{dx} = \frac{8d}{L}\left[\frac{1}{h}\left\{\frac{x}{L} - \frac{\bar{W}}{2}(1-2r)\right\} - \frac{x}{L}\right] \tag{55a}$$

$$\left(\frac{dv}{dx}\right)^2 = \frac{64d^2}{L^2}\left[\frac{1}{h^2}\left\{\frac{x^2}{L^2} - \frac{x}{L}\cdot\bar{W}(1-2r) + \frac{\bar{W}^2}{4}(1-2r)^2\right\} - \frac{2x}{L}\cdot\frac{1}{h}\left\{\frac{x}{L} - \bar{W}(1-2r)\right\}\right.$$
$$\left. + \frac{x^2}{L^2}\right] \tag{55b}$$

Substituting values of $\frac{dy}{dx}$, $\frac{dv}{dx}$ and $\left(\frac{dv}{dx}\right)^2$ from equations (54), (55a) and (55b) along with the following substitutions

$$G = 32\frac{d^2}{L^2} \quad \text{(inside the integration sign)}$$

$$F = 32\frac{d^2}{L^2} \quad \text{(outside the integration sign)}$$

$$K = \frac{\bar{W}}{2}(1 - 2r)$$

In equation (53) we have

$$\frac{2F}{L}\cdot\int_{-L/2}^{rL}\left\{x - G\cdot\frac{x^3}{L^2}\right\}\left\{\frac{1}{h}\left(\frac{x}{L} - K\right) - \frac{x}{L}\right\}.dx + F\int_{-L/2}^{rL}\left(1 - 3G\cdot\frac{x^2}{L^2}\right)\cdot$$

$$\left[\frac{1}{h^2}\cdot\left(\frac{x^2}{L^2} - 2K\frac{x}{L} + K^2\right) - \frac{2x}{L}\cdot\frac{1}{h}\left(\frac{x}{L} - K\right) + \frac{x^2}{L^2}\right].dx \tag{56}$$

In spite of having the same value G and F have been separately

denoted, because by equating G to zero, it will be seen that the denominater term reduces to unity.

On integrating and rearranging the terms we have

$$\Delta l_1 = \frac{2F}{L}\left[\frac{1}{h^2}\left(\frac{K^2L}{2}\cdot x - \frac{K}{2}\cdot x^2 + \frac{1}{6L}\cdot x^3 - \frac{K^2G}{2L}\cdot x^3 + \frac{3}{4}\frac{GK}{L^2}\cdot x^4 - \frac{3}{10}\frac{G}{L^3}\cdot x^5\right)\right.$$

$$\left. + \frac{1}{h}\left(-\frac{GK}{2L^2}\cdot x^4 + \frac{2G}{5L^3}\cdot x^3\right) - \frac{x^3}{6L} - \frac{G}{10L^3}\cdot x^5\right]_{x=-L/2}^{x=rL} \tag{57}$$

Change in length from $x'=rL$ to $x = L/2$, Δl_2

Differentiating equation (5b) we have

$$\frac{dv}{dx} = \frac{8d}{L}\cdot\left[\frac{1}{h}\cdot\left\{\frac{x}{L}+\frac{\bar{W}}{2}(1+2r)\right\} - \frac{x}{L}\right]$$

Putting $M = \frac{\bar{W}}{2}(1+2r)$ we obtain

$$\frac{dv}{dx} = \frac{8d}{L}\cdot\left\{\frac{1}{h}\left(\frac{x}{L}+M\right) - \frac{x}{L}\right\} \tag{58a}$$

and $$\left(\frac{dv}{dx}\right)^2 = \frac{64d^2}{L^2}\left\{\frac{1}{h^2}\cdot\left(\frac{x^2}{L^2}+2M\frac{x}{L}+M^2\right) - \frac{2x}{L}\cdot\frac{1}{h}\left(\frac{x}{L}+M\right) + \frac{x^2}{L^2}\right\} \tag{58b}$$

It will be noted that the term $\bar{W}^2$ enters the expressions through $\left(\frac{dv}{dx}\right)^2$ and hence if the second term in equation (53) is to be excluded, $\bar{W}^2$ should be equated to zero.

Substituting values of $\frac{dv}{dx}$ and $\left(\frac{dv}{dx}\right)^2$ from equations (58a) and (58b) in equation (53) we have

$$\Delta l_2 = \frac{2F}{L}\int_{rL}^{L/2}\left(x-\frac{G}{L^2}\cdot x^3\right)\left\{\frac{1}{h}\left(\frac{x}{L}+M\right)-\frac{x}{L}\right\}dx \;+\; F\cdot\int_{rL}^{L/2}\left(1-\frac{3G}{L^2}\cdot x^2\right)\cdot$$

$$\left\{\frac{1}{h^2}\cdot\left(\frac{x^2}{L^2}+2M\cdot\frac{x}{L}+M^2\right)-\frac{1}{h}\cdot\frac{2x}{L}\cdot\left(\frac{x}{L}+M\right)+\frac{x^2}{L^2}\right\}dx \tag{59}$$

On integrating and rearranging terms we have

$$\Delta l_2 = \frac{2F}{L}\left[\frac{1}{h^2}\cdot\left(\frac{M^2L}{2}\cdot x+\frac{M}{2}\cdot x^2+\frac{1}{6L}\cdot x^2-\frac{M^2G}{2L}\cdot x^3-\frac{3}{4}\cdot\frac{MG}{L^2}\cdot x^4-\frac{3G}{10L^3}\cdot x^5\right)\right.$$

$$\left.+\frac{1}{h}\left(\frac{MG}{2L^2}\cdot x^4+\frac{2G}{5L^3}\cdot x^5\right)-\frac{1}{6L}\cdot x^3-\frac{G}{10L^3}\cdot x^5\right]_{rL}^{L/2} \tag{60}$$

Total change in length Δl can now be obtained from equations (57) and (60) as

$$\Delta l = \Delta l_1 + \Delta l_2 = \frac{2F}{L}\left[\frac{1}{h^2}\left\{(K^2-M^2)\cdot rL-\frac{1}{2}(K+M)\cdot r^2L^2-\frac{G}{2L}(K^2-M^2)\cdot r^3L^3+\frac{3}{4}\frac{G}{L^2}(K+M)r^4L^4\right\}\right.$$

$$+\frac{1}{h^2}\cdot\left\{(K^2+M^2)\cdot\frac{L^2}{4}+(K+M)\cdot\frac{L^2}{8}+\frac{L^2}{24}-G(K^2+M^2)\cdot\frac{L^2}{16}-G(K+M)\cdot\frac{3L^2}{64}-\frac{3G}{160}\cdot L^2\right\}$$

$$\left.-\frac{1}{h}\cdot\frac{G}{2L^2}(K+M)\,r^4L^4+\frac{1}{h}\left[G(K+M)\cdot\frac{L^2}{32}+G\cdot\frac{L^2}{40}\right]-\frac{L^2}{24}-\frac{GL^2}{160}\right] \tag{61a}$$

Putting the following values in equation (61a) we have

$$K+M = \bar{W} \qquad , \qquad K-M = -2r\bar{W} \qquad ,$$

$$K^2+M^2 = 0\cdot5\left(1+4r^2\right)\bar{W}^2 \quad , \quad K^2-M^2 = -2r\bar{W}^2$$

$$\Delta l = \frac{FL}{4} \cdot \frac{1}{h^2} \cdot \left[-\left(\frac{G}{20} + \frac{1}{3}\right) \bar{h}^2 - 4G\bar{w}r^4\bar{h} + G\left(\frac{\bar{w}}{4} + \frac{1}{5}\right)h \right.$$

$$-\left\{ 4\left(1 - \frac{3}{2}Gr^2\right)\bar{w}r^2 + 8\left(1 - Gr^2\right)\bar{w}^2r^2 \right\} + \left\{ \left(1 + 4r^2\right)\bar{w}^2 + \bar{w} + \frac{1}{3} \right\}$$

$$\left. -G\left\{ \frac{1}{4}\left(1 + 4r^2\right)\bar{w}^2 + \frac{3}{8}\bar{w} + \frac{3}{20} \right\} \right] \tag{61b}$$

The right hand side in equation (52)

$$= \quad S \cdot \frac{hL}{AE}$$

$$or \quad S \cdot \frac{HL}{AE} \cdot \frac{h}{H}$$

$$or \quad U(\bar{h} - 1) \quad \text{where} \quad U = S \cdot \frac{HL}{AE} \tag{62}$$

Equation (52) now becomes, by substitution from equations (61b) and (62)

$$\frac{12\,U}{FL} \cdot \bar{h}^3 + \left(\cdot 15\,G + 1 - \frac{12\,U}{FL}\right) \cdot \bar{h}^2 + G\left(12\bar{w}r^4 - 0.75\bar{w} - 0.6\right) \cdot \bar{h}$$

$$+ 12\left(1 - 1.5Gr^2\right) \cdot \bar{w}r^2 + 24\left(1 - Gr^2\right) \cdot \bar{w}^2r^2 - \left\{ 1 + 3\bar{w} + 3\left(1 + 4r^2\right)\bar{w}^2 \right\}$$

$$+ G \left\{ 0.75\left(1 + 4r^2\right)\bar{w}^2 + 1.125\,\bar{w} + 0.45 \right\} = 0 \tag{63}$$

and is identical to equation (36). Equations (37a) to (37e) are easily derived from equation (36) or (63). Extensibility of the cable can be neglected by equating U to zero.

Derivation of the value of S

If it is assumed that

(i)   length of the cable l = span L

(ii)   initial tension in the cable = H , throughout its length, and

(iii)   increment in cable tension = h , throughout its length

then the extension of the cable due to h = $\dfrac{hL}{AE}$ and S = 1.

The above assumptions are justifiable for a small ratio of dip to span. A more accurate expression for the extensibility of the cable is derived here. The change in cable tension $\Delta \bar{T}$ for an applied load P (see Figure 3) can be evaluated by considerations of statics.

$$\Delta \bar{T}_{(x = -L/2 \text{ to } rL)} = \left\{ (V_A - w.x)^2 + (h+H)^2 \right\}^{1/2} - \left\{ \left(\frac{wL}{2} - wx \right)^2 + H^2 \right\}^{1/2} = \Delta \bar{T}_1 \qquad (64a)$$

and $\quad \Delta \bar{T}_{(x = rL \text{ to } L/2)} = \left\{ (V_A - P - wx)^2 + (h+H)^2 \right\}^{1/2} - \left\{ \left(\frac{wL}{2} - wx \right)^2 + H^2 \right\}^{1/2} = \Delta \bar{T}_2 \qquad (64b)$

The initial length of a small element of the cable dL is given by equation (48a) as

$$= \left\{ 1 + \left(\frac{dy}{dx} \right)^2 \right\}^{1/2} \quad \text{or} \quad \left\{ 1 + \frac{w^2 x^2}{H^2} \right\}^{1/2}$$

The extension of the cable becomes

$$e'_1{}_{(x = -L/2 \text{ to } rL)} = \frac{1}{AE} \int_{-L/2}^{rL} \Delta \bar{T}_1 \cdot \left(1 + \frac{w^2 x^2}{H^2} \right)^{1/2} \cdot dx \qquad (65a)$$

$$e'_2{}_{(x = rL \text{ to } L/2)} = \frac{1}{AE} \int_{rL}^{L/2} \Delta \bar{T}_2 \cdot \left(1 + \frac{w^2 x^2}{H^2} \right)^{1/2} \cdot dx \qquad (65b)$$

The value of S is evaluated here for $r = 0$, in which case the equations (65a) and (65b) are identical and the total extension becomes

$$e = 2e_1' \tag{66}$$

The value of e is obtained by numerically integrating the expression in equation (66), and S can be evaluated as

$$S = \frac{e}{hL/AE}$$

The calculations have been done for a cable of span 100 in. and weight 1 lb./in. of span. It will be seen from the following values that the value of $\overline{W}$ does not appreciably affect S .

d/L	$\overline{W}$	S
0.05	0.1	1.012656
0.05	1.0	1.013007

Values of S have been obtained for $\overline{W} = 0.1$ for other values of d/L and are given below

d/L	S
0.05	1.012656
0.10	1.048925
0.20	1.190880

These values of S are very nearly equal to $(1 + 4.8 \frac{d^2}{L^2})$ and this expression has been adopted for general use to express the extensibility of the cable. The empirical constant of 4.8 could have been calculated with greater accuracy but it was considered needless because the results are not affected even if S is taken as unity (see Figures 5 and 6).

Appendix B

The computer programmes written to employ the 'Influence coefficient method' and the 'General method' to solve numerical problems are described here. The limitations of each programme are enumerated and their working is described by means of flow-diagrams. The symbols used and not covered by the general notation are defined by their use in the flow-diagram or defined separately.

Programme 1. Influence coefficient method for solving a plane system

The programme has the following limitations:-

(i)   Structure should be symmetrical about the y-axis and the x-axis passing through the centre point between the vertices of the two main cables.

(ii) $n \not> 20$

(iii)   n x total number of applied loads $\not> 400$

(iv)   At least one load must be applied on each cable, however its value can be put equal to zero.

(v) $R \not> 50$

(vi) $Q \not> 511$

The symbols not included in the general notation and also not clearly defined by the flow-diagram are given below:-

R   =   Number of loading cases

N'   =   Number of applied loads in each loading case on the upper cable

M'   =   "   "   "   "   "   "   "   "   "   lower   "

A_{22} $=$ $24 \omega t \; \dfrac{H^2}{WL}_2$

A_{23} $=$ ωt

$\bar{W}$ =   Unit load as proportion of wL

W⁴   =   Value of unit load in units of wL

Matrix A' = n x n sized left hand side matrix in equation (43)

Matrix B' = the right hand side matrix for R loading cases, size n x R

$$
\text{Matrix } \bar{T} =
\begin{array}{c}
\\
T_1 \\
\\
\\
T_h \\
\\
\\
\\
\\
T_n
\end{array}
\begin{vmatrix}
1 & 2 & 3 & \text{-------R} \\
\end{vmatrix}
\qquad \text{Size } n \times R.
$$

Programme 2. General method for solving a plane system

The programme is written to assume the geometry of the main wires, correct it if necessary and then solve the structure for applied loading or movements at the supports. The structure should be symmetrical about the y-axis and n should not be greater than 20.

Following are the symbols needing separate defination:-

M = Number of iterative cycles required to correct the initially assumed geometry.

S = Number of iterative cycles required to obtain a solution for applied loading.

Matrix A = Matrix consisting of the coefficients of the unknown matrix $\bar{U}$, and is generated from the left hand side of Equation (33). Size of the matrix is (4n x 4n).

$$
\text{Matrix } \bar{U} =
\begin{vmatrix}
\vdots \\
V_h \\
U_h \\
\vdots \\
\vdots \\
V_h \\
U_h \\
\vdots
\end{vmatrix}
\begin{array}{l}
\left.\begin{array}{c} \\ \\ \end{array}\right\} \text{Upper Cable} \\[2em]
\left.\begin{array}{c} \\ \\ \end{array}\right\} \text{Lower Cable}
\end{array}
$$

$$h = 1, 2 \cdots \cdots n$$

Matrix B = Right hand side matrix which is also produced from
equation (33) and its size is (4n x 1)

Matrix B = $B_1 + B_2$

where,

$$\text{Matrix } B_1 = \begin{vmatrix} \vdots \\ \dot{Y}_{\hbar} \\ X_{\hbar} \\ \vdots \\ Y_{\hbar} \\ X_{\hbar} \\ \vdots \end{vmatrix} \begin{matrix} \left.\vphantom{\begin{matrix}a\\b\end{matrix}}\right\} \text{Upper Cable} \\ \\ \left.\vphantom{\begin{matrix}a\\b\end{matrix}}\right\} \text{Lower Cable} \end{matrix} \quad \hbar = 1,2 \cdots\cdots n$$

and

$$\text{Matrix } B_2 = \begin{vmatrix} \vdots \\ Ky_{\hbar} \\ Kx_{\hbar} \\ \vdots \\ Ky_{\hbar} \\ Kx_{\hbar} \\ \vdots \end{vmatrix} \begin{matrix} \left.\vphantom{\begin{matrix}a\\b\end{matrix}}\right\} \text{Upper Cable} \\ \\ \left.\vphantom{\begin{matrix}a\\b\end{matrix}}\right\} \text{Lower Cable} \end{matrix} \quad \hbar = 1,2 \cdots\cdots n$$

Output block No.1:

Prints matrix $\bar{U}$ in a block by itself with a maximum of L' numbers on a line. —

Output block No.2:

Prints ΔFo_i for the upper cable
    " ΔFo_i " " lower "
    " ΔFo_i " " hanger
   The output is in a block by itself with 3 numbers per line
   i = 1, 2, 3 .... n for hangers
   i = 0, 1, 2, 3 .... n for cables

Programme 3.   Solution of a three-cable system

The programme either reads in as data the values of x_k, y_k, z_k, lo_i and Fo_i or establishes the initial geometry of the structure and then finds solutions for applied loads. The structure should be symmetrical about the y-axis and the value of n should not exceed 9.

The following notation needs separate definition:-

Matrix A = The matrix containing the coefficients of the unknown matrix $\bar{U}$ and is produced by using equation (33). It is (9n x 9n) in size.

$$
\text{Matrix } \bar{U} =
\left|
\begin{array}{l}
\vdots \\
u_h \\
w_h \\
v_h \\
\vdots \\
u_h \\
w_h \\
v_h \\
\vdots \\
u_h \\
w_h \\
v_h \\
\vdots
\end{array}
\right|
\begin{array}{l}
\left.\begin{array}{l} \\ \\ \\ \end{array}\right\} \text{Cable 1 (fig.36)} \\
\left.\begin{array}{l} \\ \\ \\ \end{array}\right\} \text{Cable 2 (,,)} \\
\left.\begin{array}{l} \\ \\ \\ \end{array}\right\} \text{Cable 3 (,,)} \\
h = 1, 2, \cdots \cdots n
\end{array}
\qquad \text{Size } (9n \times 1)
$$

Matrix B is the right hand side matrix produced from equation (33).
It is (9n x 1) in size.

Matrix B = B_1 + B_2

where,

$$
\text{Matrix } B_1 =
\left|
\begin{array}{l}
\vdots \\
X_h \\
Z_h \\
Y_h \\
\vdots \\
X_h \\
Z_h \\
Y_h \\
\vdots \\
X_h \\
Z_h \\
Y_h \\
\vdots
\end{array}
\right|
\begin{array}{l}
\left.\begin{array}{l} \\ \\ \\ \end{array}\right\} \text{Cable 1} \\
\left.\begin{array}{l} \\ \\ \\ \end{array}\right\} \text{Cable 2} \\
\left.\begin{array}{l} \\ \\ \\ \end{array}\right\} \text{Cable 3} \\
h = 1, 2 \cdots \cdots n
\end{array}
$$

$$\text{Matrix } B_2 = \begin{vmatrix} \begin{matrix} \vdots \\ K_{x_h} \\ K_{z_h} \\ K_{y_h} \\ \vdots \end{matrix} \Big\} \text{ Cable 1} \\ \begin{matrix} \vdots \\ K_{x_h} \\ K_{z_h} \\ K_{y_h} \\ \vdots \end{matrix} \Big\} \text{ Cable 2} \\ \begin{matrix} \vdots \\ K_{x_h} \\ K_{z_h} \\ K_{y_h} \\ \vdots \end{matrix} \Big\} \text{ Cable 3} \end{vmatrix} \qquad h = 1, 2 \cdots \cdots n$$

$$\text{Matrix } \bar{V} = \begin{vmatrix} \begin{matrix} \vdots \\ \bar{w}'_h \\ \bar{v}'_h \\ \vdots \end{matrix} \Big\} \text{ Cable 1} \\ \begin{matrix} \vdots \\ \bar{w}'_h \\ \bar{v}'_h \\ \vdots \end{matrix} \Big\} \text{ Cable 2} \\ \begin{matrix} \vdots \\ \bar{w}'_h \\ \bar{v}'_h \\ \vdots \end{matrix} \Big\} \text{ Cable 3} \end{vmatrix} \qquad \text{Size } (6n \times 1)$$

$$h = 1, 2 \cdots \cdots n$$

Matrix C = Matrix consisting of the coefficient of $\bar{V}$ is calculated from the left hand side of equations (25 b and c).

Matrix D = Right hand side matrix produced from equations (23 b and c).

Output block No. 1:

(i)   Prints F'_i for cables 1, 2 and 3 and prints l'_i for cables 1, 2 and 3 in a block by itself with 6 numbers on each line;

i = 0, 1, 2 .... n

(ii)   Prints l'_i for hangers 1, 2 and 3 in a block by itself, with 3 numbers on each line; i = 1, 2, ... n.

(iii) Prints z_k for cables 1, 2 and 3 and prints y_k for cables 1, 2 and 3 in a block by itself with 6 numbers on each line;

k = 0, 1, 2 .... (n + 1)

Output block No. 2

(i)   Prints z_k for cables 1, 2 and 3 and y_k for cables 1, 2 and 3 in a block by itself with 6 numbers on each line;

k = 0, 1, 2 .... (n + 1)

(ii) Prints $l'^{(v)}_i$ for cables 1, 2 and 3 and $l'^{(v)}_i$ for hangers 1, 2 and 3 in a block by itself with 6 numbers on each line except when i = 0 and there are only 3 numbers on the line;

i = 1, 2, ... n for the hangers; i = 0, 1, 2 .... n for the cables.

Output block No. 3

Prints ΔFo_i for cables 1, 2 and 3 and prints ΔFo_i for hangers 1, 2 and 3 in a block by itself, with 6 numbers on each line except when i = 0 and there are only three numbers on the line;

i = 1, 2 .... n for the hangers; i = 0, 1, 2 .... n for the cables

START

READS O', Q'

K' = 1

READS L, $1/(AE)_c$, $(r)_{m=1}$, a/L, $(r)_{n=n}$, $(\delta)_{n=1}$, a/L, $(\delta)_{n=n}$, d_U, d_-, D, $1/(AE)_n$, A_{22}, A_{23}, R, M', N'

READS M' VALUES OF $\bar{W}$
" " " " r
" N' " " $\bar{W}$
" " " " T

S = 1

S = S+1

S > R? NO / YES

READS w, w', ń, G

EVALUATES MATRIX A' AND PUTS A' = 1000 A'

EVALUATES MATRIX B' AND PUTS B' = 1000 B'

PRINTS 0.5 × B COLUMN BY COLUMN. EACH COLUMN GIVES THE VALUES OF 1000×ll_h OR 1000 × ℓ_h FOR A LOADING CASE, AND IS OUTPUT IN SEPERATE BLOCKS, WITH O' NUMBERS PER LINES

INVERTS A AND EVALUATES $\bar{T}$, $\bar{T} = A^{-1}B$

$\bar{G} = w'\bar{T}$

PRINTS $\bar{G}$ IN THE SAME WAY AS B'

S = 1

EVALUATES h_U/H AND h_L/H AND PRINTS EACH ON A SEPARATE LINE

S = S+1

S > R? NO / YES

K' = K'+1

K' > Q' ? YES END

FLOW-DIAGRAM FOR PROGRAMME 1

START

READS $L', 0', S, M, n, T, J',$ $(AE)c_U, (AE)c_L, (AE)_h, a,$ $X_1, X_2, X_{(n+1)}, D, d_U, d_L,$ R_U, R_L, H_U, H_L

$N' = 1$

ASSUMES INITIAL SHAPE; EVALUATES ℓ'_i AND F_{i} FOR CABLES. $i = 0, 1 \cdots n$

$M = 0$?

NO → CORRECTS THE INITIALLY ASSUMED SHAPE IN M CYCLES OF ITERATION

YES

EVALUATES ℓ_{0i} FOR HANGERS AND EQUATES F_{0i} TO T $i = 1, 2 \cdots n$

SETS UP MATRIX A; PUTS A = ·0001 A; EVALUATES A^{-1}

$M' = 1$

READS NEXT PROBLEM

NO

YES

$N' > J$?

$N' = N + 1$

$M' > J$? NO → READS NEXT CASE OF LOADING.

YES

$M' = M' + 1$

READS MATRIX ·0001 B_1, Y_{U1}, β_{U1}, Y_{U2}, β_{U2}, Y_{L1}, β_{L1}, Y_{L2}, β_{L2}

$S' = 1$

EQUATES U AND U AT THE SUPPORT TO Y_{U1}, β_{U1} ETC.

$O' = 1$

END

$O' = 0$ $O' = ?$ $O' = 2$

ASSUME $\bar{U}^{(S')} = 0$

YES

$S' > S$? NO

SETS UP MATRIX B_2; PUTS $B_2 = ·0001 B_2$; PUTS $B = B_1 + B_2$

ASSUME $\bar{U}^{(S')} = \frac{1}{2} \bar{U}^{(S')} + \frac{1}{2} \bar{U}^{(S-1)}$

OUTPUT BLOCK NO. 2

EVALUATES ℓ_i AND FROM IT THE VALUES OF ΔF_{0i} FOR ALL MEMBERS

ASSUME $\bar{U}^{(S')} = \bar{U}^{(S-1)}$

EVALUATES $\bar{U}^{(S')}$ AS, $\bar{U}^{(S')} = A^{-1} B$

OUTPUT BLOCK NO. 1

$S' = S + 1$

NO $S' > 2$? YES

FLOW-DIAGRAM FOR PROGRAMME 2

START

READS A'

$B' = 1$

READS $W', L', (n+2),$ $S', C_0, D, C_1, D_1, T_0, C_2,$ $D_2, T_1, C_3, D_3, T_2, X_1, a.$

$W' = 0$? — YES

NO

$S = 1$

ASSUMES y_k AND $\mathcal{z}_k$ FOR THE CABLES; $k = 1, 2 \cdots n.$

EQUATES F_i' FOR THE HANGERS TO T_0', T_1 AND T_2 RESPECTIVELY

EVALUATES l_i' AND F_i' FOR THE CABLES; AND l_i' FOR HANGERS

OUTPUT BLOCK NO. 1

READS M'

$I' = 1$

SETS UP MATRICES C AND D

EVALUTES MATRIX $\bar{V}$ $\bar{V} = C^{-1} D$

PUTS $y_k = y_k + U_k$, $\mathcal{z}_k = \mathcal{z}_k + W_k$ AND EVALUATES $l_i'^{(w)}$

OUTPUT BLOCK NO. 2

$I' > M'$? — NO

YES

$S = S + 1$

$S > S'$? — NO ... YES

READS y_k FOR CABLES 1, 2, 3; " $\mathcal{z}_k$ " " " $k = 0, 1, 2 \cdots (n+1)$

READS F_{0i} FOR CABLES 1, 2, 3; " l_{0i} " " " $i = 1, 2, \cdots n$

READS l_{0i} FOR HANGERS 1, 2 AND 3 $i = 1, 2 \cdots n$

READS $S', Z', (AE)c_{1;2;3},$ $(AE)_{h_{1;2;3}}, L'.$

SETS UP MATRIX A AND PUTS $A = .0001$

$Z' = 0$? — NO — PRINTS A' ROW BY ROW

YES

EVALUATES A^{-1}

$S = 1$

READS R'

READS $.0001 \times B_1$

$Q' = 1$

ASSUME $\bar{U}^{(Q')} = 0$

EVALUATES B_2 PUTS $B = B_1 + B_2$

EVALUATES $\bar{U}^{(Q')}$ $\bar{U}^{(Q')} = A^{-1} B$

PRINTS $\bar{U}^{(Q')}$ WITH L' NUMBERS ON EACH LINE

$Q' = Q' + 1$

$Q' > 2$? — NO

YES

ASSUME $\bar{U}^{(Q')}$ $= 0.5 \bar{U}^{(Q')} + 0.5 \bar{U}^{(Q'-1)}$

EVALUATES l_i AND ΔF_{0i} FOR THE CABLES AND THE HANGERS.

OUTPUT BLOCK NO. 3

$Q' > R'$? — NO

YES

$S = S + 1$

$S > S'$? — NO

YES

$B' = B' + 1$

$B' > A'$? — NO

YES

END

READS THE NEXT CASE OF LOADING

READS THE NEXT PROBLEM

FLOW-DIAGRAM FOR PROGRAMME 3

FIGURES

FIGURES 1, 2, 3 and 4 are on pages

5, 6, 9 and 18 respectively.
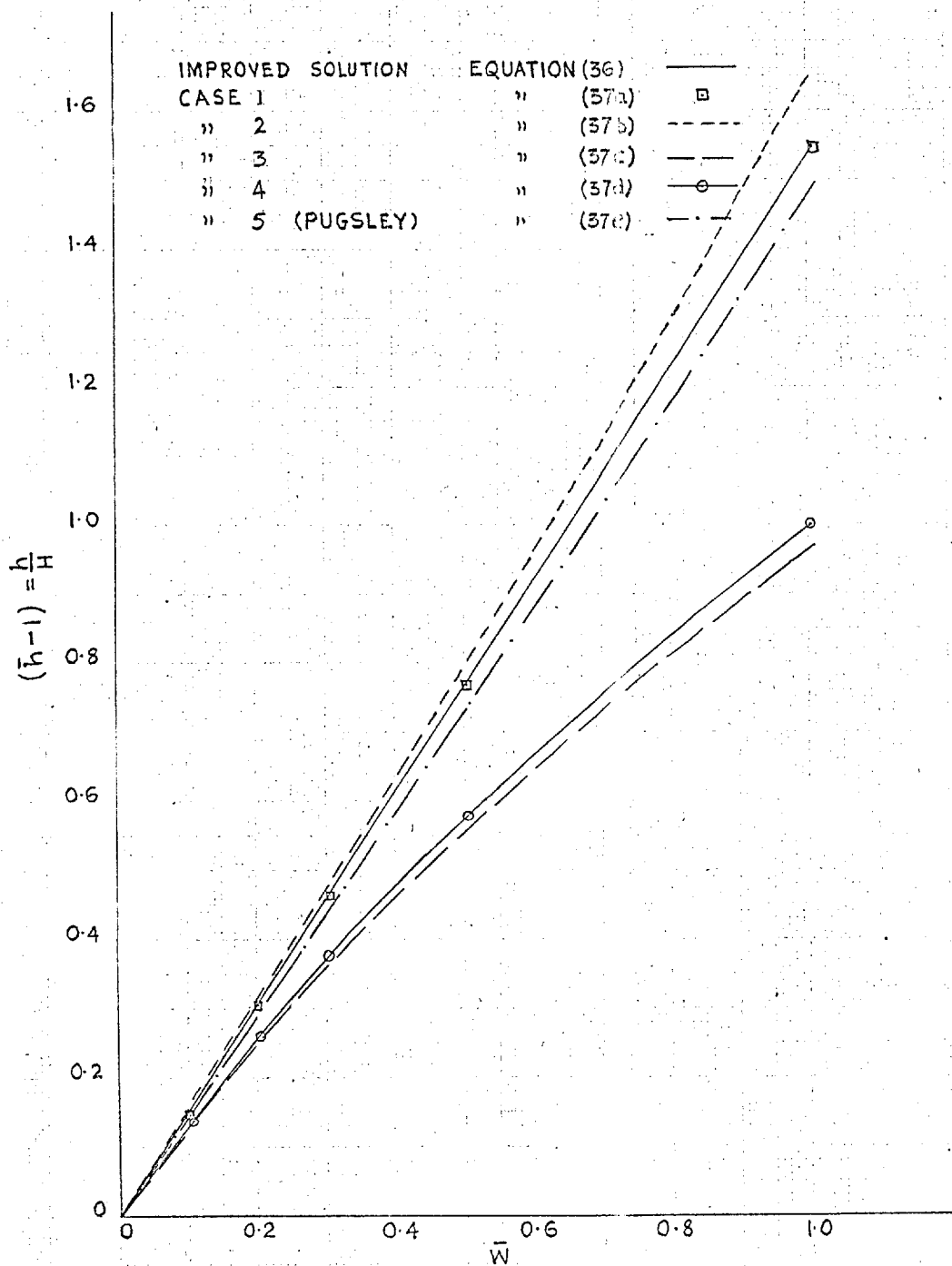
FIG.5 : LOAD $\bar{W}$ APPLIED TO A SINGLE CABLE
AT THE CENTRE POINT
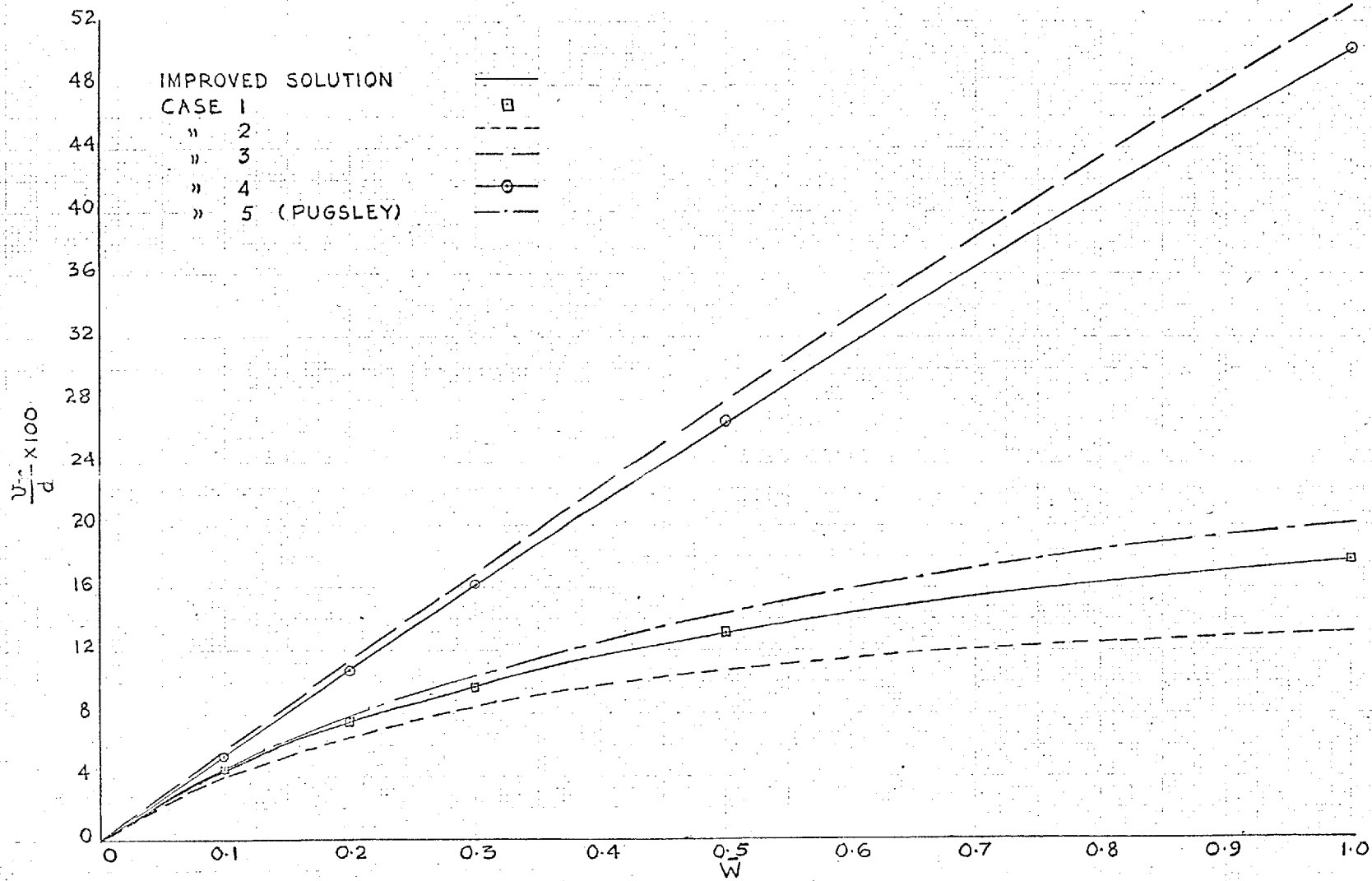
FIG. 6 : LOAD $\bar{W}$ APPLIED TO A SINGLE CABLE
AT THE CENTRE POINT
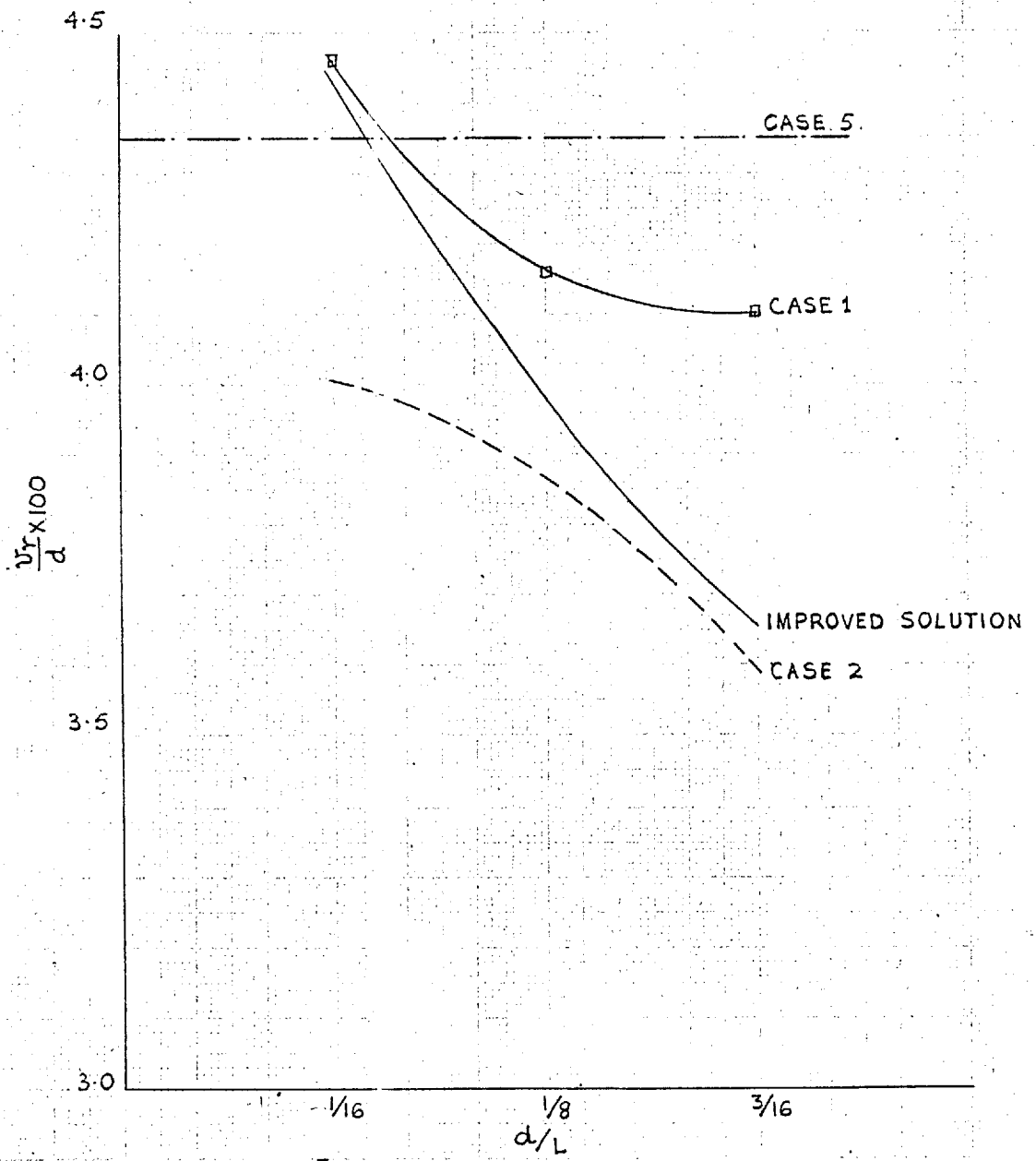
FIG. 7   LOAD W̄ APPLIED TO A SINGLE CABLE AT THE CENTRE POINT.
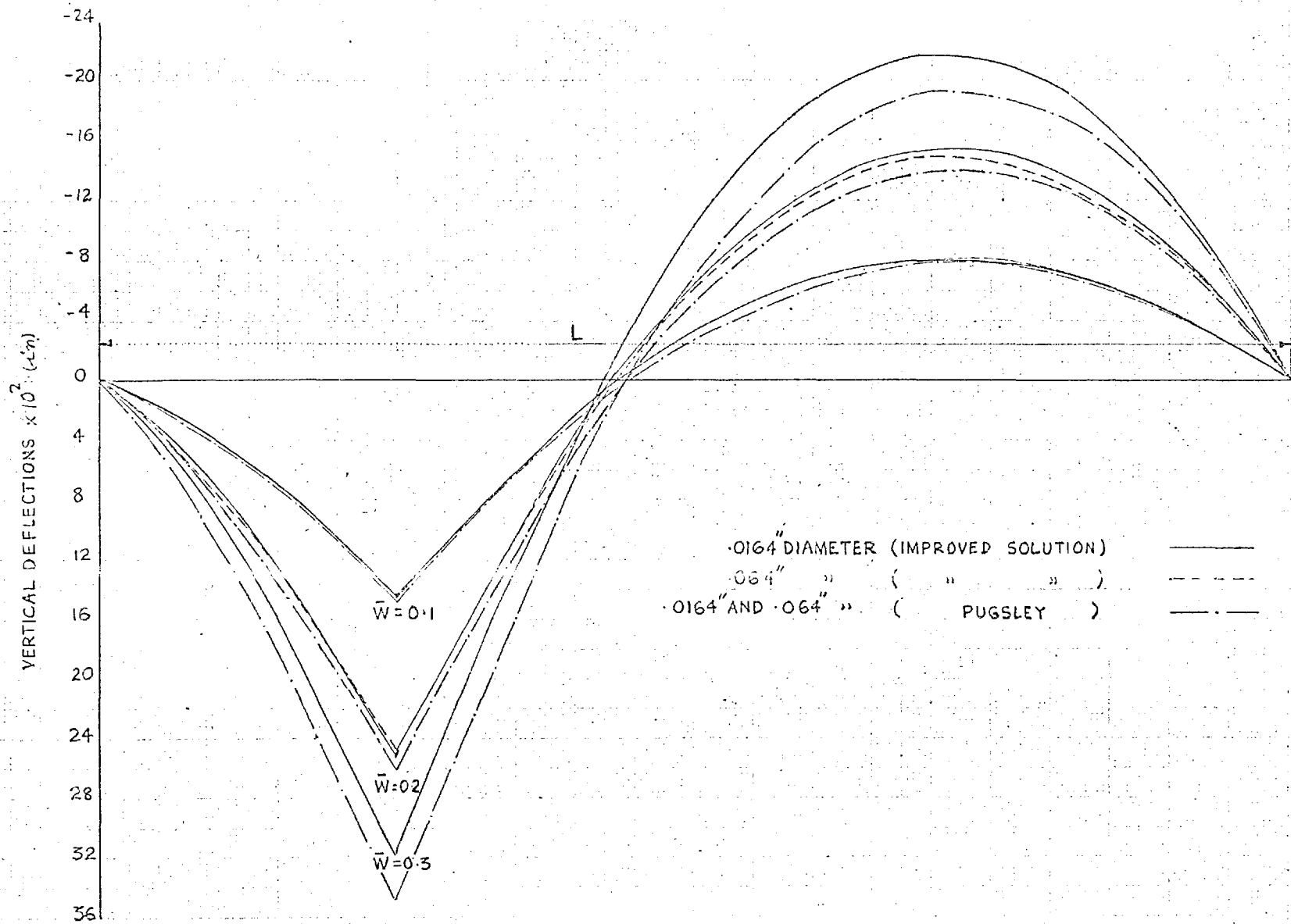
FIG. 8   POINT LOAD APPLIED AT THE QUARTER POINT TO
·0164" AND ·064" DIAMETER SINGLE CABLES.
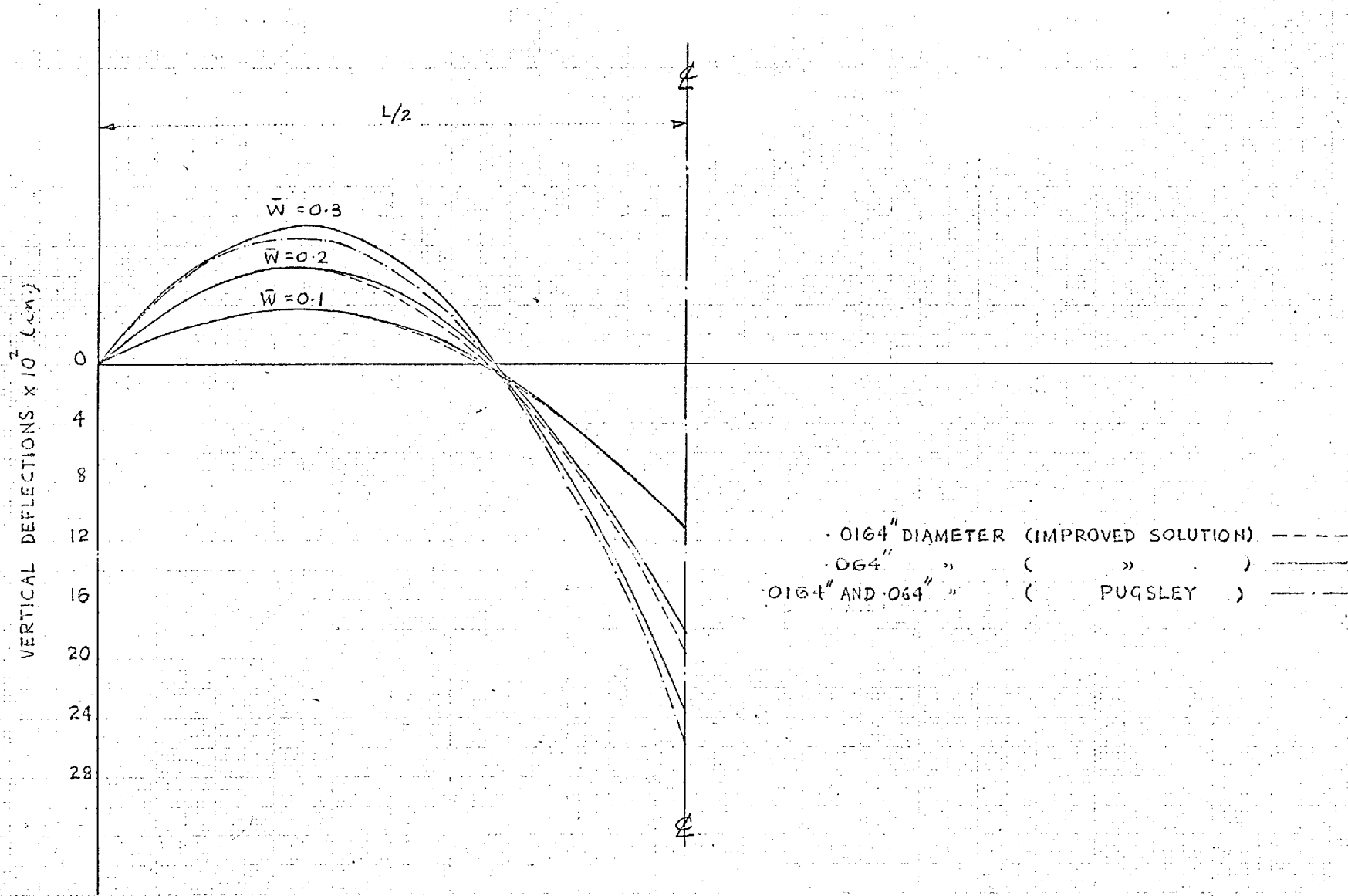
FIG. 9 POINT LOAD APPLIED AT THE CENTRE POINT TO
.0164" AND .064" DIAMETER SINGLE CABLES
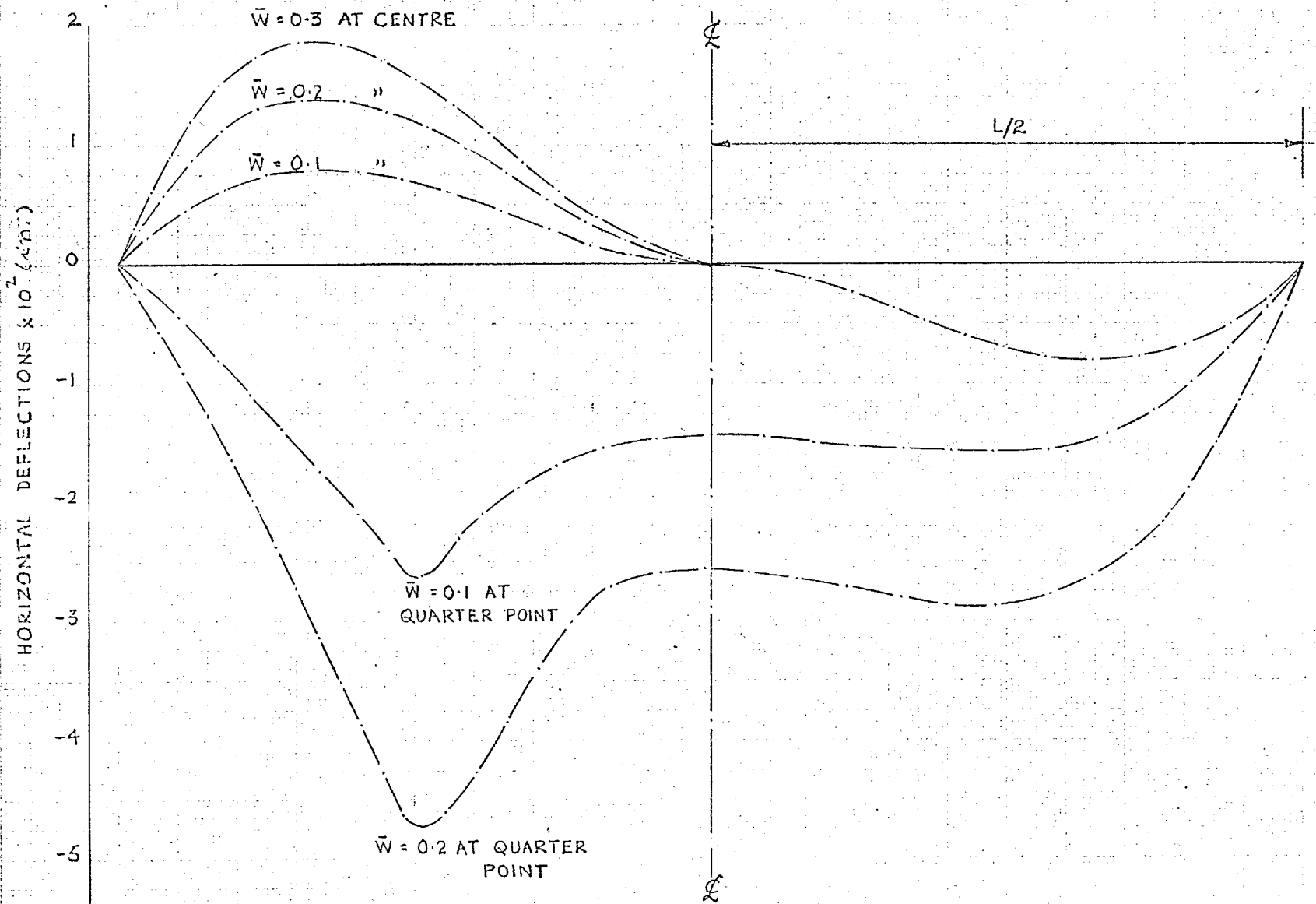
FIG.10   POINT LOAD APPLIED TO A SINGLE CABLE

FIGURES 11a and 11b are on page 32.

CHANGE IN HANGER TENSION (lb.)

0·1
0·0
-0·1
-0·2
-0·3
-0·4
-0·5
-0·6
-0·7

L

P = 2·5 lb. AT QUARTER POINT

GENERAL METHOD ———
INFLUENCE COEFFICIENT ,, — — —
EXPERIMENT —-⊙-—
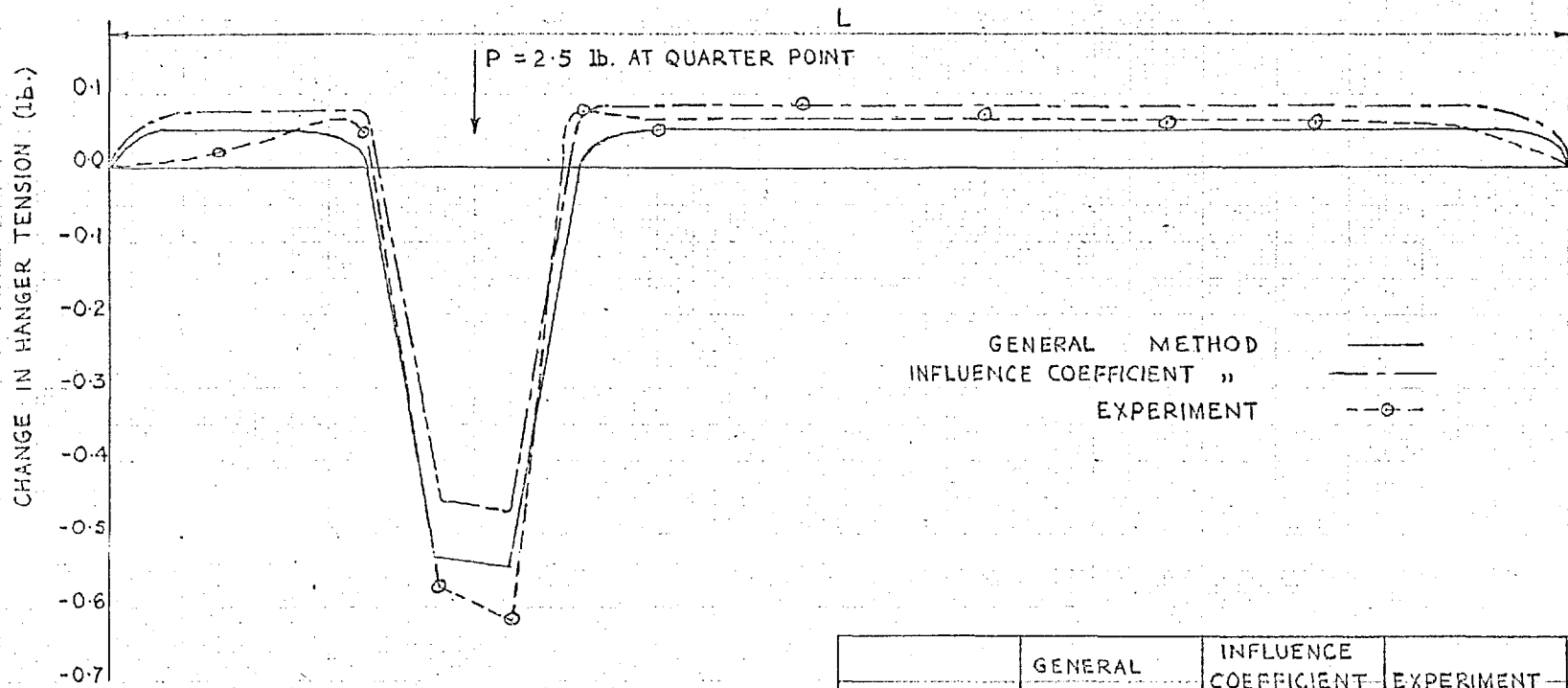
	GENERAL METHOD	INFLUENCE COEFFICIENT METHOD	EXPERIMENT
h_U (lb.)	4·80	6·70	4·70
h_L (lb.)	-0·60	1·00	-0·90

FIG. 12.   PLANE SYSTEM : POINT LOAD APPLIED
TO THE UPPER CABLE
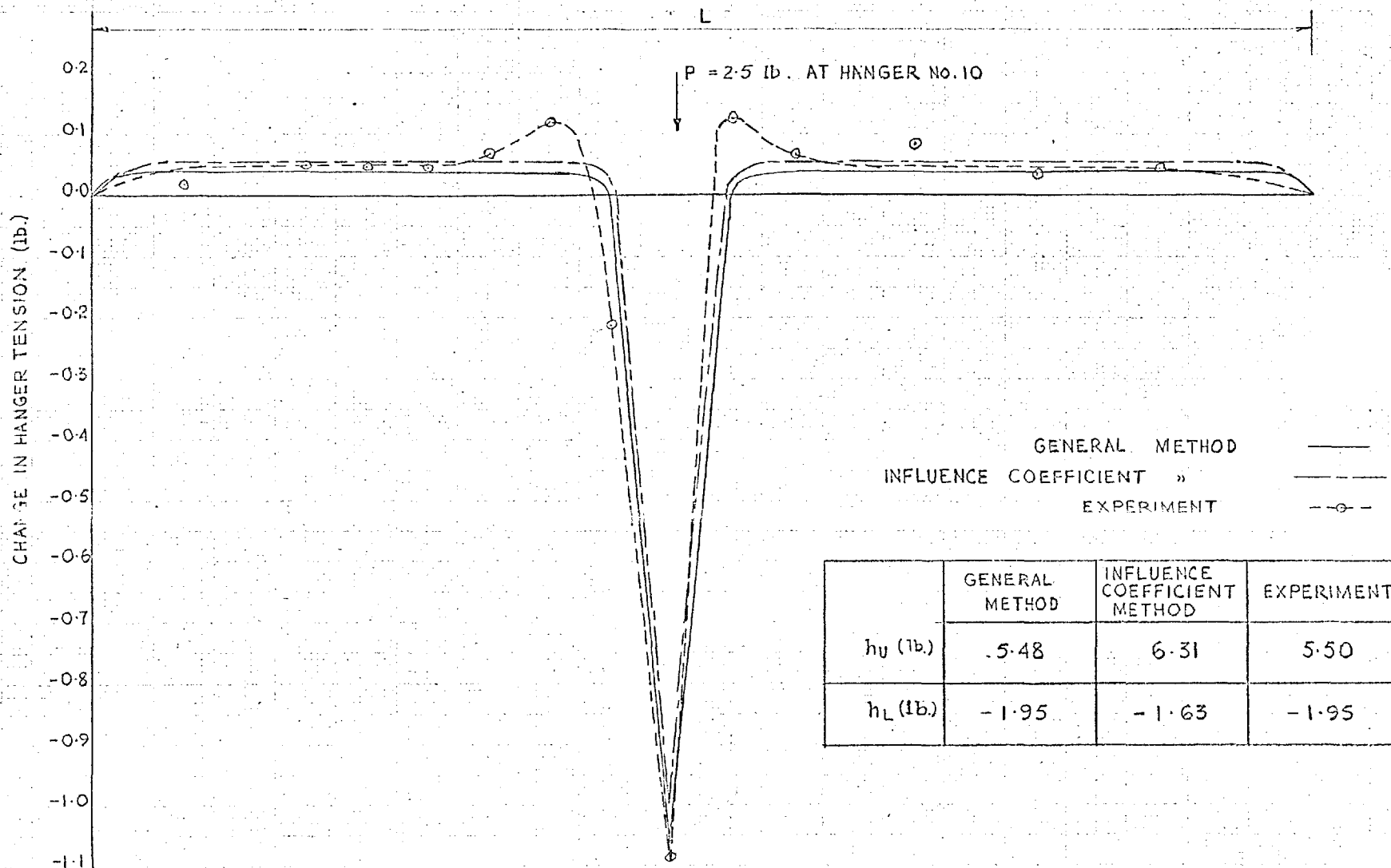
FIG.13. PLANE SYSTEM: POINT LOAD APPLIED
TO THE UPPER CABLE.
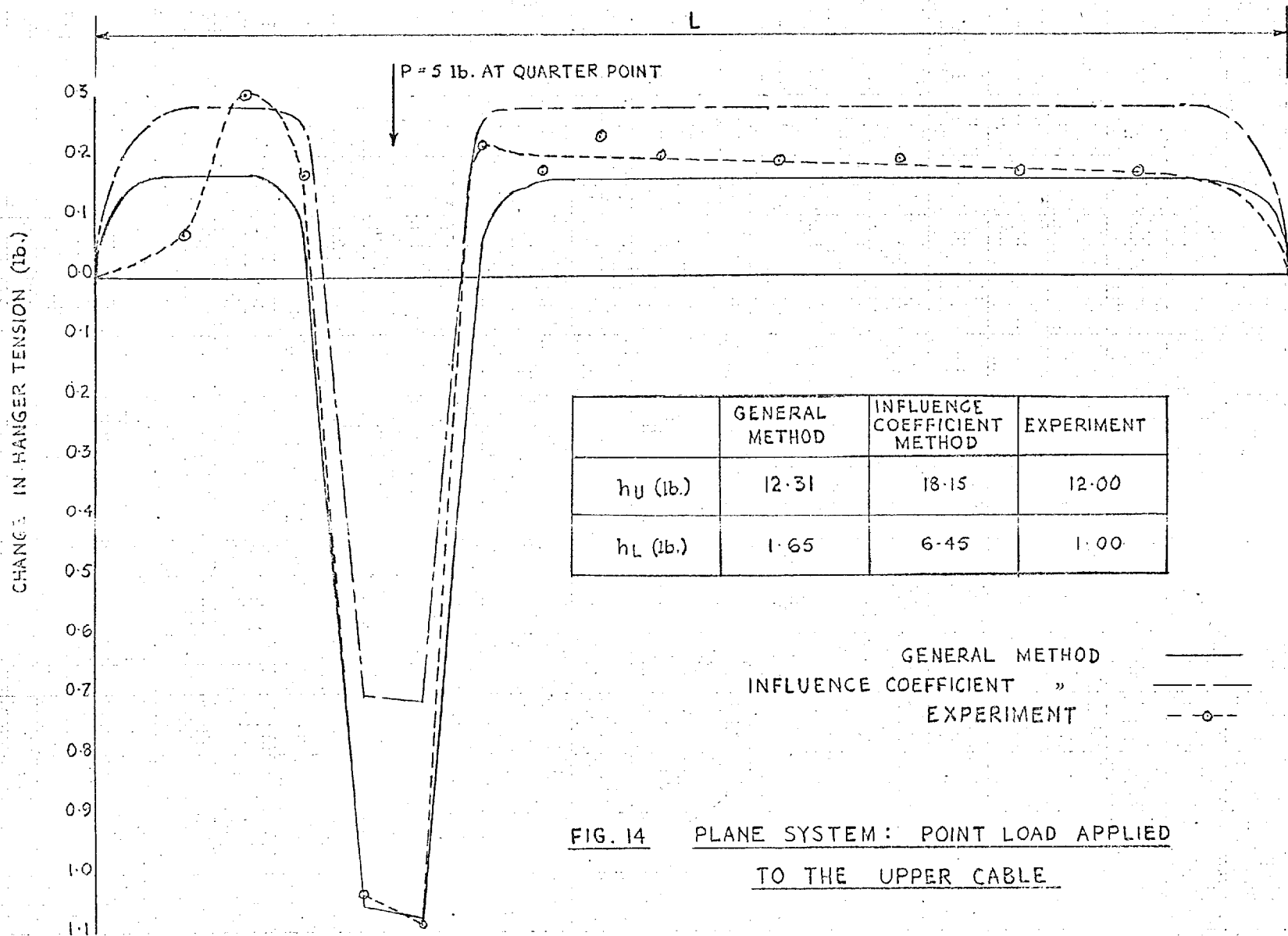
FIG. 14   PLANE SYSTEM: POINT LOAD APPLIED
TO THE UPPER CABLE
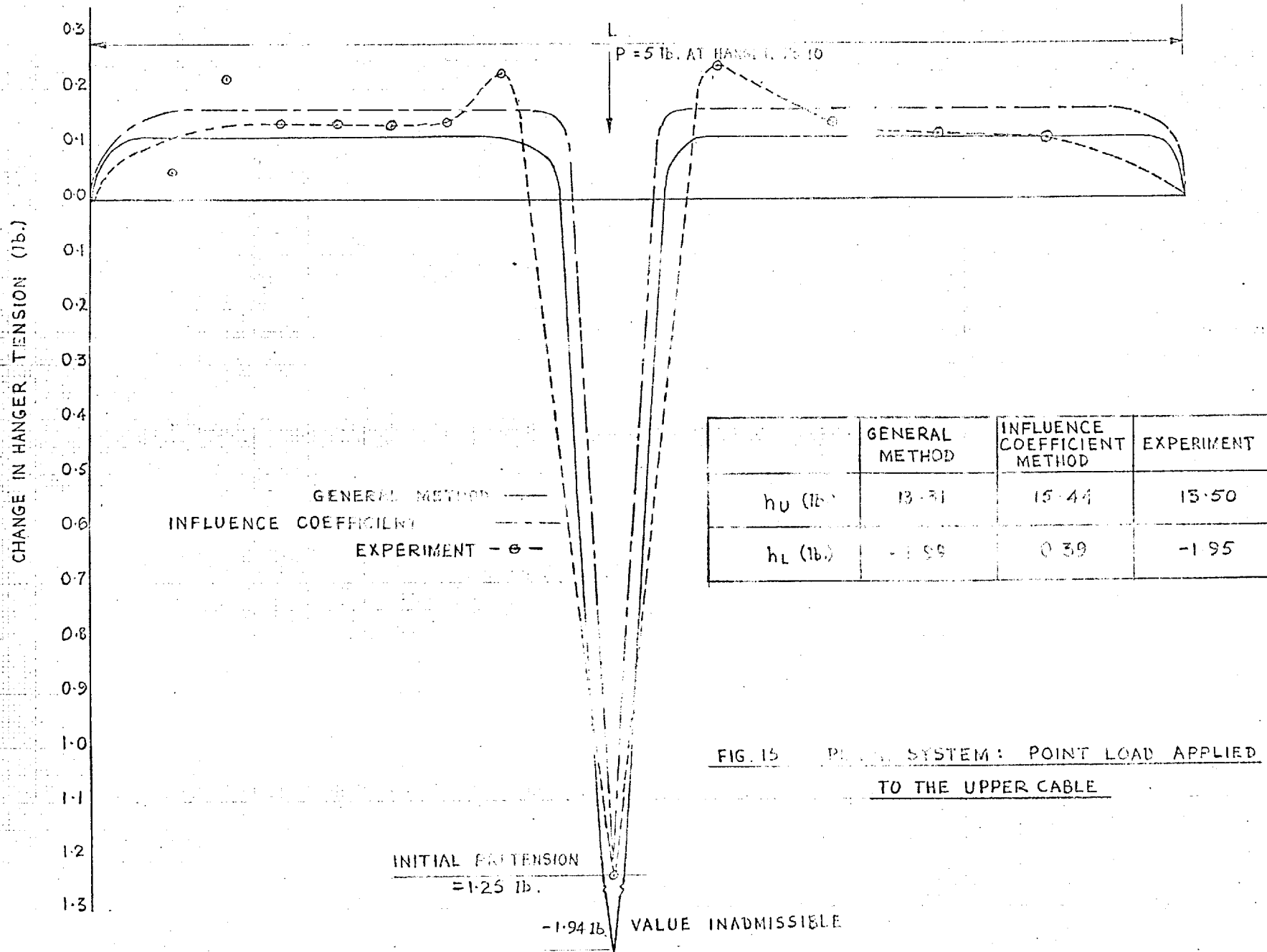
FIG. 15   PLATE SYSTEM : POINT LOAD APPLIED
           TO THE UPPER CABLE
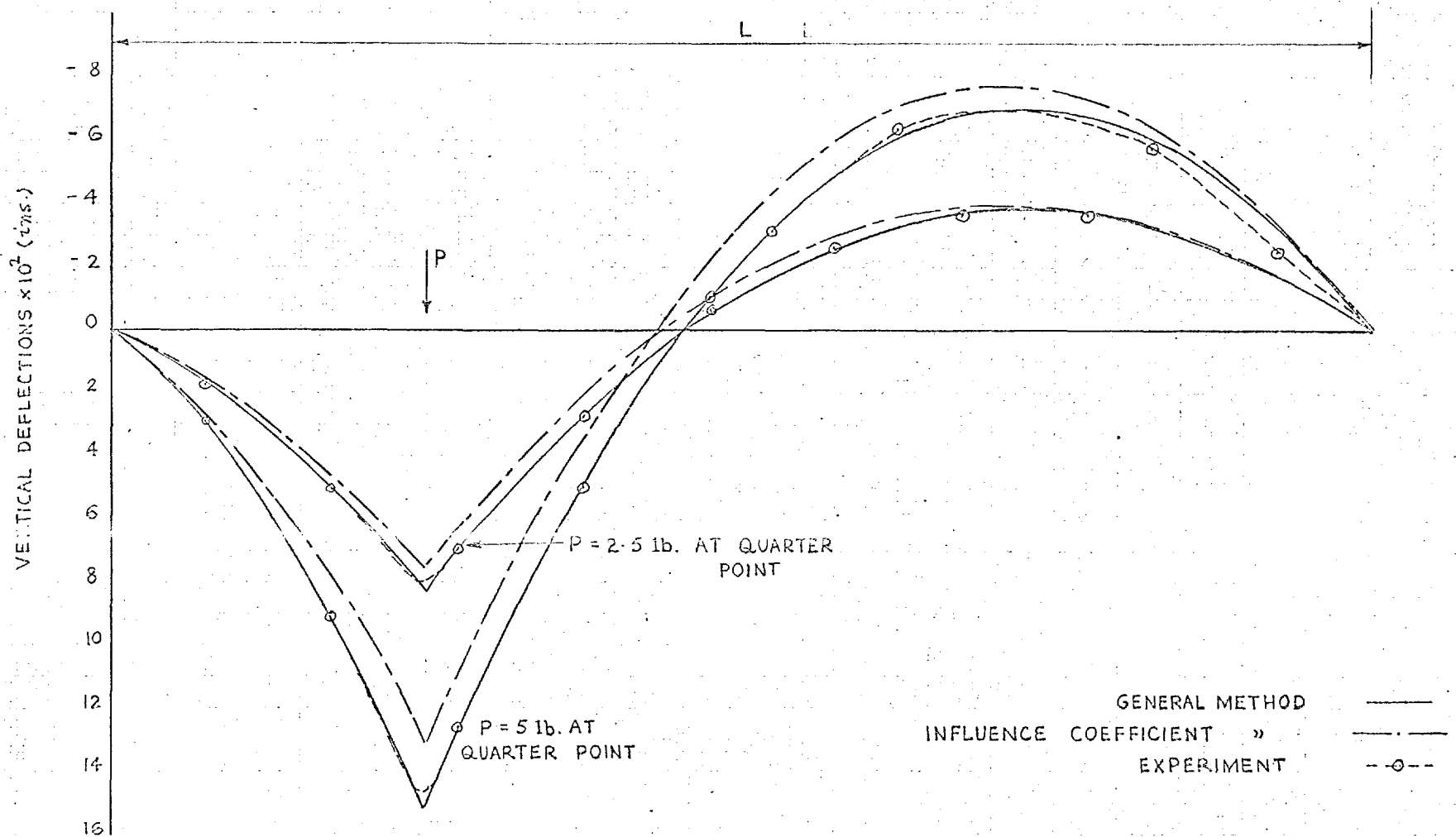
FIG.16   PLANE SYSTEM: POINT LOAD APPLIED
TO THE UPPER CABLE
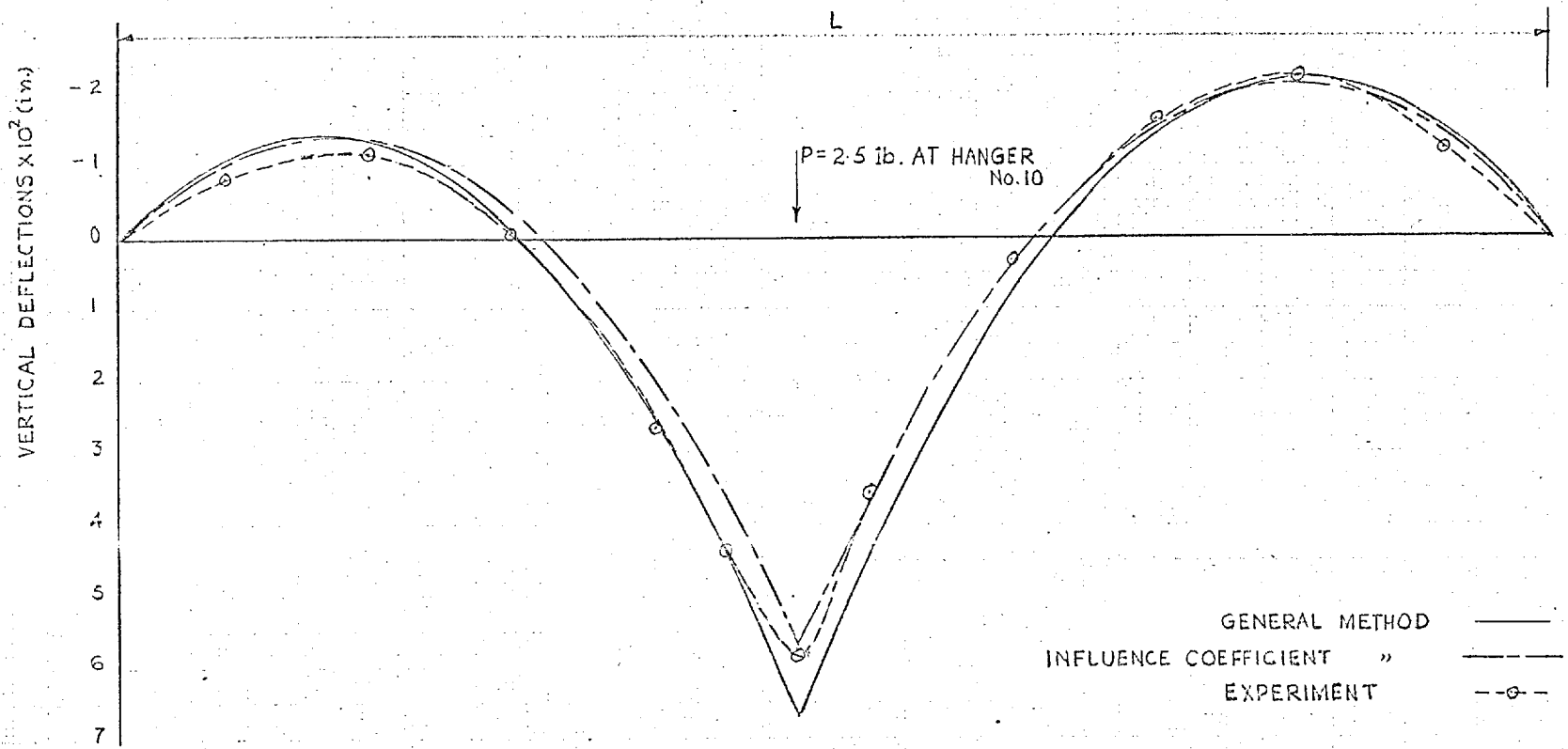
FIG.17.   PLANE SYSTEM : POINT LOAD APPLIED TO
                THE UPPER CABLE .
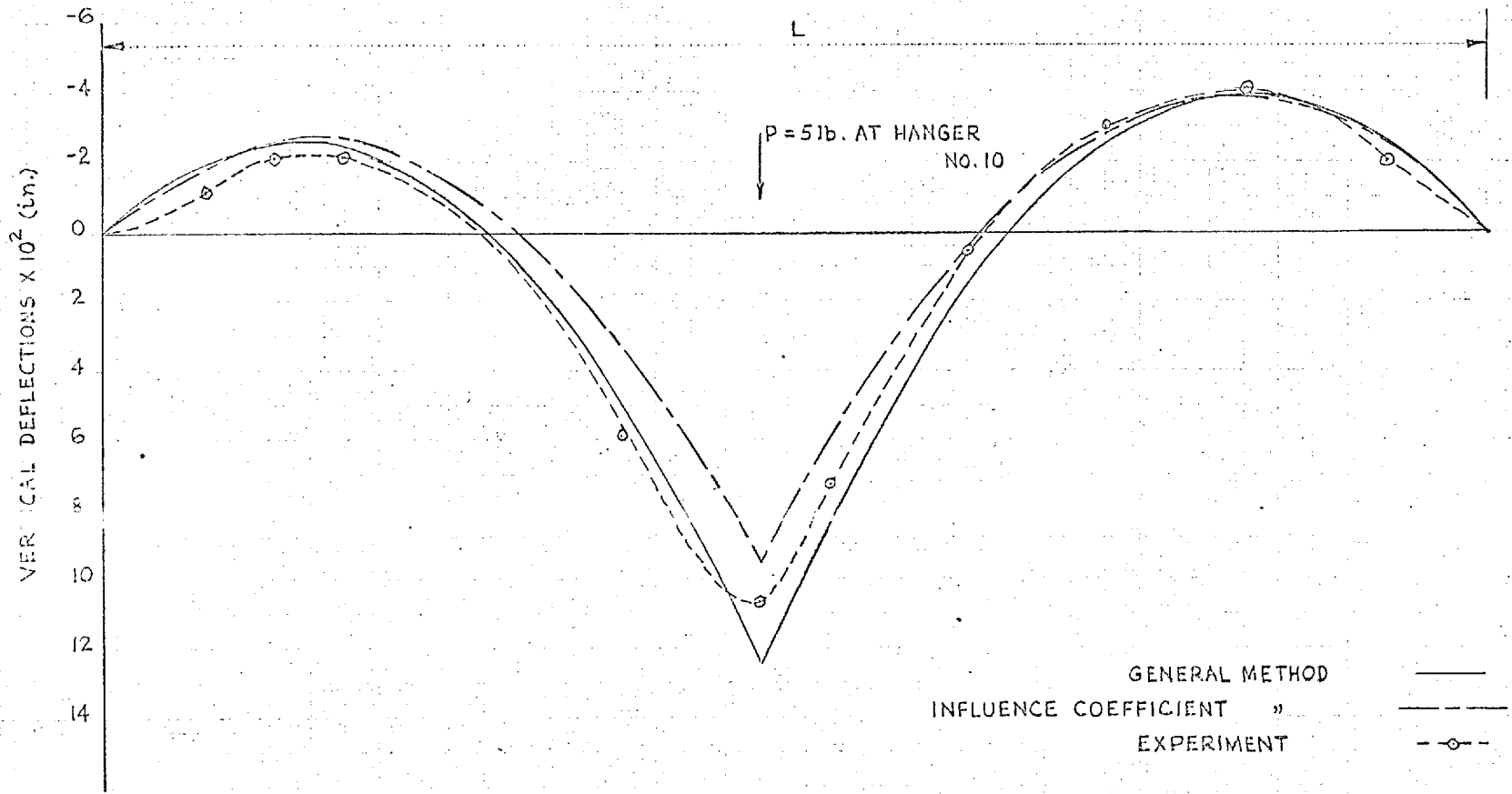
FIG. 18   PLANE SYSTEM :   POINT LOAD APPLIED
TO THE UPPER CABLE
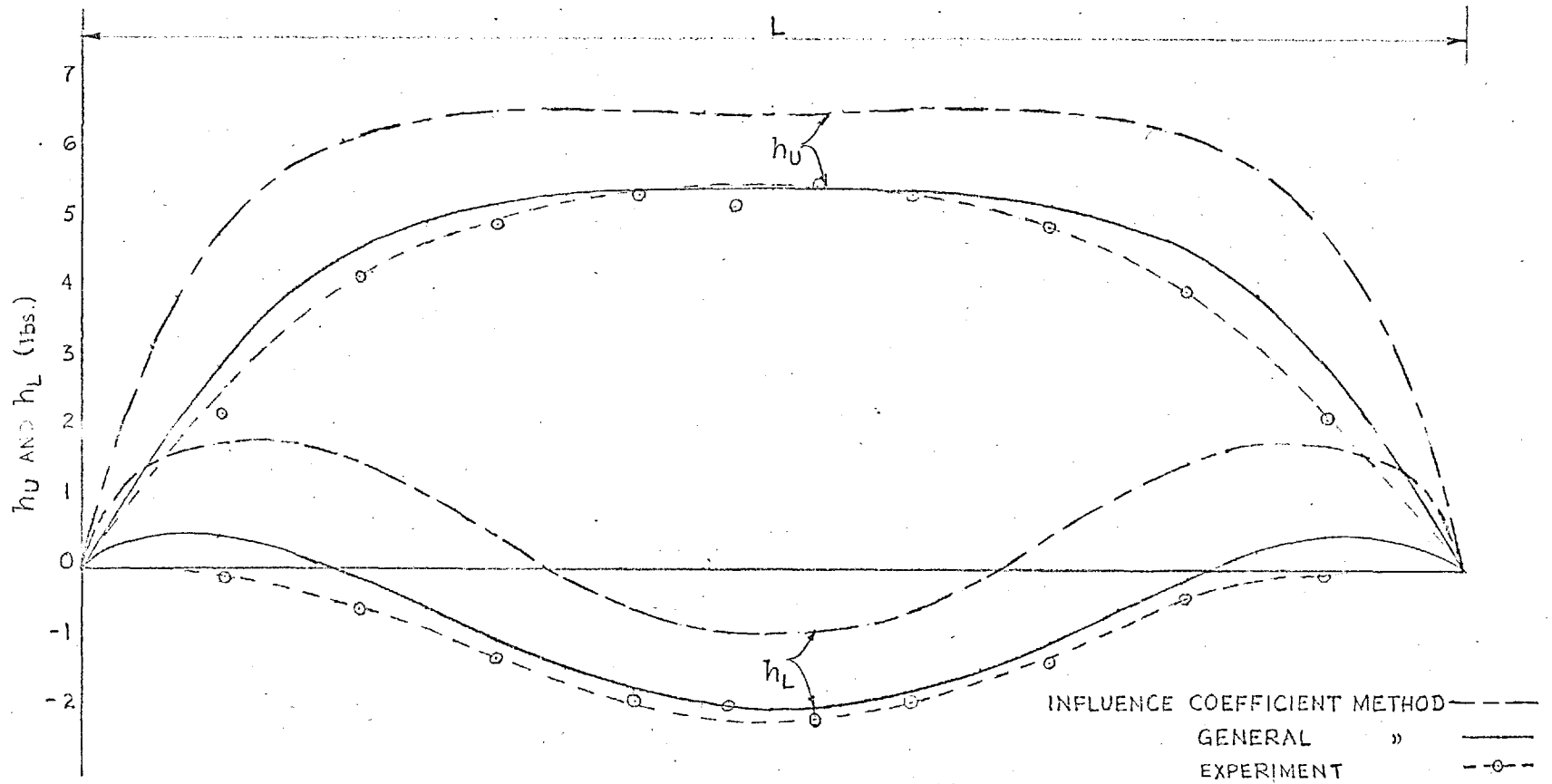
FIG. 19 INFLUENCE LINE FOR h_U AND h_L FOR A UNIT LOAD OF 2·5 lb.
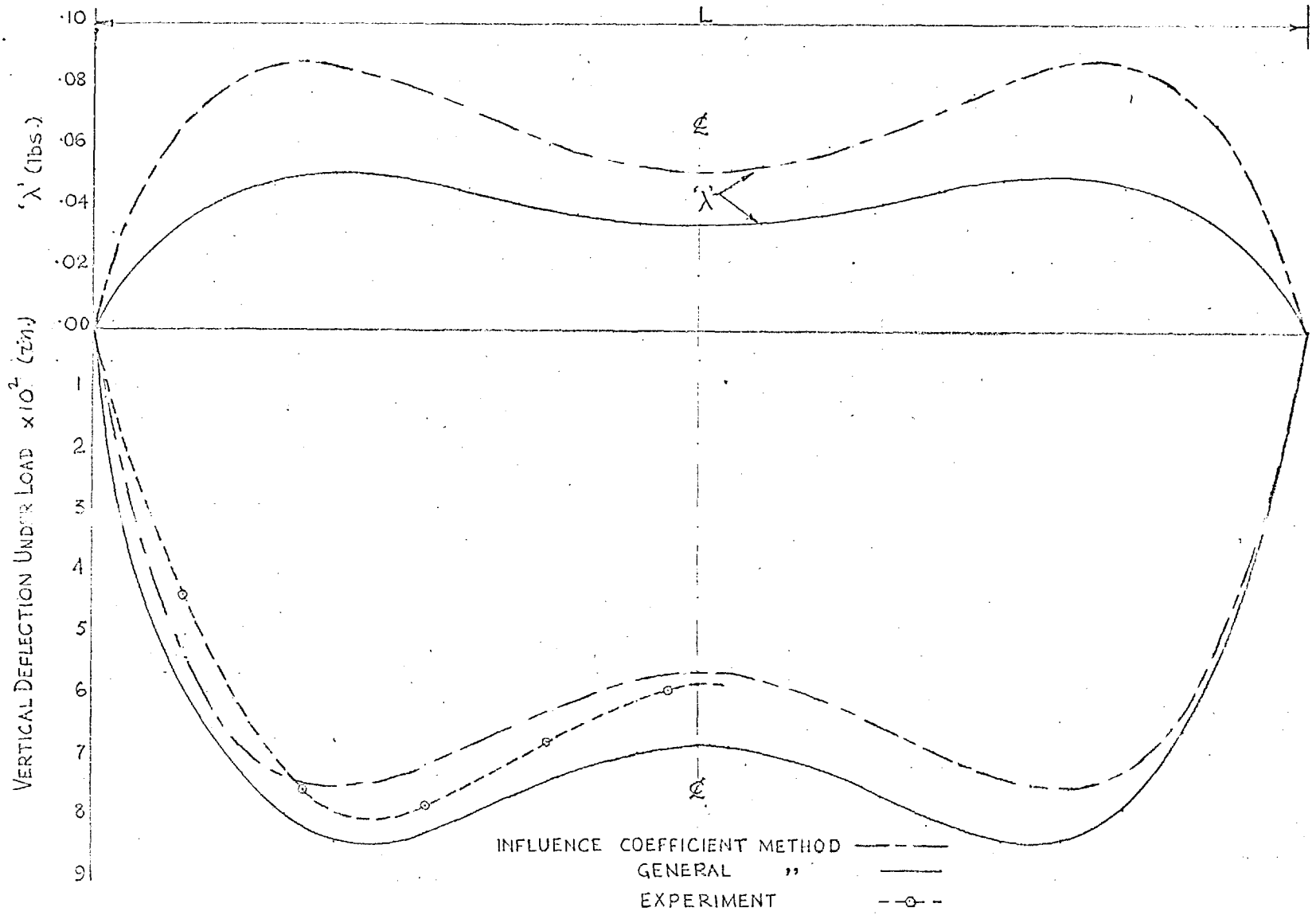
FIG. 20   INFLUENCE LINE FOR 'λ' AND DEFLECTIONS UNDER A UNIT
LOAD OF 2·5 lbs.
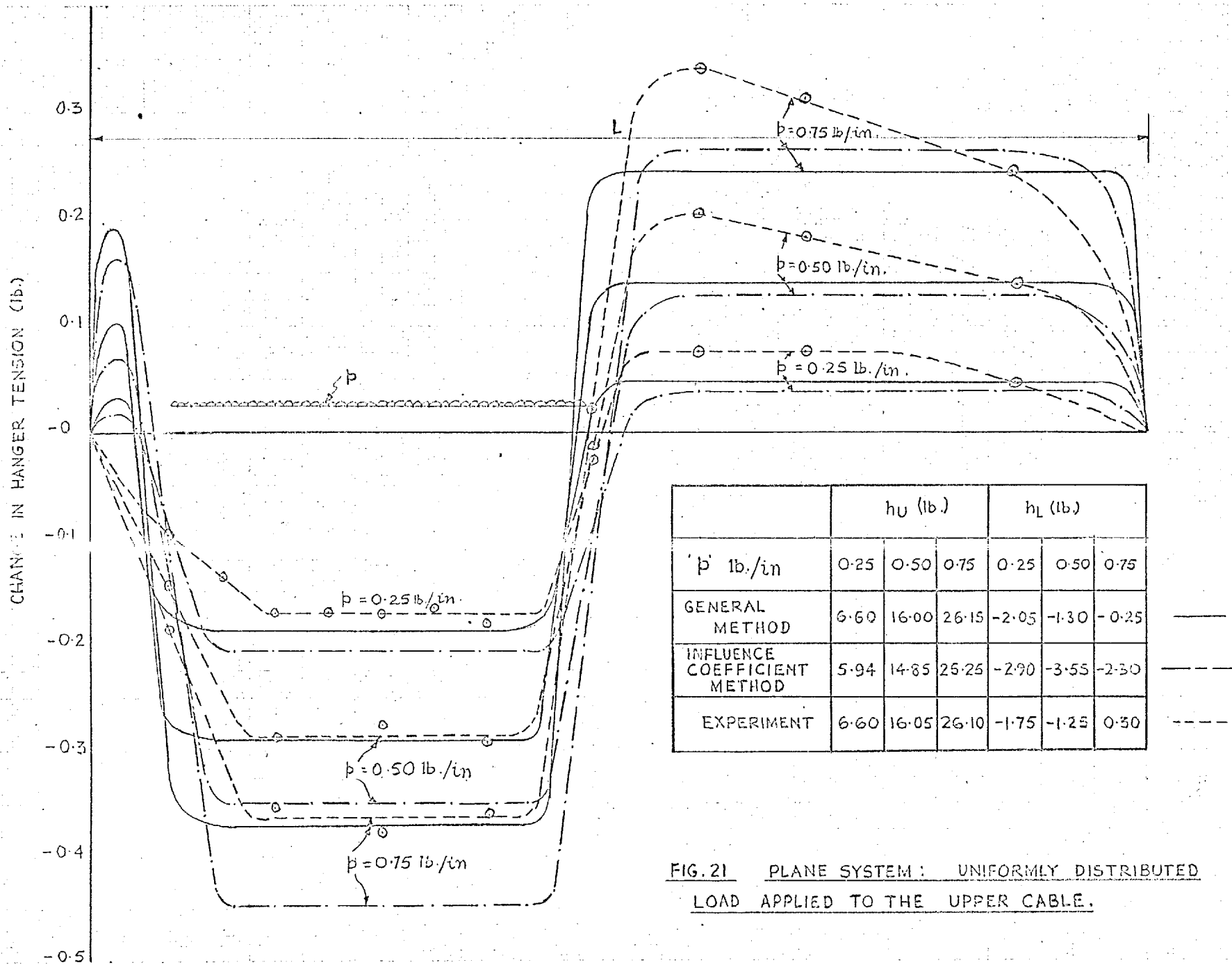
'p' lb./in	h_U (lb.)			h_L (lb.)			
	0.25	0.50	0.75	0.25	0.50	0.75	
GENERAL METHOD	6.60	16.00	26.15	-2.05	-1.30	-0.25	————
INFLUENCE COEFFICIENT METHOD	5.94	14.85	25.25	-2.90	-3.55	-2.30	— — —
EXPERIMENT	6.60	16.05	26.10	-1.75	-1.25	0.30	- - - -

FIG. 21   PLANE SYSTEM: UNIFORMLY DISTRIBUTED LOAD APPLIED TO THE UPPER CABLE.

		h_U (lb.)		h_L (lb.)	
p lb./in.	0·25	0·50	0·25	0·50	
GENERAL METHOD	6·18	15·00	-2·33	-1·90	————
INFLUENCE COEFFICIENT METHOD	5·65	14·85	-2·95	-2·65	— — —
EXPERIMENT	6·40	15·15	-2·15	-1·95	- - - -
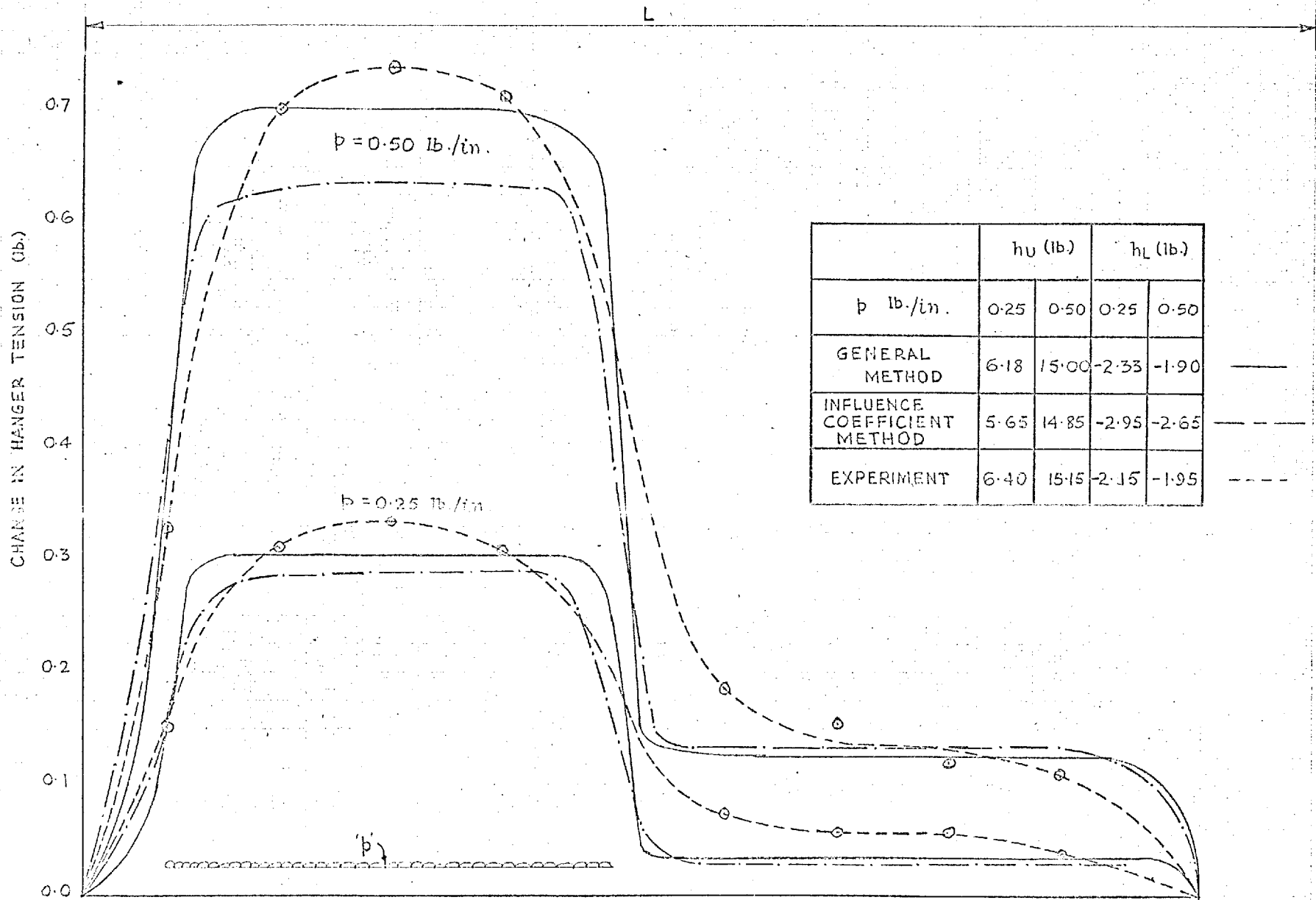
FIG. 22   PLANE SYSTEM : UNIFORMLY DISTRIBUTED LOAD APPLIED TO THE LOWER CABLE
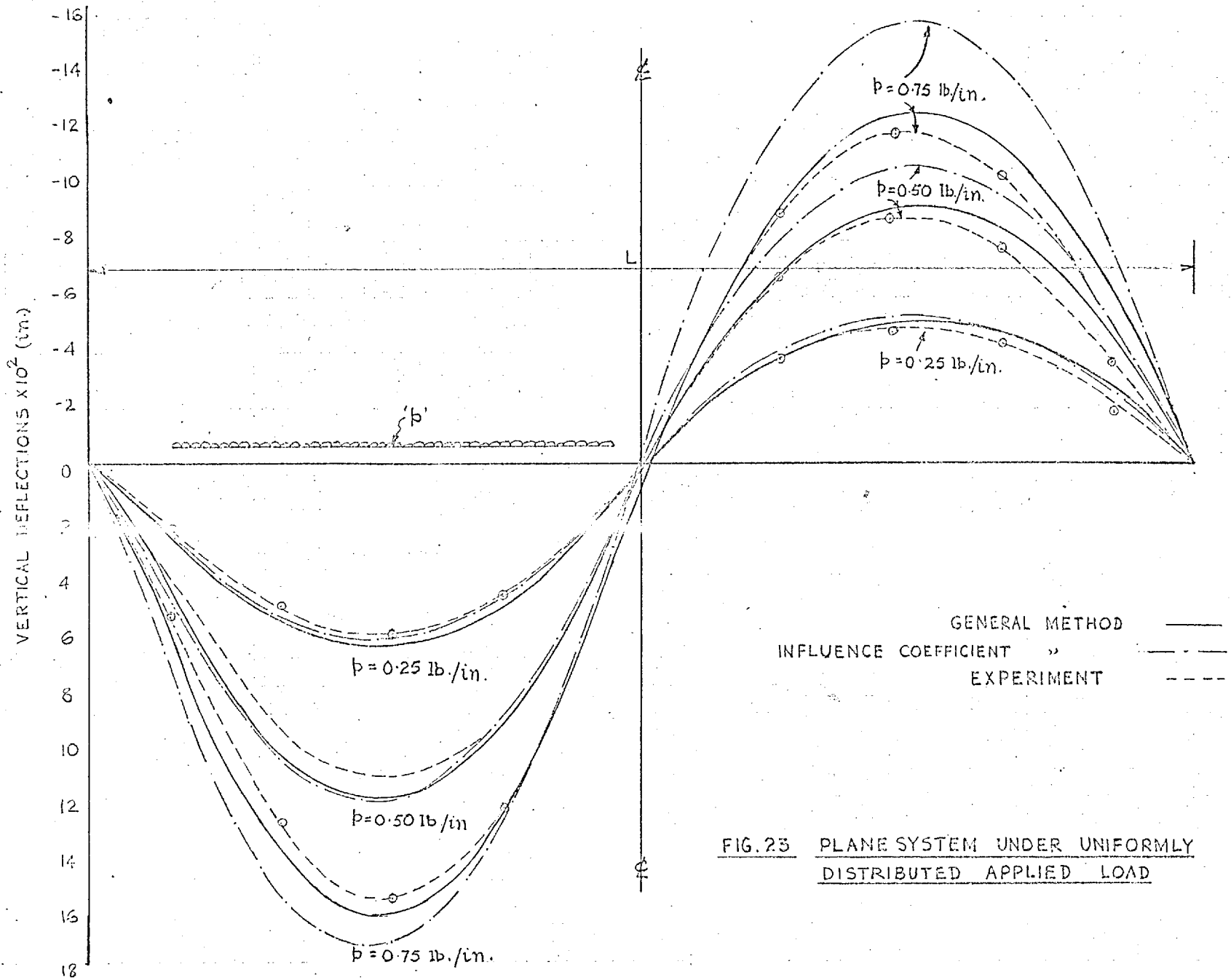
FIG. 23 PLANE SYSTEM UNDER UNIFORMLY DISTRIBUTED APPLIED LOAD
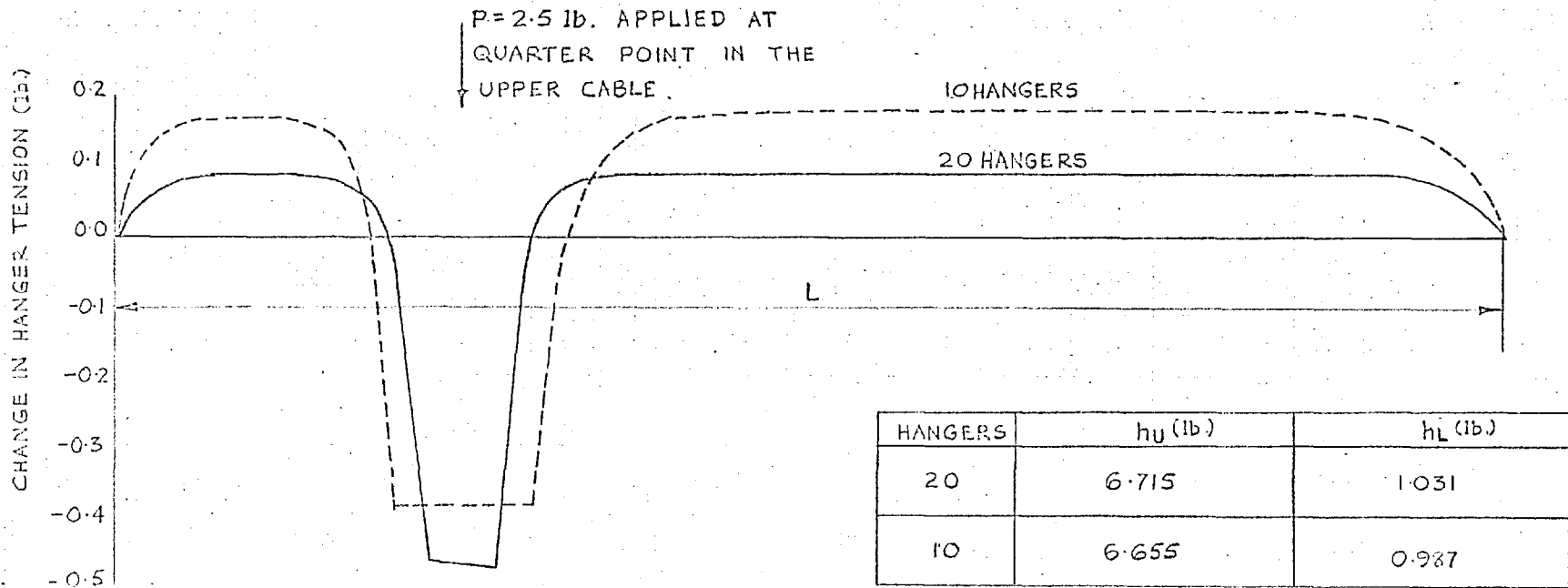
FIG. 24   EFFECT OF GROUPING HANGERS TOGETHER
IN INFLUENCE COEFFICIENT METHOD

P = 2·5 lb. APPLIED AT
QUARTER POINT IN
THE UPPER CABLE

VERTICAL DEFLECTIONS ×10² (in.)

L
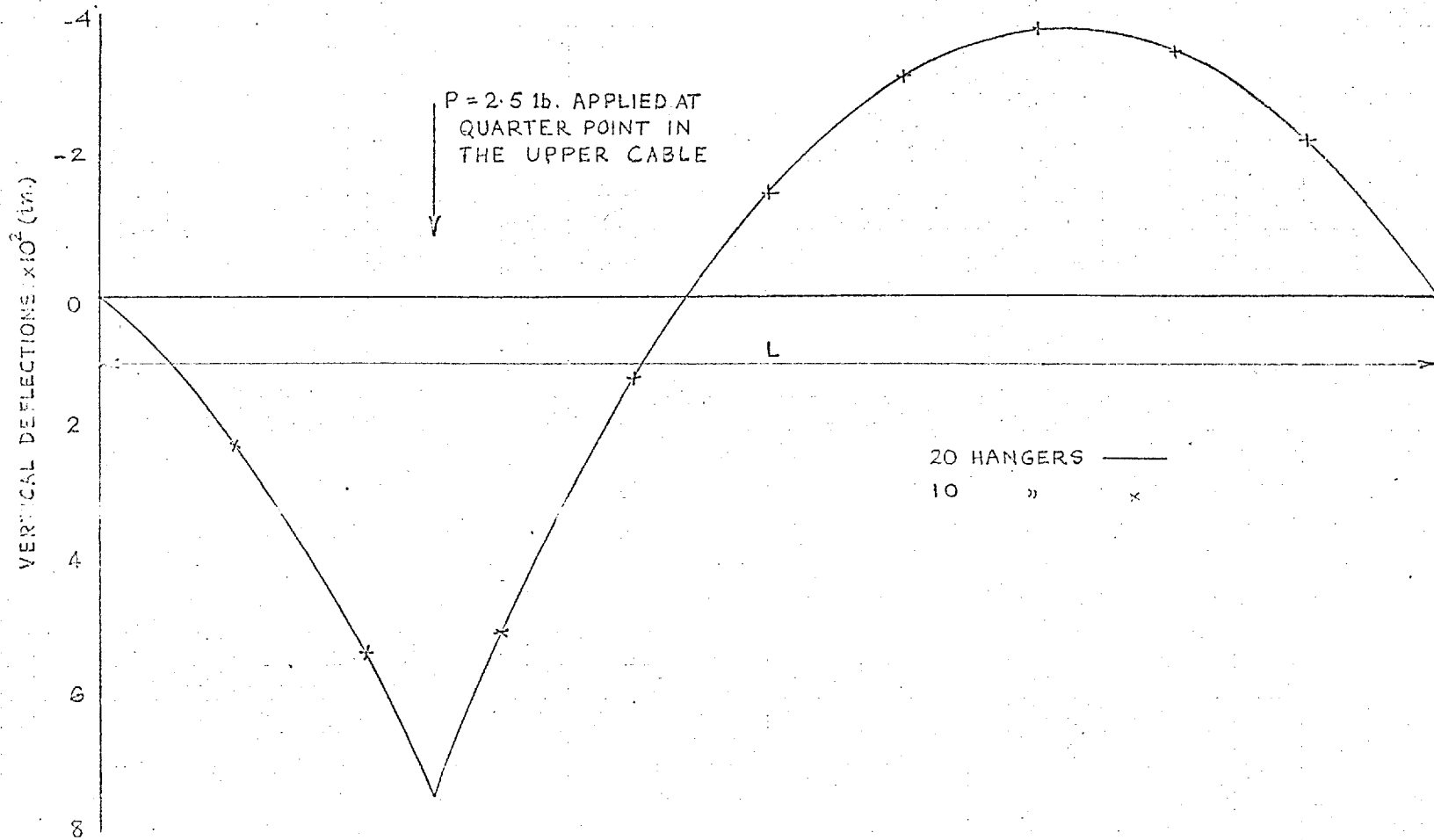
20 HANGERS ———
10   ,,   ×

FIG.25   EFFECT OF GROUPING HANGERS TOGETHER
IN INFLUENCE COEFFICIENT METHOD
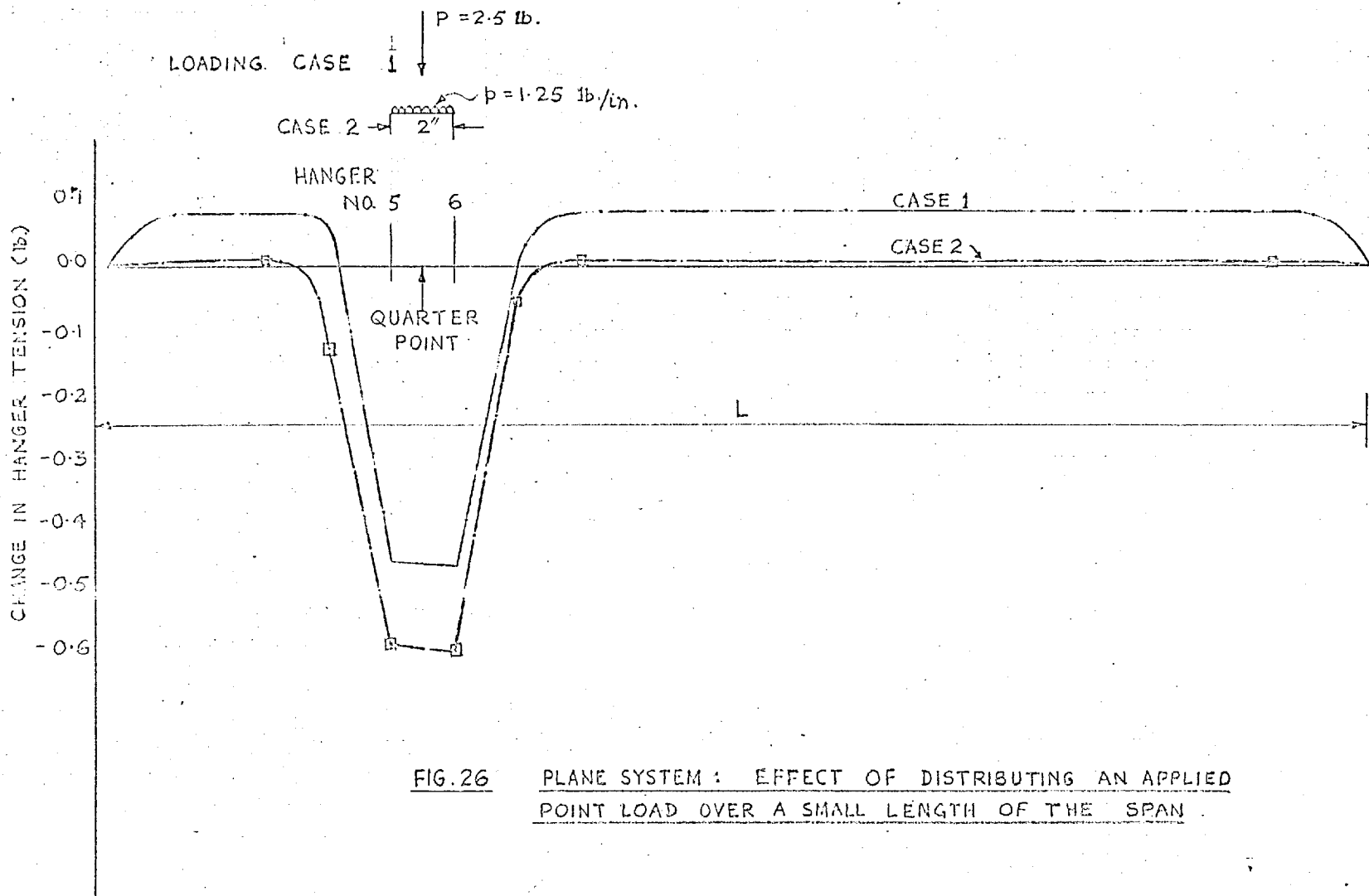
FIG. 26   PLANE SYSTEM :   EFFECT OF DISTRIBUTING AN APPLIED
POINT LOAD OVER A SMALL LENGTH OF THE SPAN.
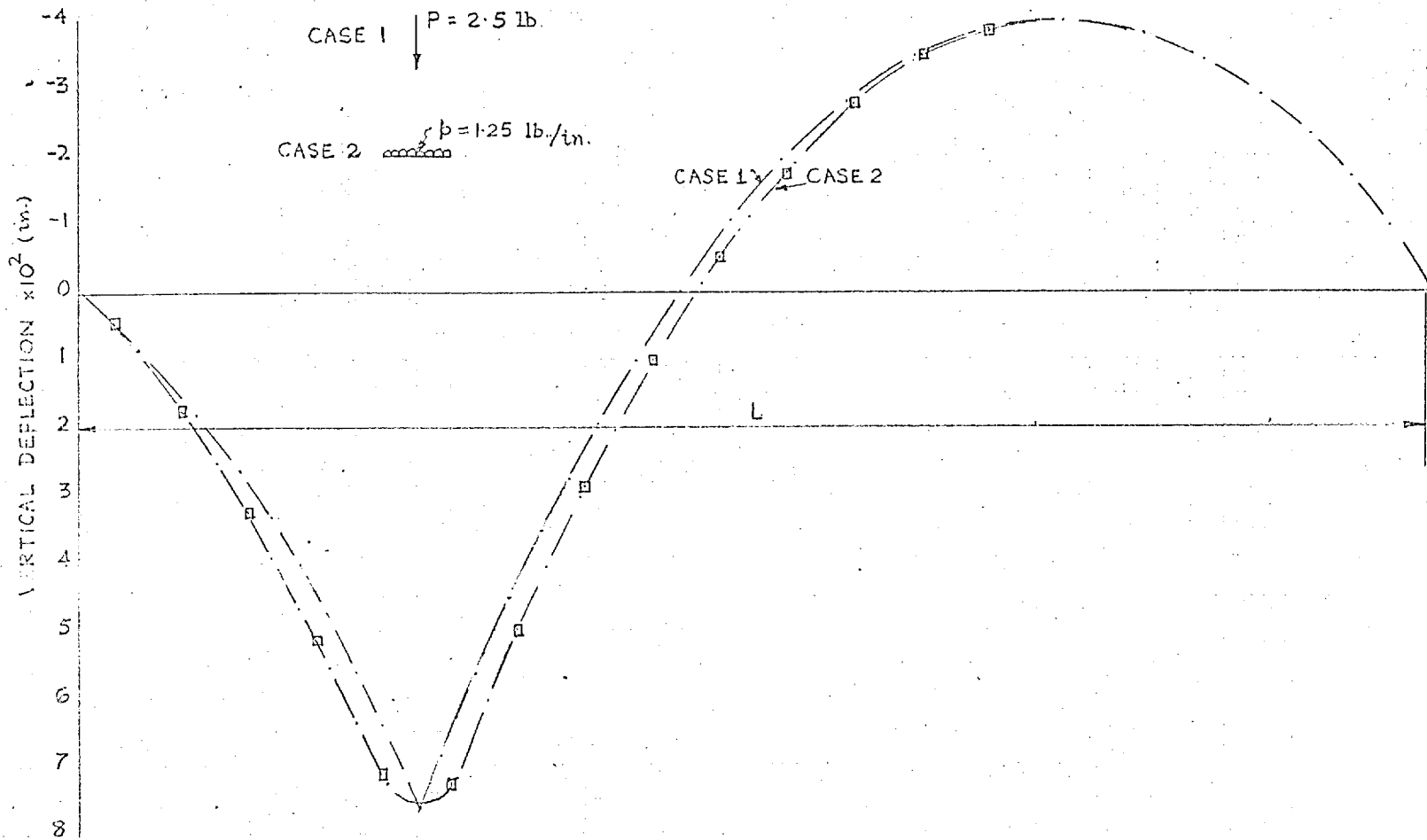
FIG. 27 PLANE SYSTEM: EFFECT OF DISTRIBUTING AN APPLIED POINT LOAD OVER A SMALL LENGTH OF THE SPAN
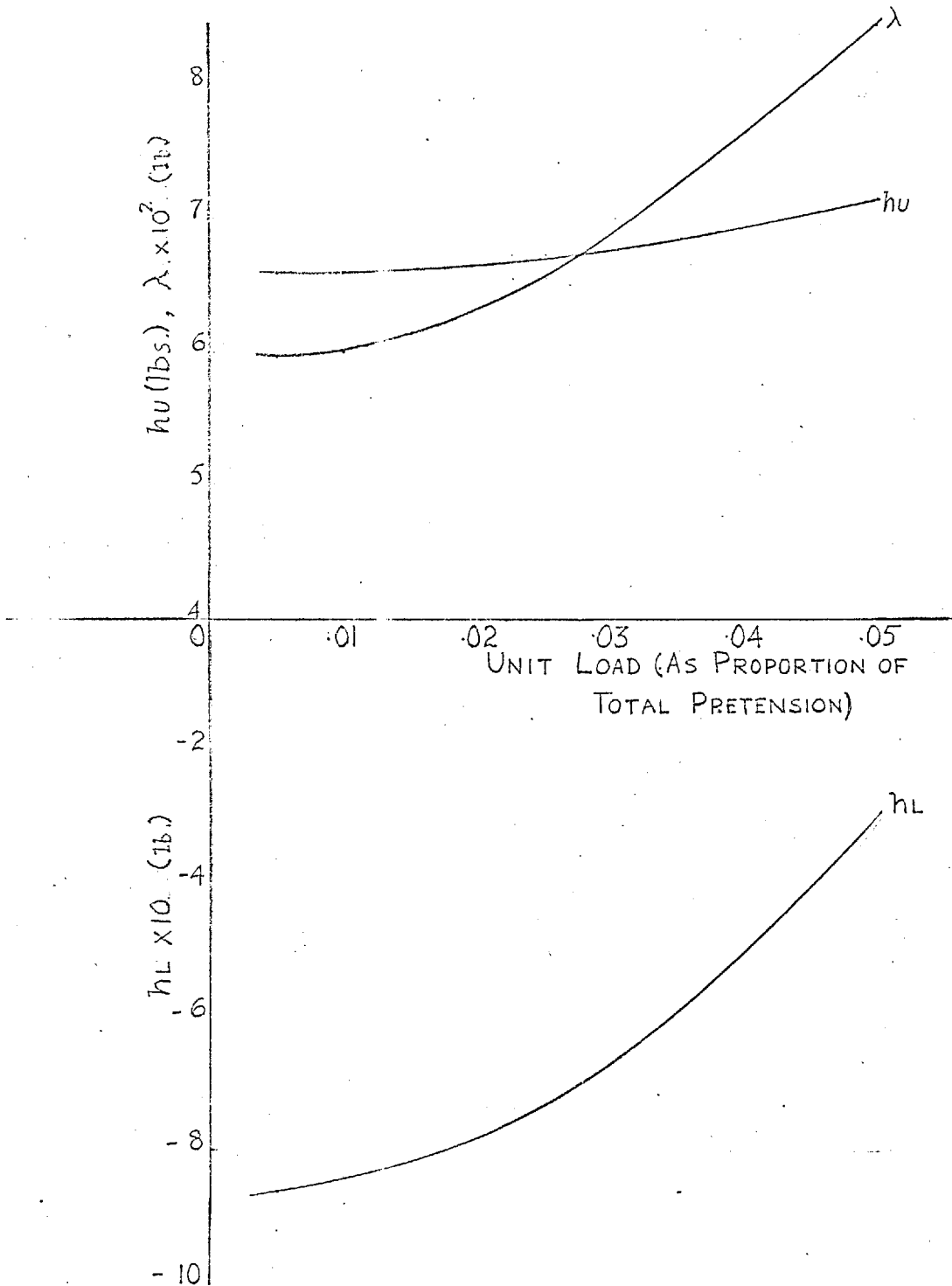
FIG. 28   VARIATION OF λ, hu AND hL WITH UNIT LOAD
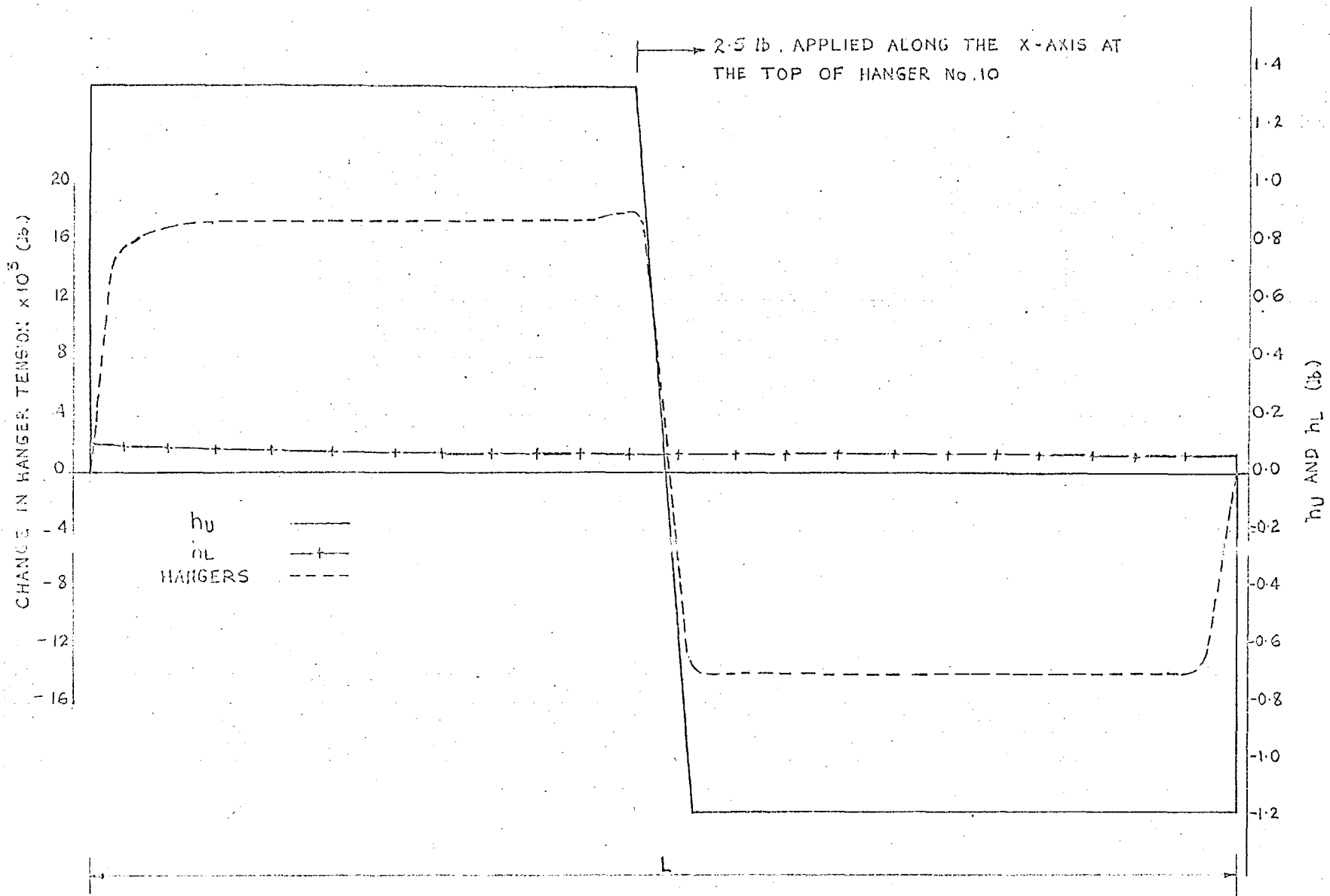
FIG.29   PLANE SYSTEM UNDER HORIZONTAL
APPLIED LOAD

FIG. 30   PLANE SYSTEM UNDER HORIZONTAL
APPLIED LOAD

LOAD 'P' ON LOWER CABLE

P lbs.	h_U lbs.	h_L lbs.
2.5	5.318	-2.114
5.0	12.915	-1.871

P = 5.0 lbs.

P = 2.5 lbs.

CHANGE IN HANGER TENSION (lbs.)

L
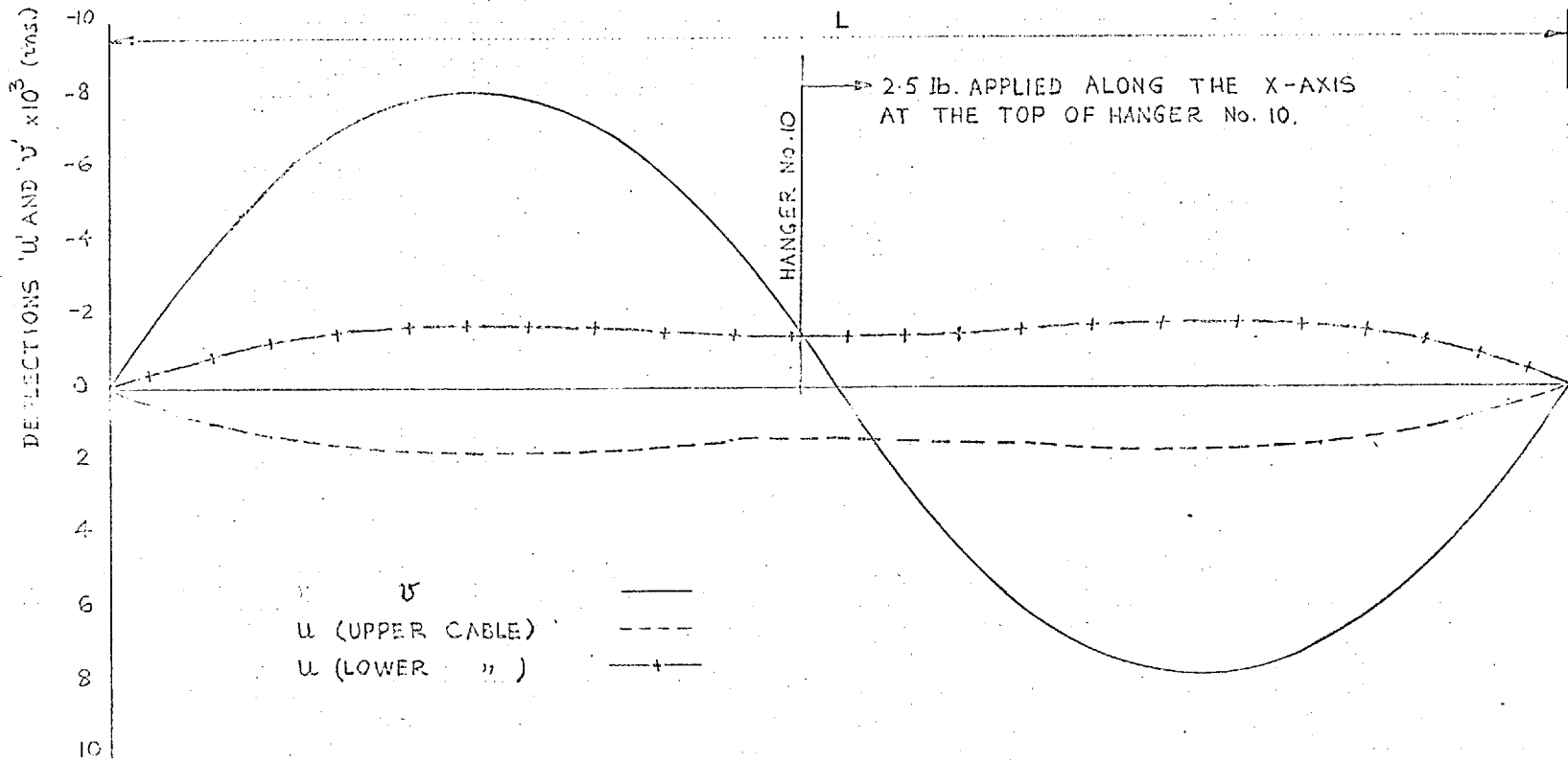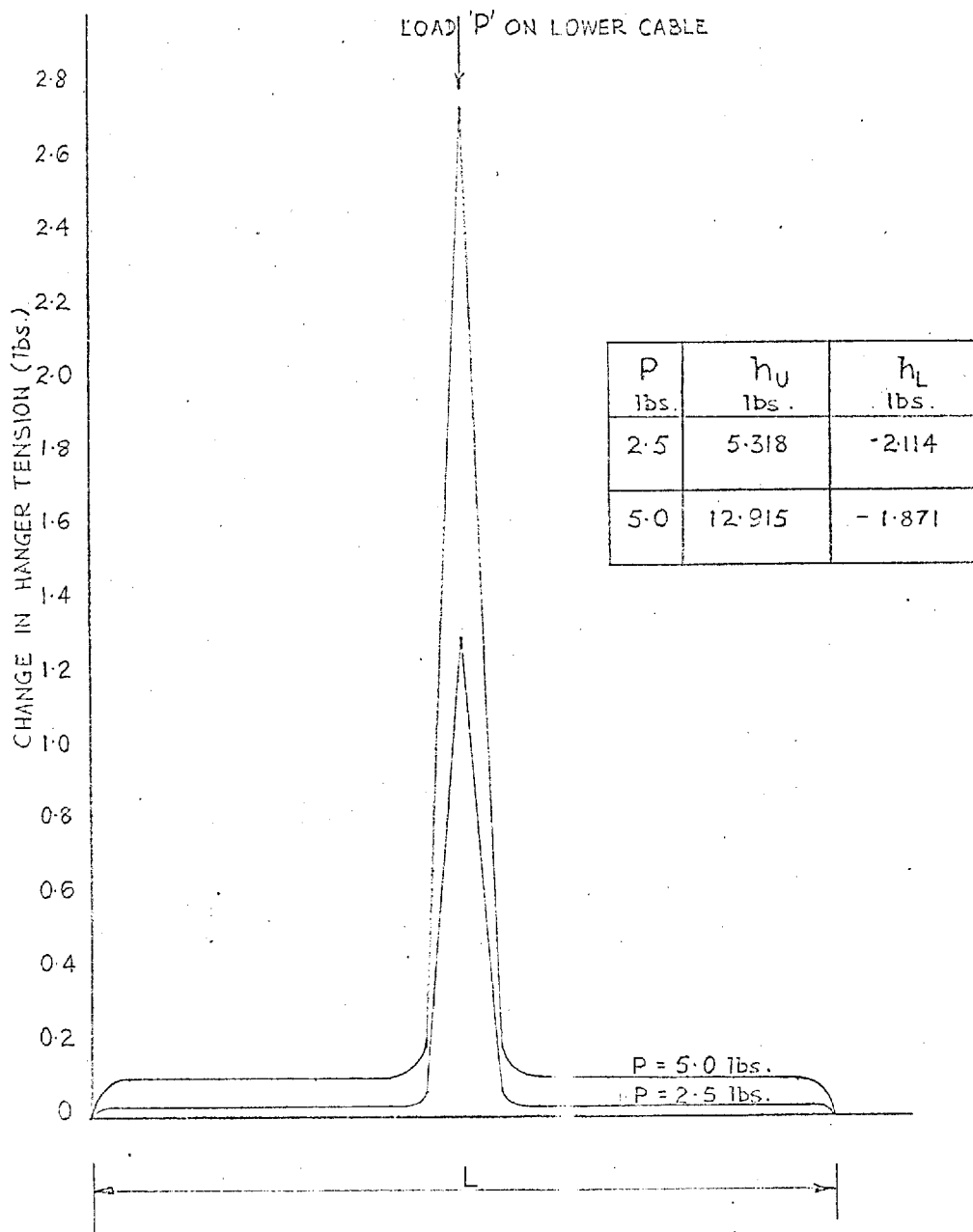
FIG. 31 CHANGE IN FORCES FOR POINT LOAD 'P'

APPLIED TO LOWER CABLE
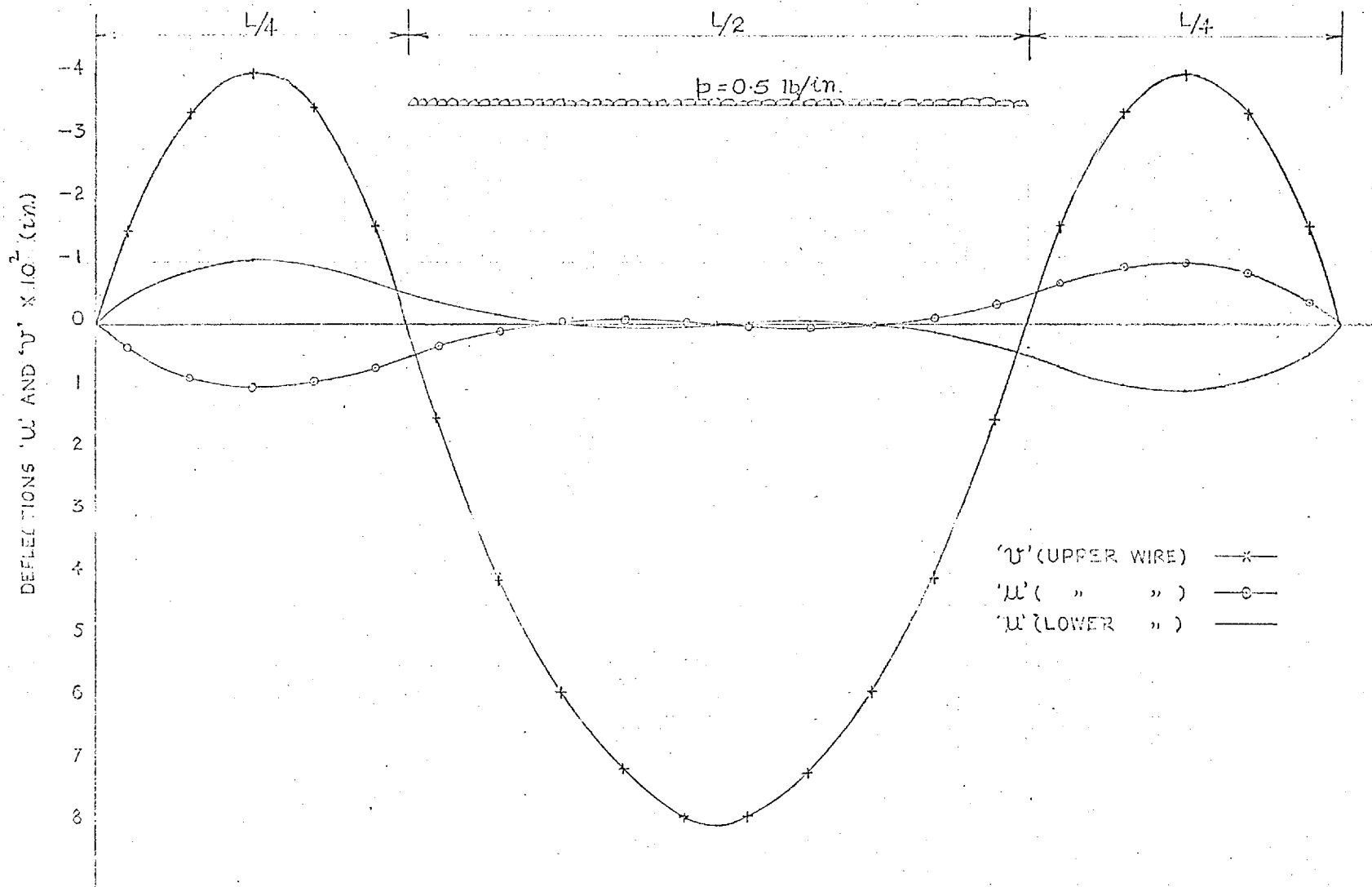
FIG.32 UNIFORMLY DISTRIBUTED LOAD ON THE
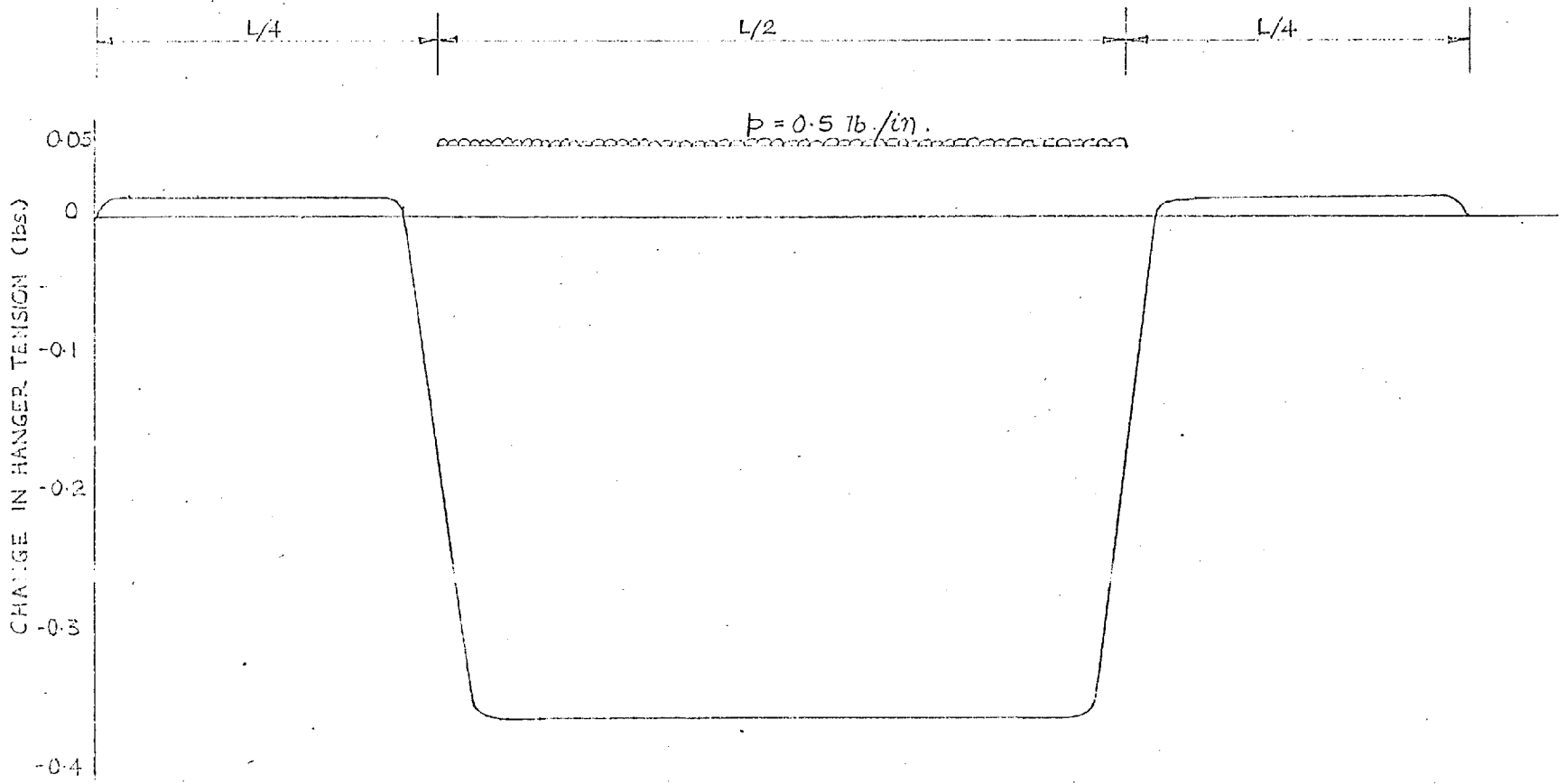
UPPER CABLE

FIG.33   UNIFORMLY DISTRIBUTED LOAD APPLIED TO
UPPER CABLE
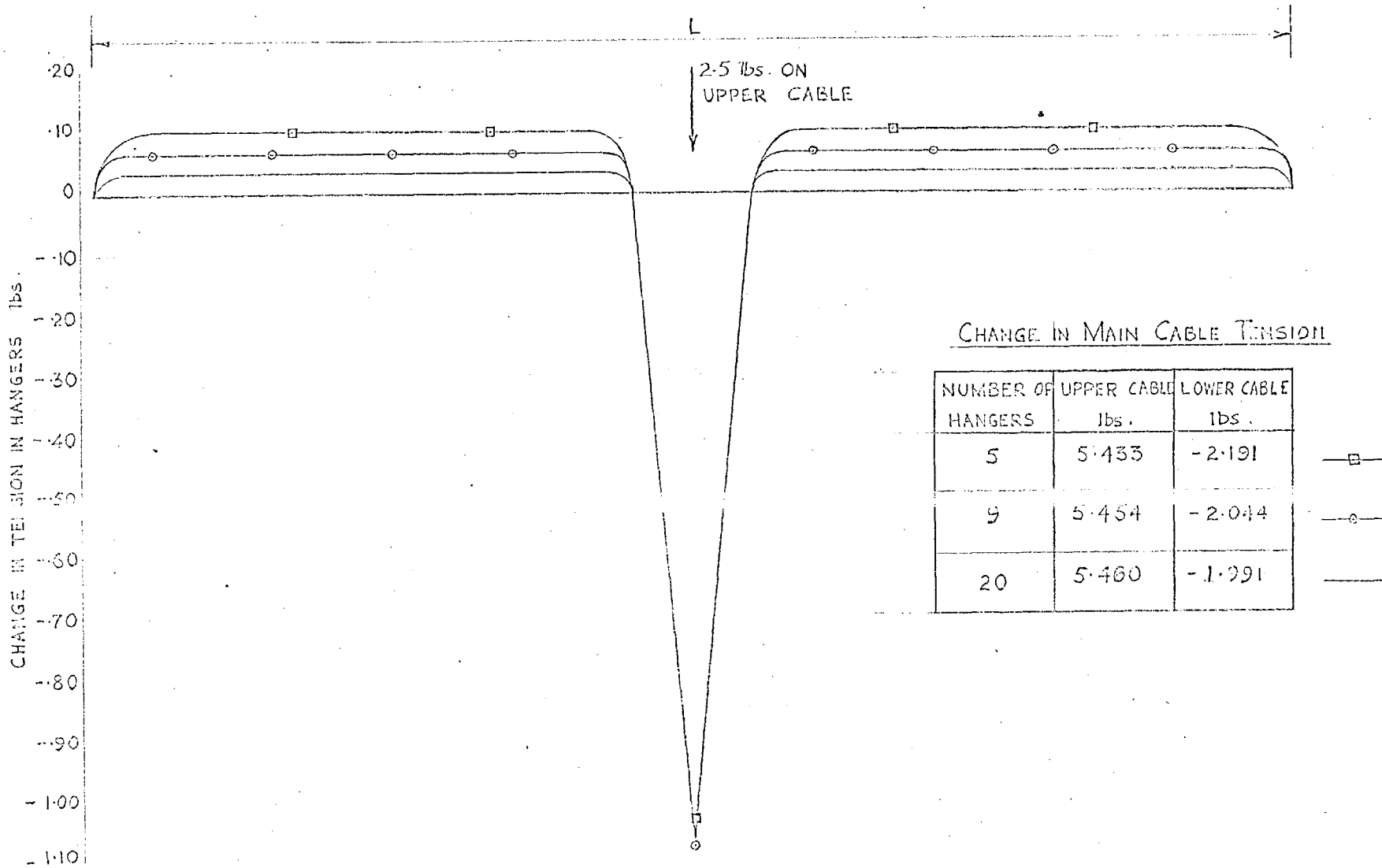
FIG. 34   EFFECT OF GROUPING HANGERS IN PLANE SYSTEM

USING THE GENERAL METHOD
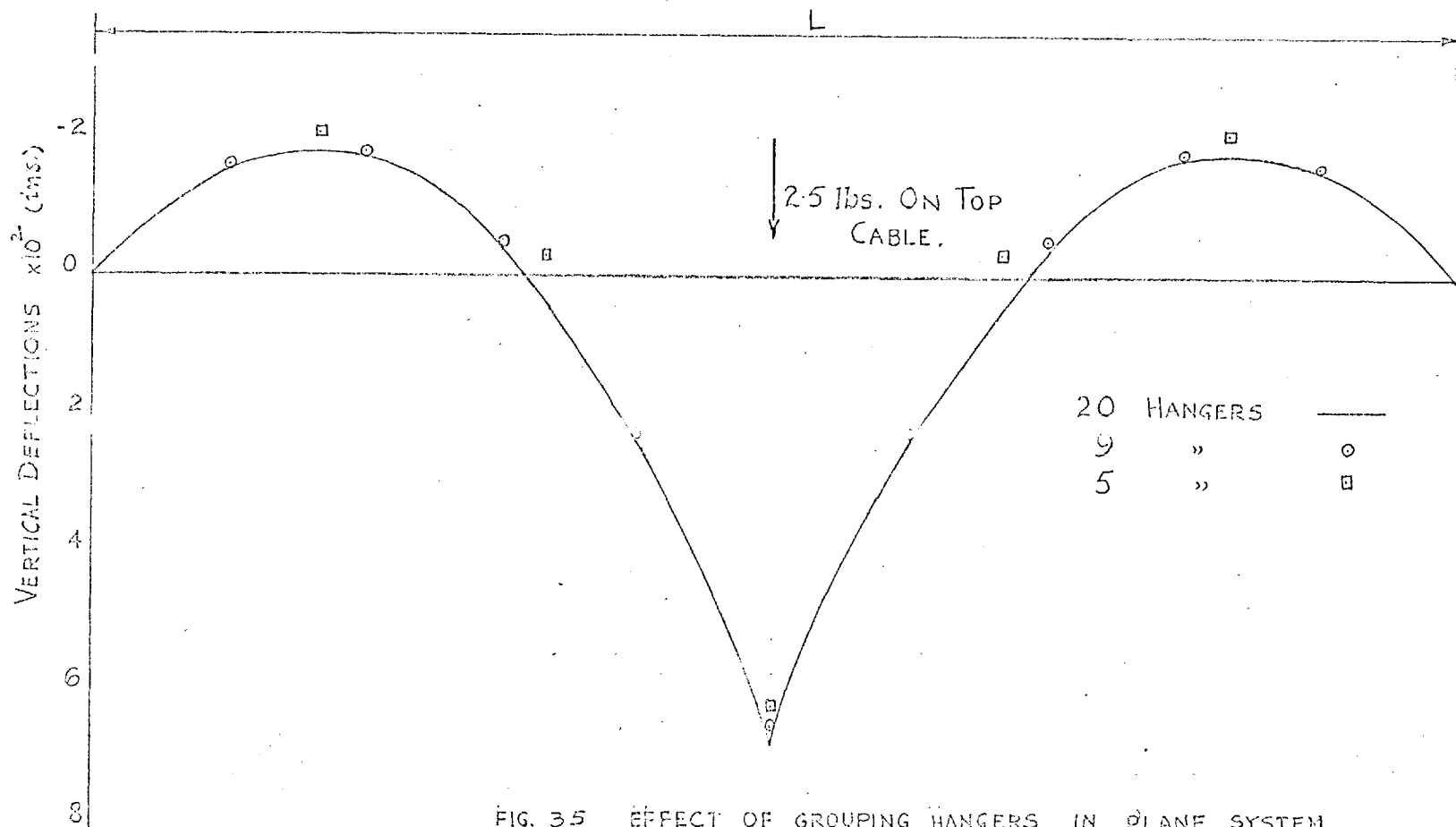
FIG. 35   EFFECT OF GROUPING HANGERS IN PLANE SYSTEM
USING THE GENERAL METHOD
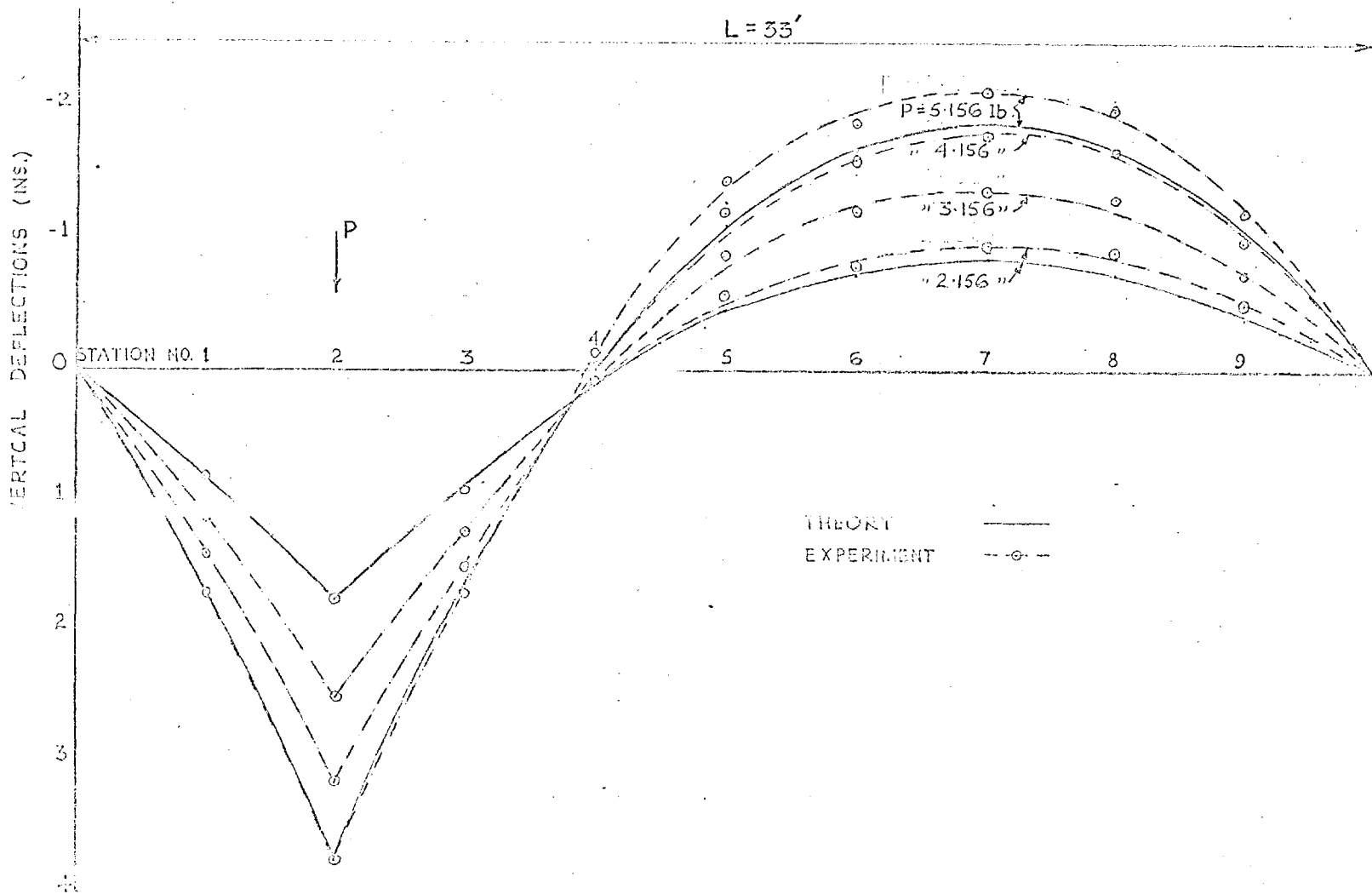
FIG. 37   VERTICAL DEFLECTIONS FOR ·032″ DIAMETER WIRE

UNDER APPLIED POINT LOAD
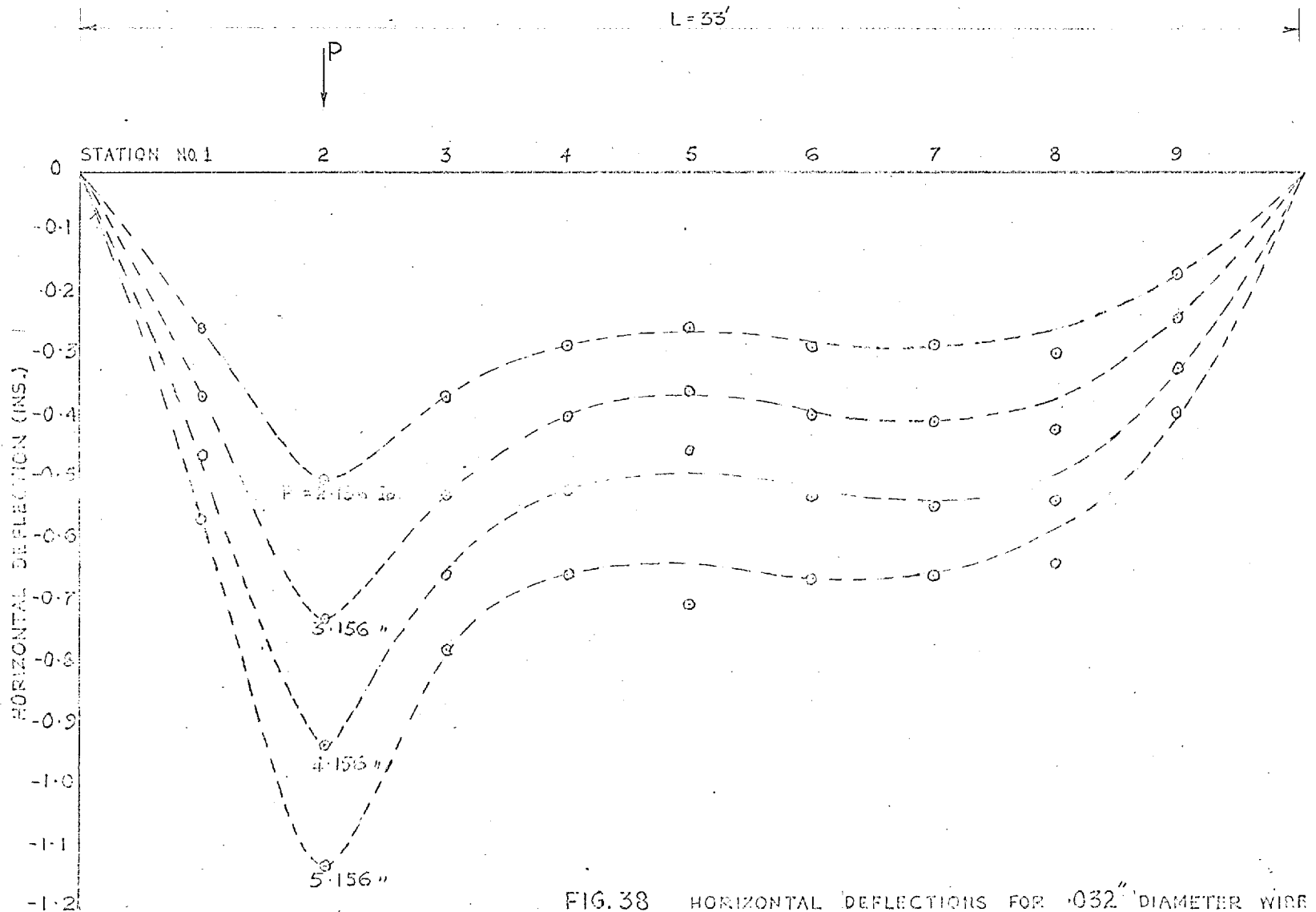
FIG. 38   HORIZONTAL DEFLECTIONS FOR ·032" DIAMETER WIRE
UNDER APPLIED POINT LOAD
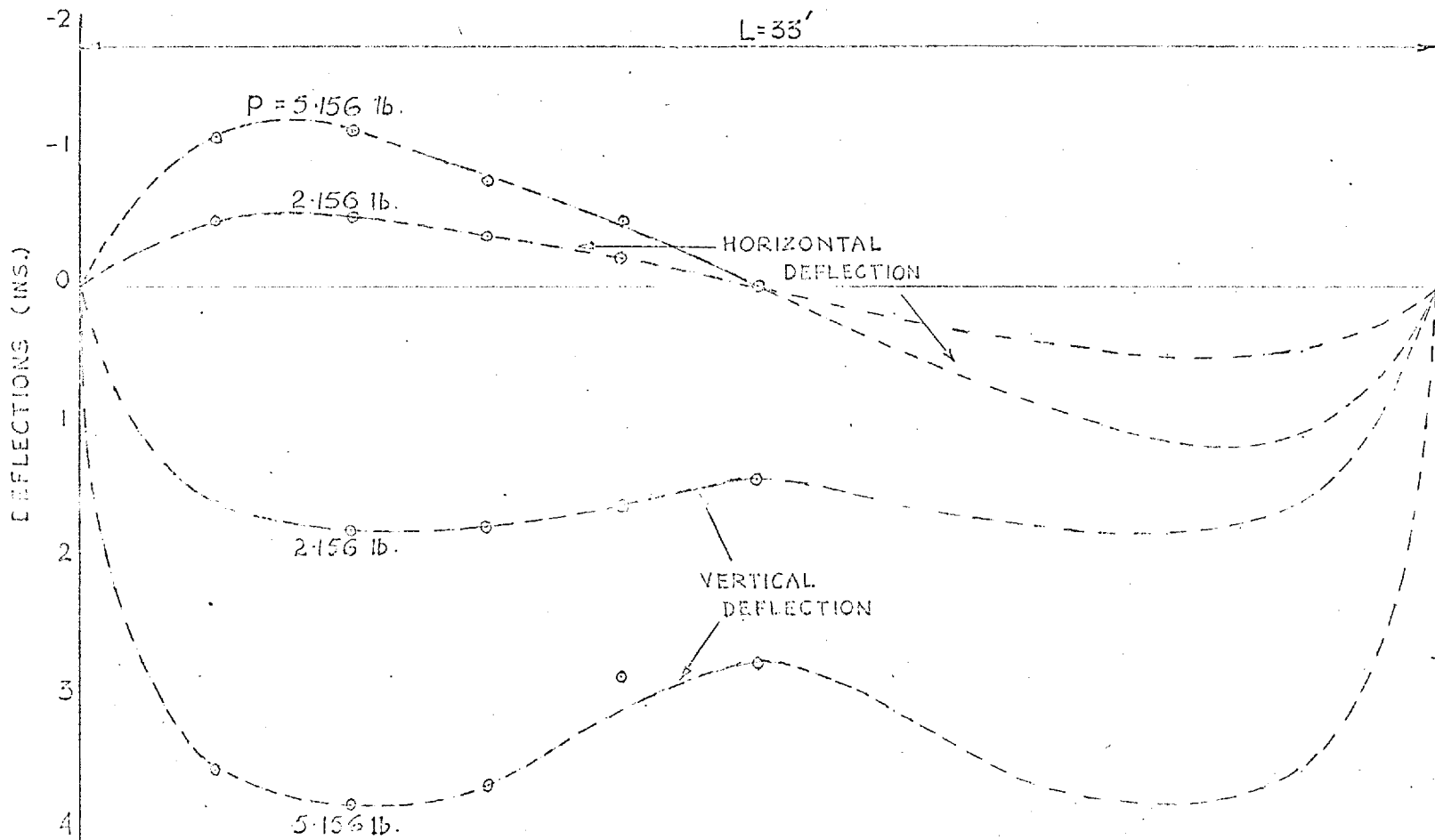
FIG. 39 - 1. VALUES OF DEFLECTION UNDER THE LOADED
POINT FOR ·032" DIAMETER WIRE.
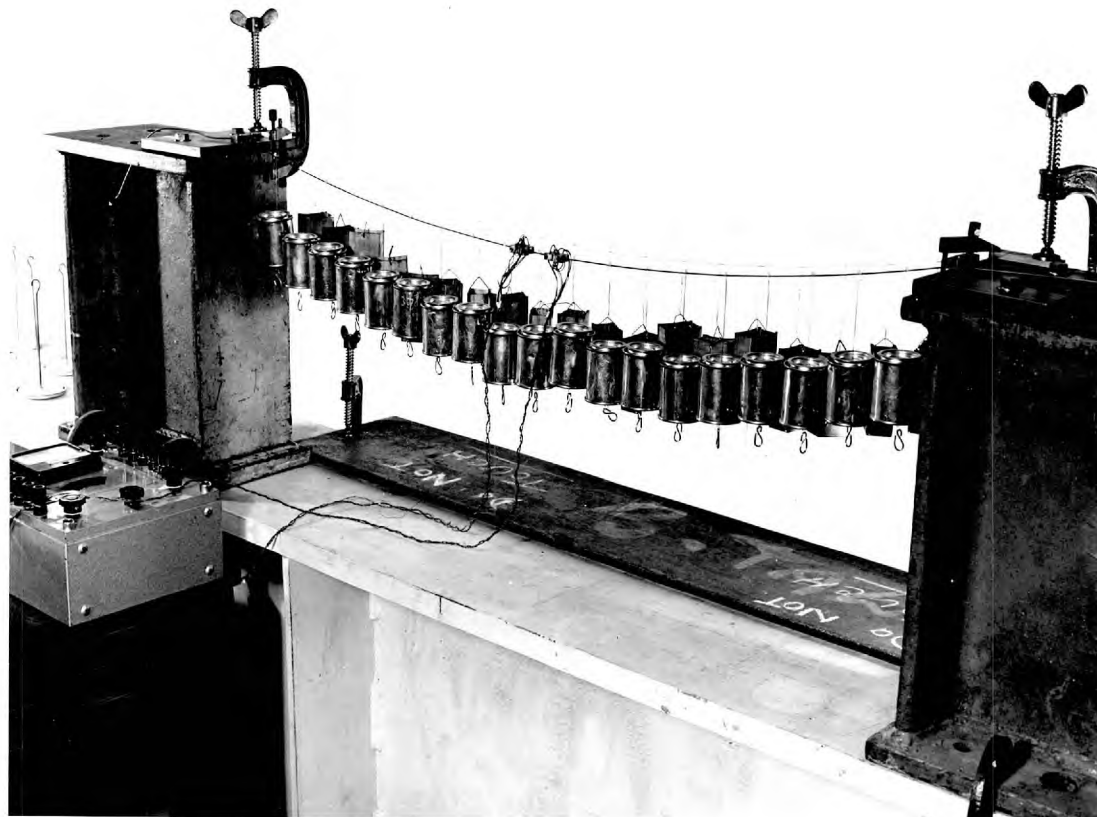
FIGURE 40   EXPERIMENTAL SET UP FOR THE .0164" AND .064" DIAMETER WIRES
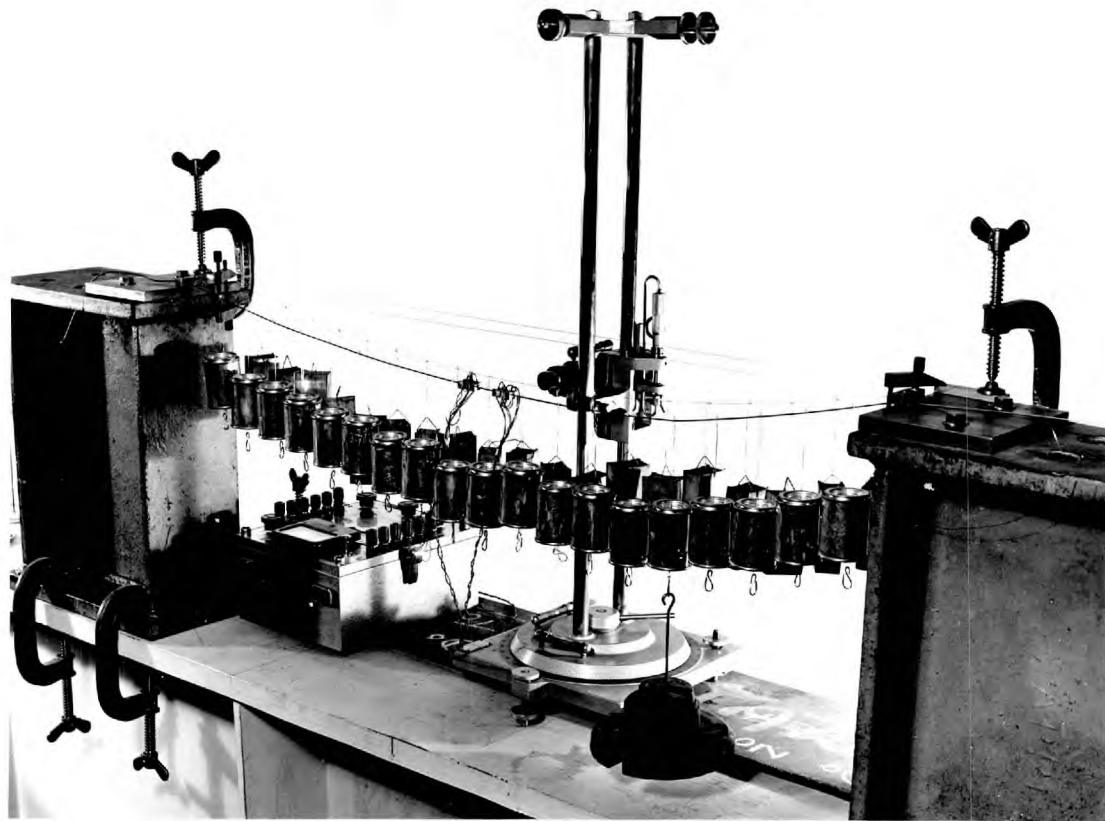
FIGURE 41   .064" DIAMETER WIRE LOADED AT THE QUARTER POINT
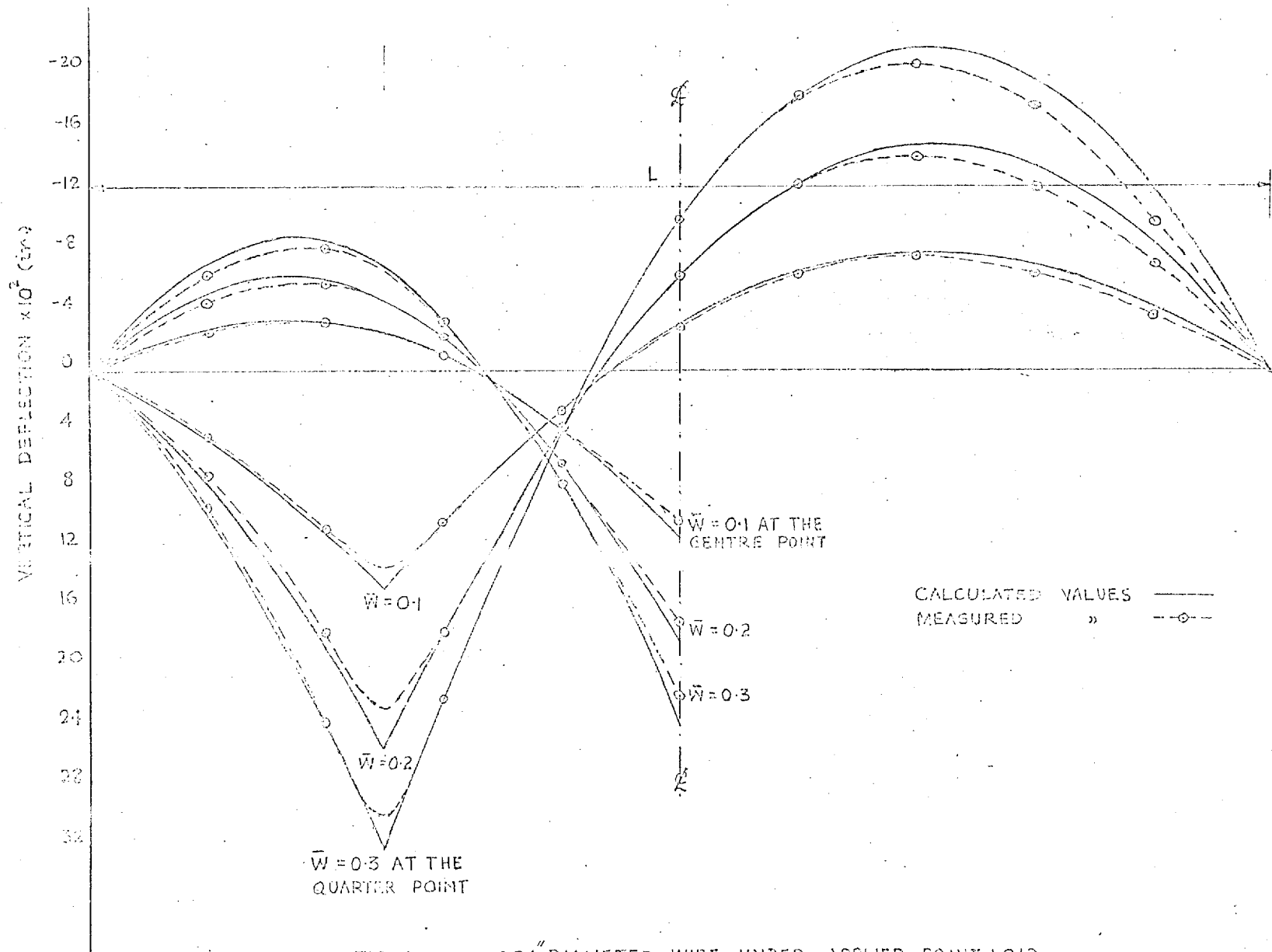
FIG. 42   ·064" DIAMETER WIRE UNDER APPLIED POINT LOAD
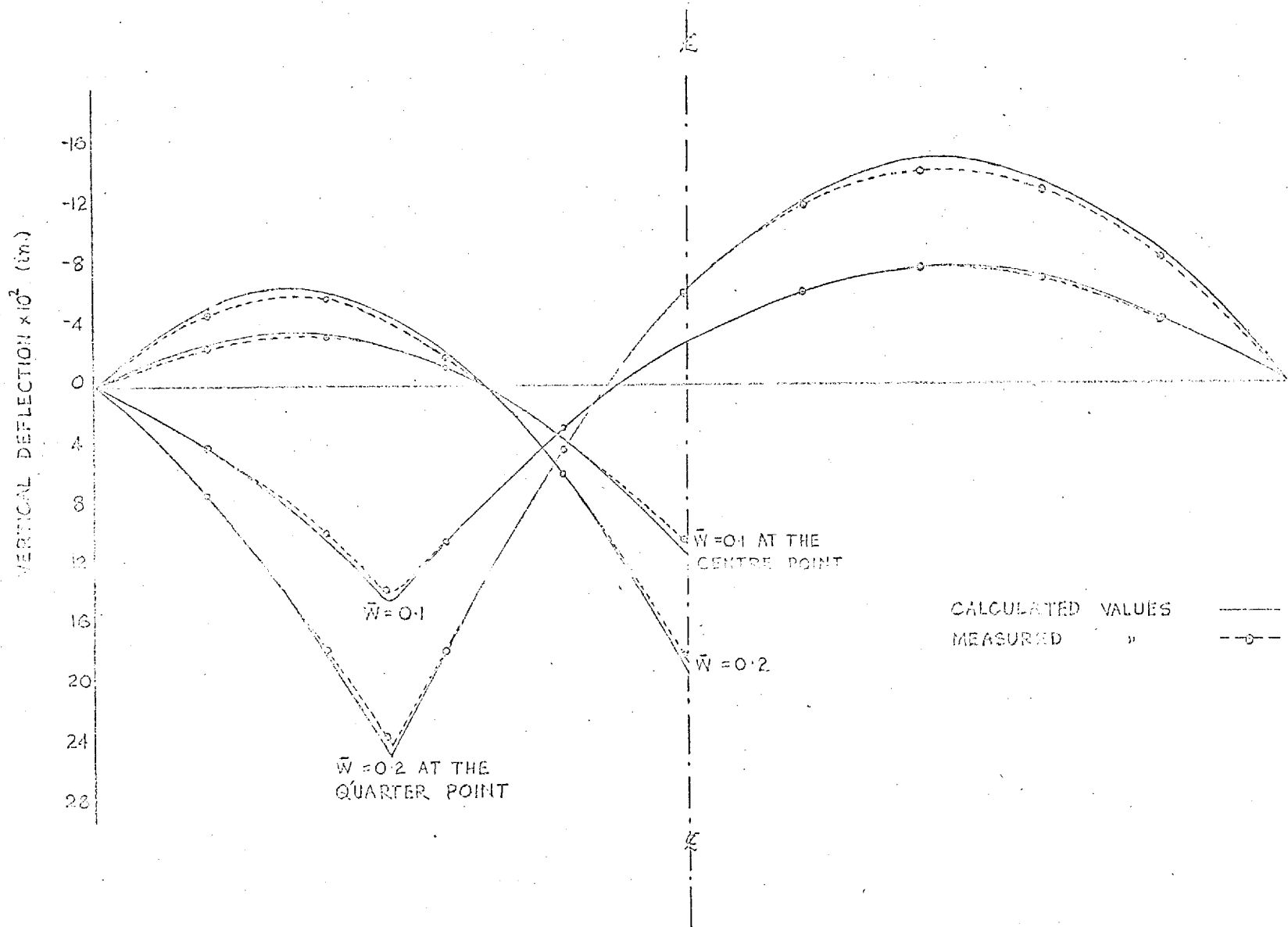
FIG. 43   ·0164" DIAMETER WIRE UNDER APPLIED POINT LOAD
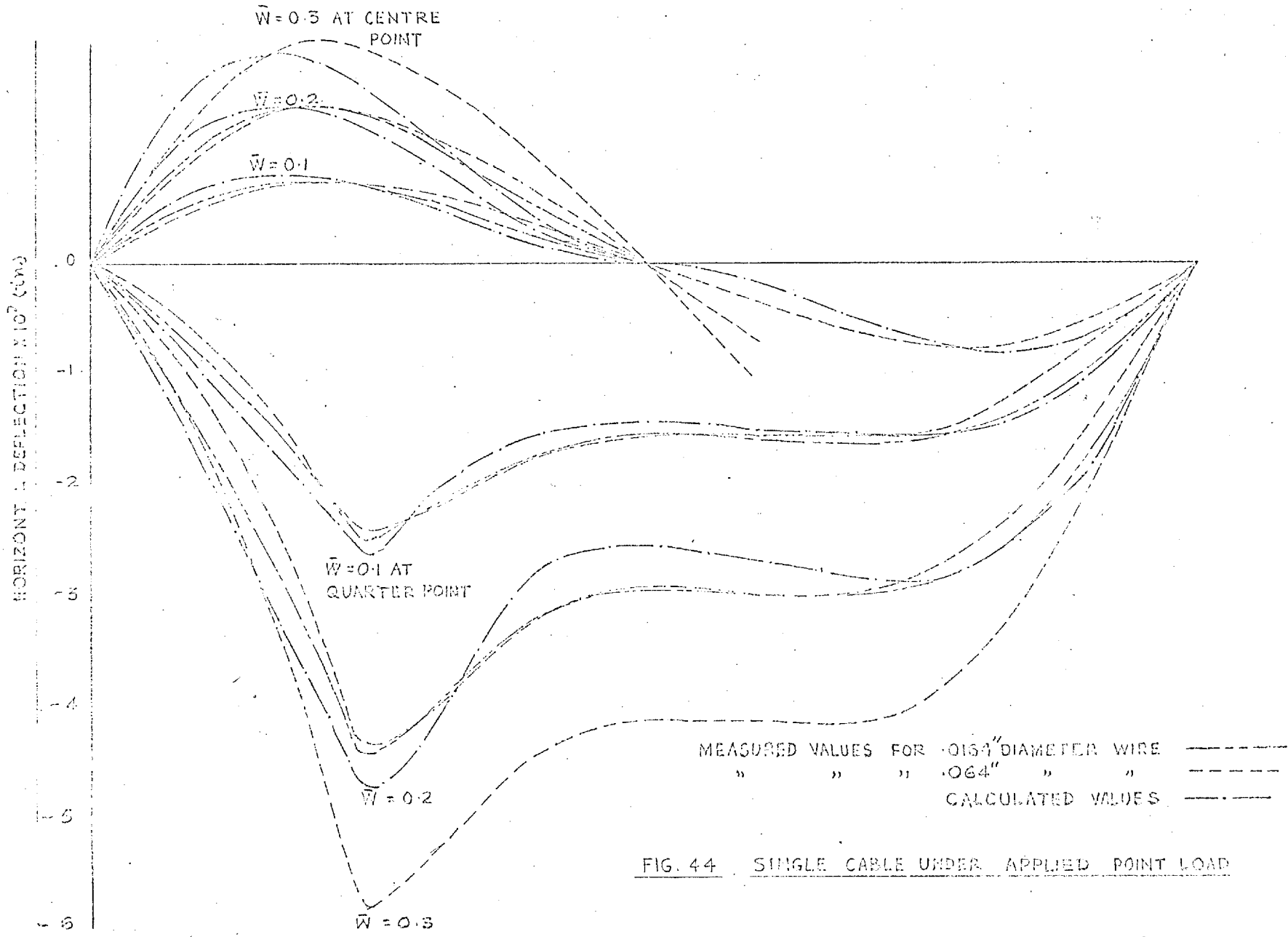
FIG. 44   SINGLE CABLE UNDER APPLIED POINT LOAD
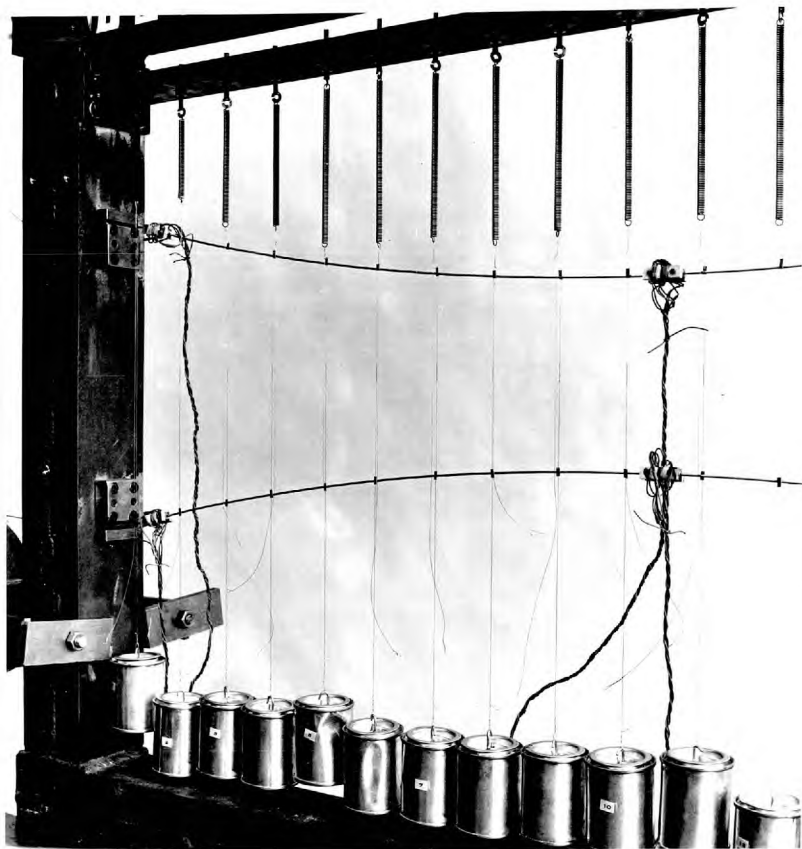
FIGURE 45   EXPERIMENTAL MODEL OF THE PLANE SYSTEM

THE PHOTOGRAPH SHOWS THE UPPER WIRE DIRECTLY
LOADED AND THE LOWER WIRE SPRING-LOADED THROUGH
A SEPARATE SET OF HANGERS DURING THE ASSEMBLY OF
THE MODEL. THE LOWER WIRE IS LOADED OVER A
PULLEY AT THE LEFT SUPPORT.

EXPERIMENTAL MODEL OF THE PLANE SYSTEM.

FIGURE 46

THE PHOTOGRAPH SHOWS THE UPPER WIRE DIRECTLY LOADED AND THE LOWER WIRE SPRING-
LOADED THROUGH A SEPARATE SET OF HANGERS DURING THE ASSEMBLY OF THE MODEL. THE
LOWER WIRE IS LOADED OVER A PULLEY AT THE LEFT SUPPORT
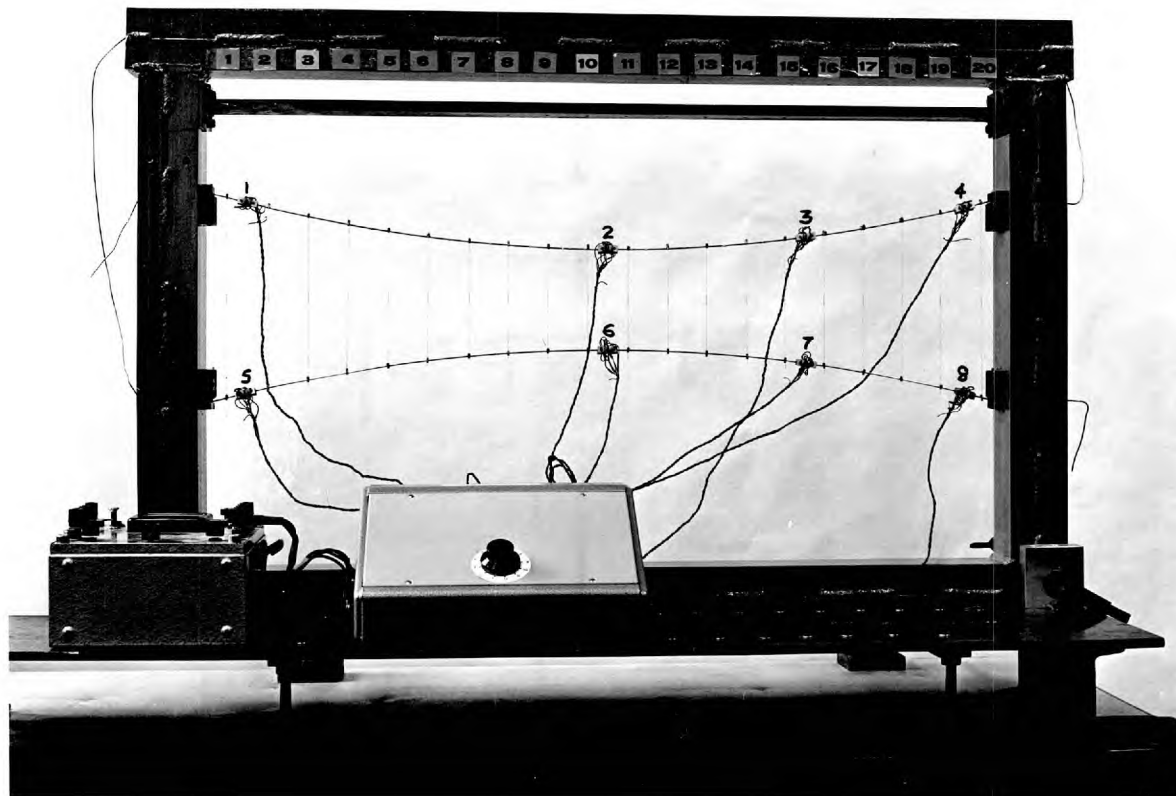
FIGURE 47   COMPLETED MODEL OF THE PLANE SYSTEM

FIGURES 48 and 49 are on page 69.

AVERAGE STRAIN = 30.66×10⁻⁶/lb.
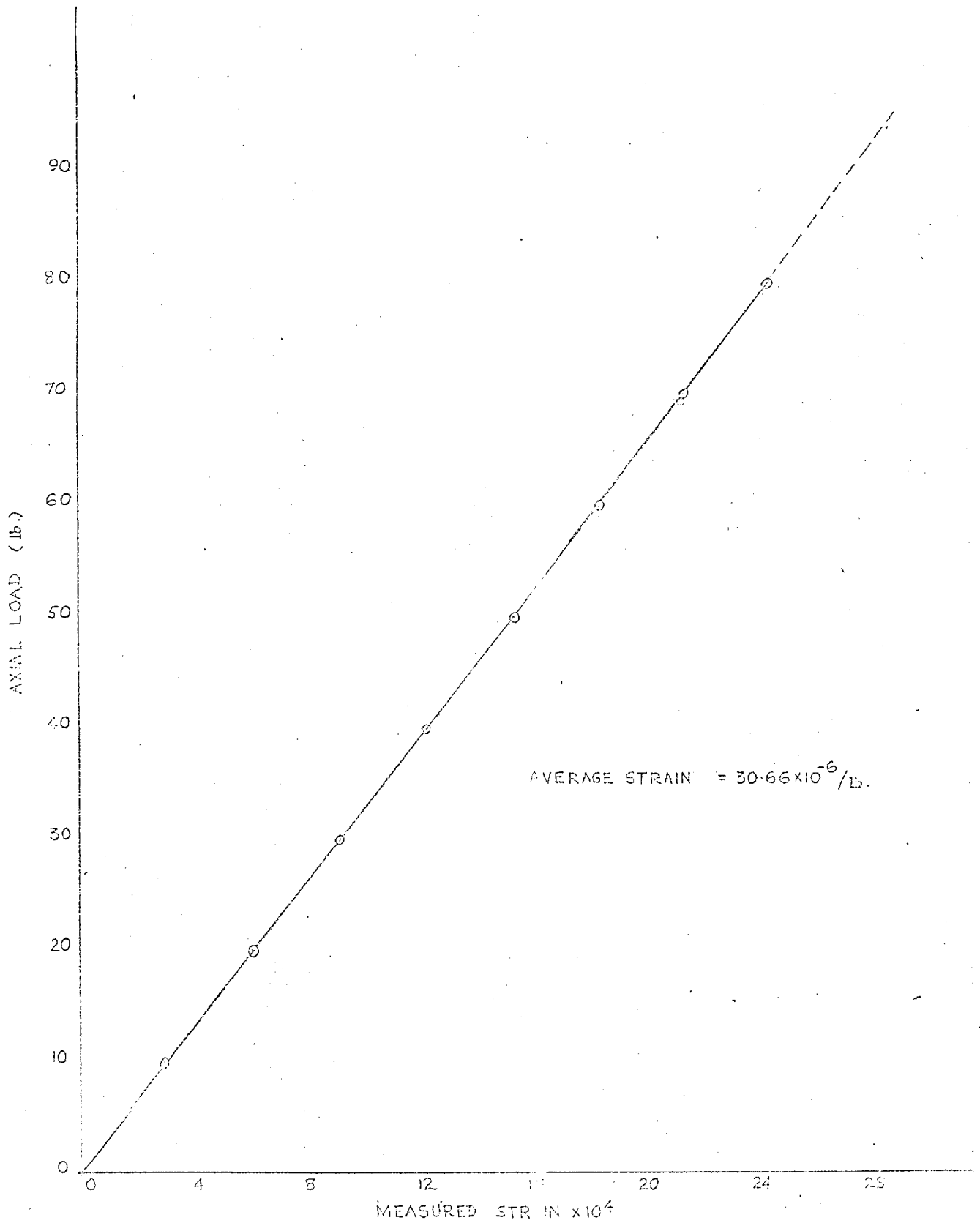
FIG. 50   CALIBRATION CURVE FOR LOAD-CELL No. I

FIGURES 51 and 52 are on pages 73 and 74

respectively.
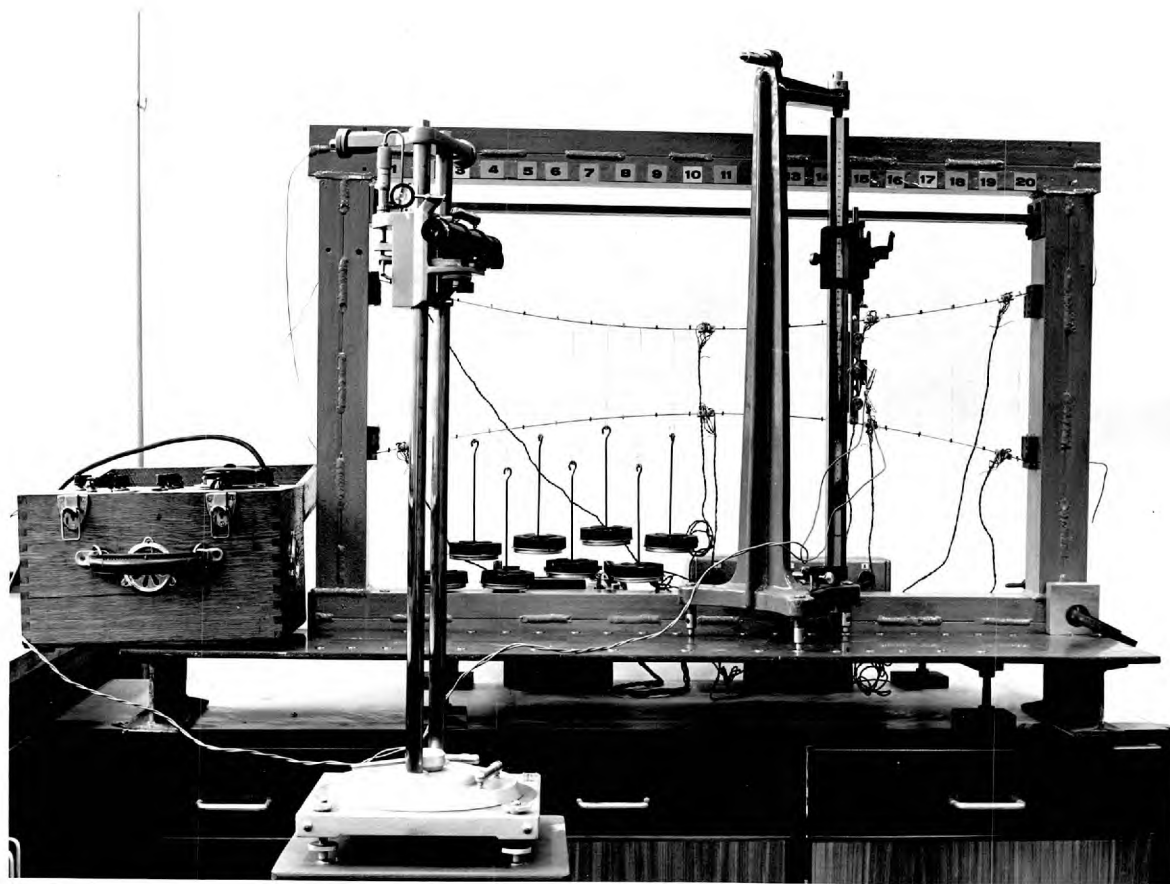
FIGURE 53   THE MODEL OF THE PLANE SYSTEM UNDER APPLIED LOADING
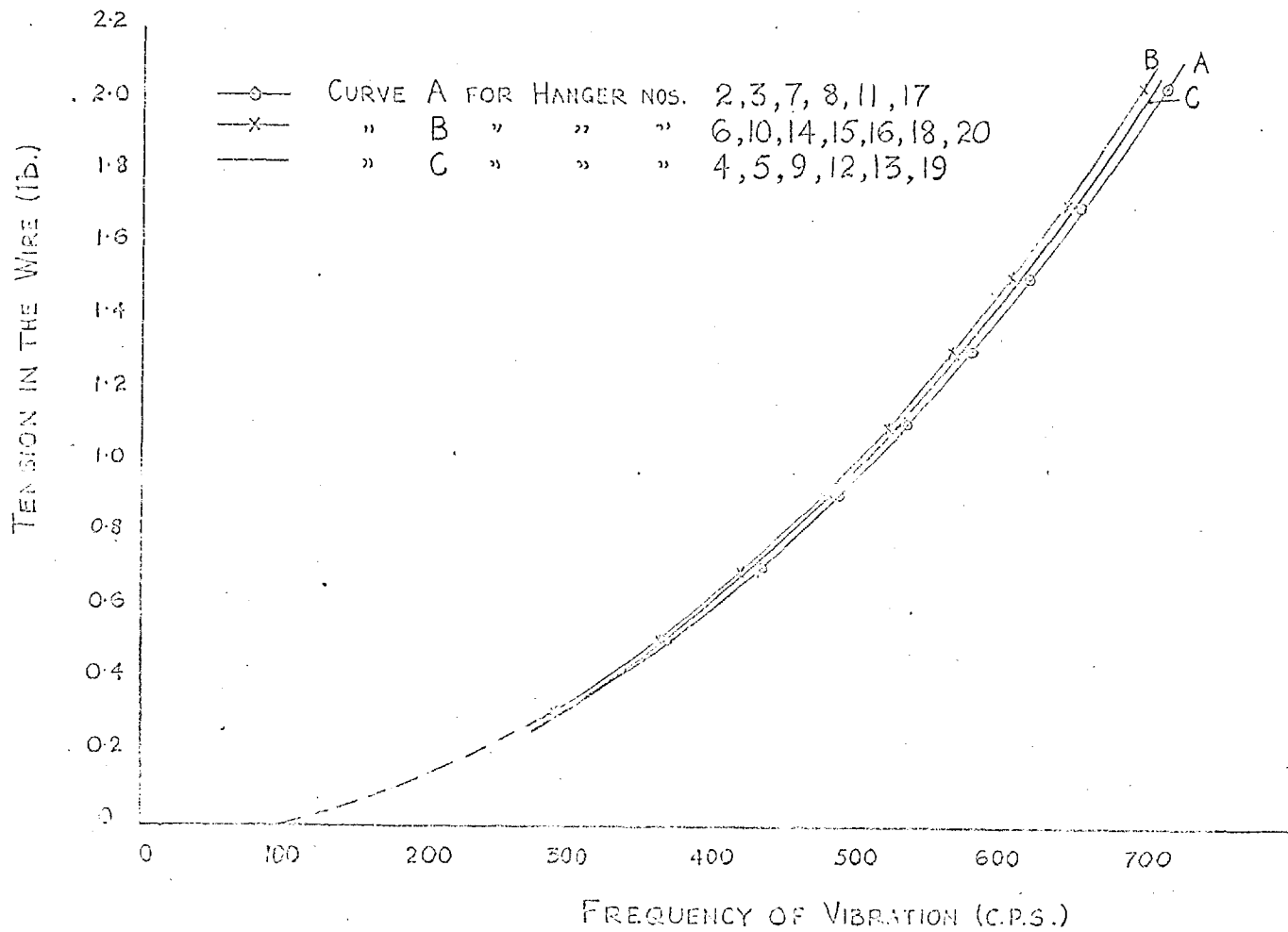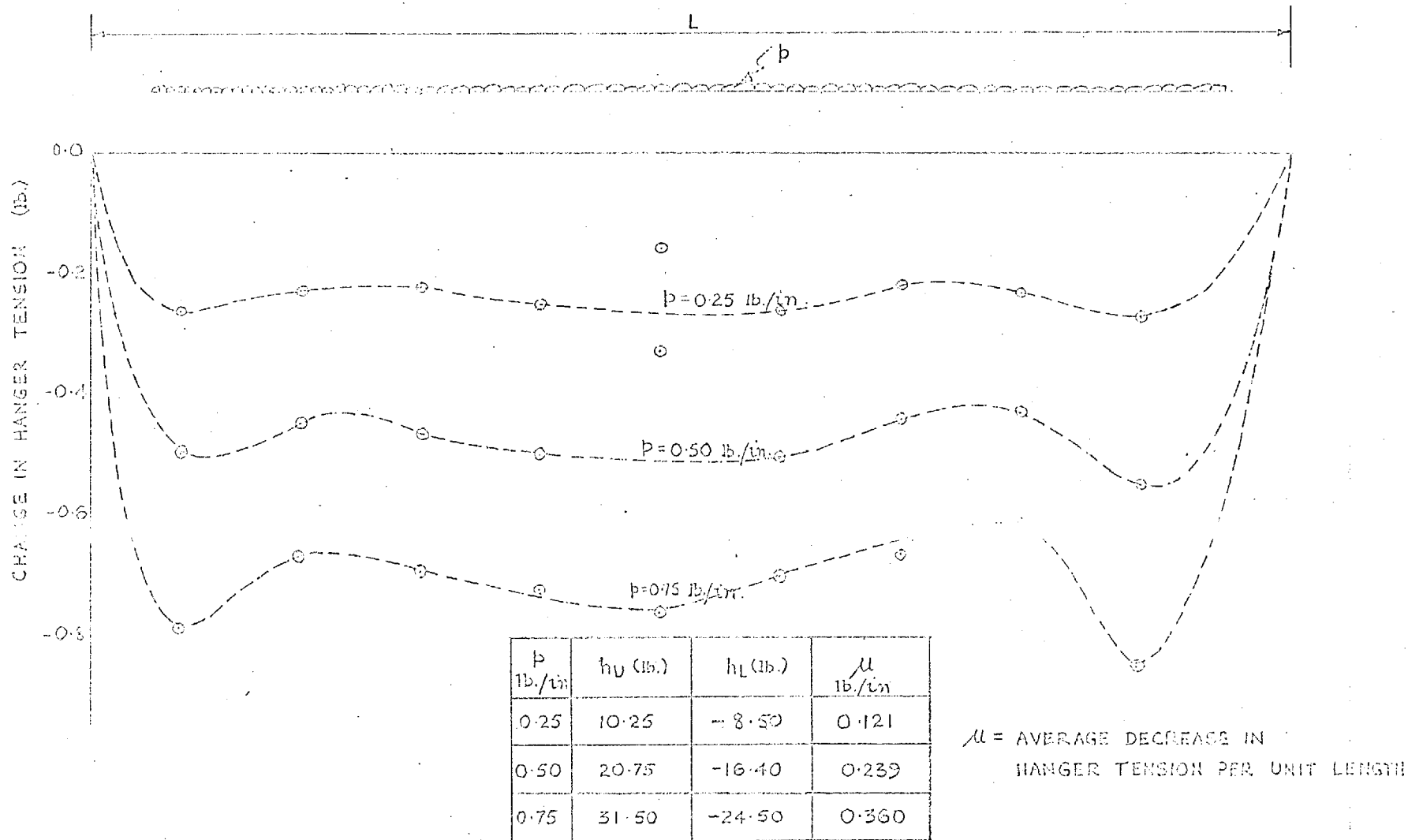THE MEASURING INSTRUMENTS ARE ALSO SEEN IN THE PHOTOGRAPH.

Curve A for Hanger nos. 2, 3, 7, 8, 11, 17
     " B " " " 6, 10, 14, 15, 16, 18, 20
     " C " " " 4, 5, 9, 12, 13, 19

FIG. 54 · CALIBRATION CURVES FOR HANGERS

p lb./in	h_U (lb.)	h_L (lb.)	μ lb./in
0.25	10.25	− 8.50	0.121
0.50	20.75	−16.40	0.239
0.75	31.50	−24.50	0.360

μ = AVERAGE DECREASE IN HANGER TENSION PER UNIT LENGTH

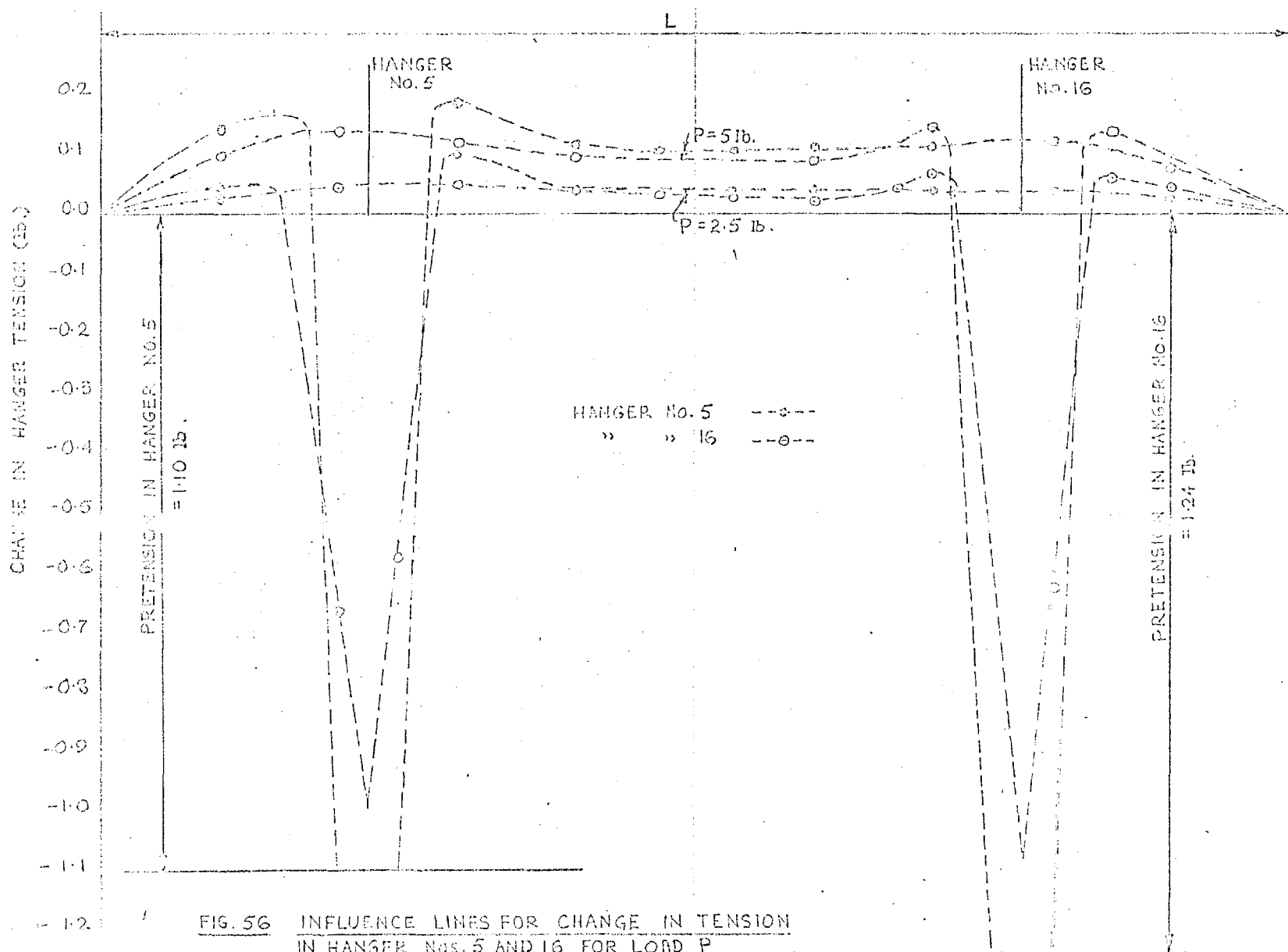FIG. 55   PLANE SYSTEM : UNIFORMLY DISTRIBUTED LOAD APPLIED TO THE UPPER CABLE

FIG. 56   INFLUENCE LINES FOR CHANGE IN TENSION
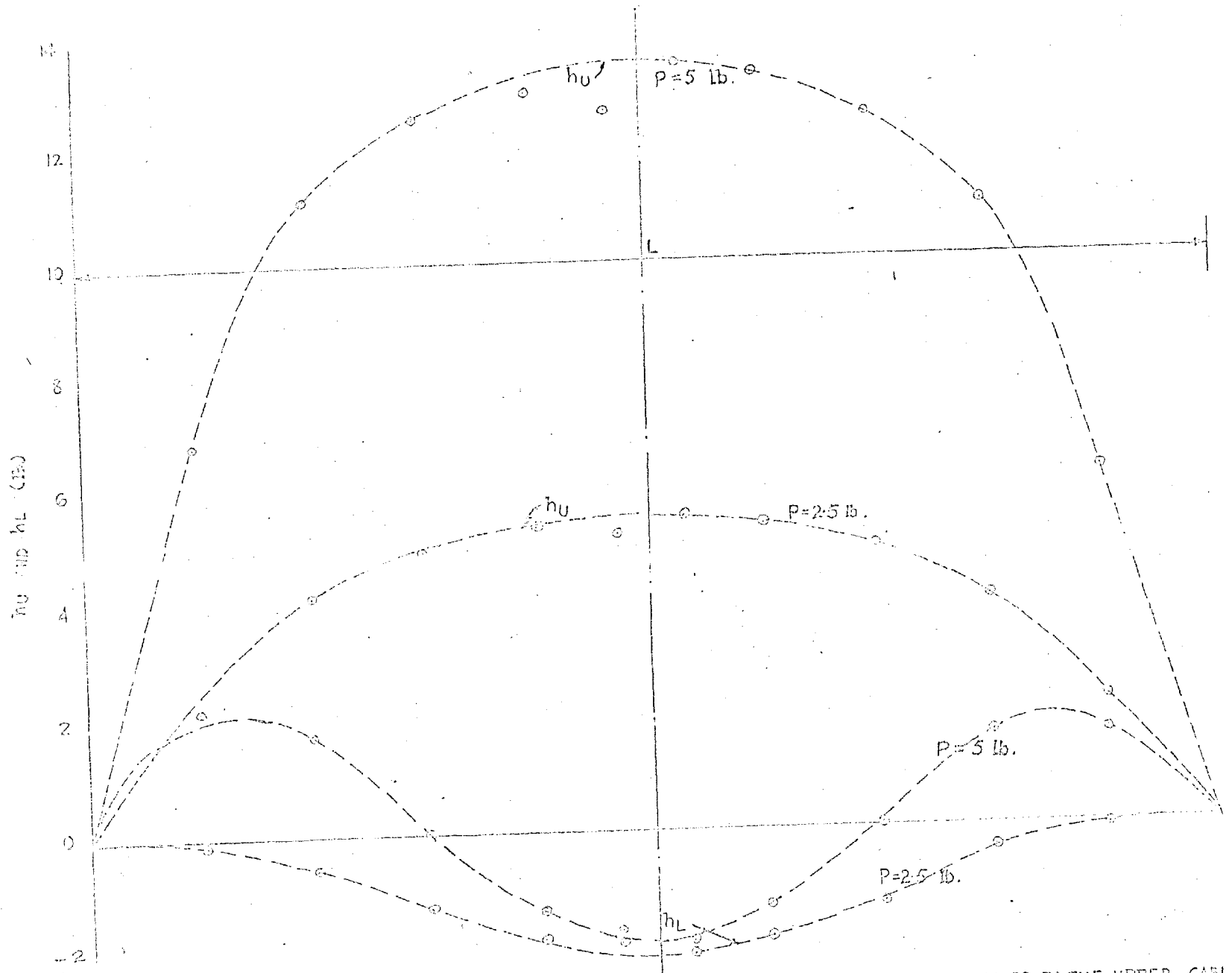IN HANGER Nos. 5 AND 16 FOR LOAD P
APPLIED TO THE UPPER CABLE

FIG. 57 INFLUENCE LINES FOR h_U AND h_L FOR LOAD P APPLIED TO THE UPPER CABLE

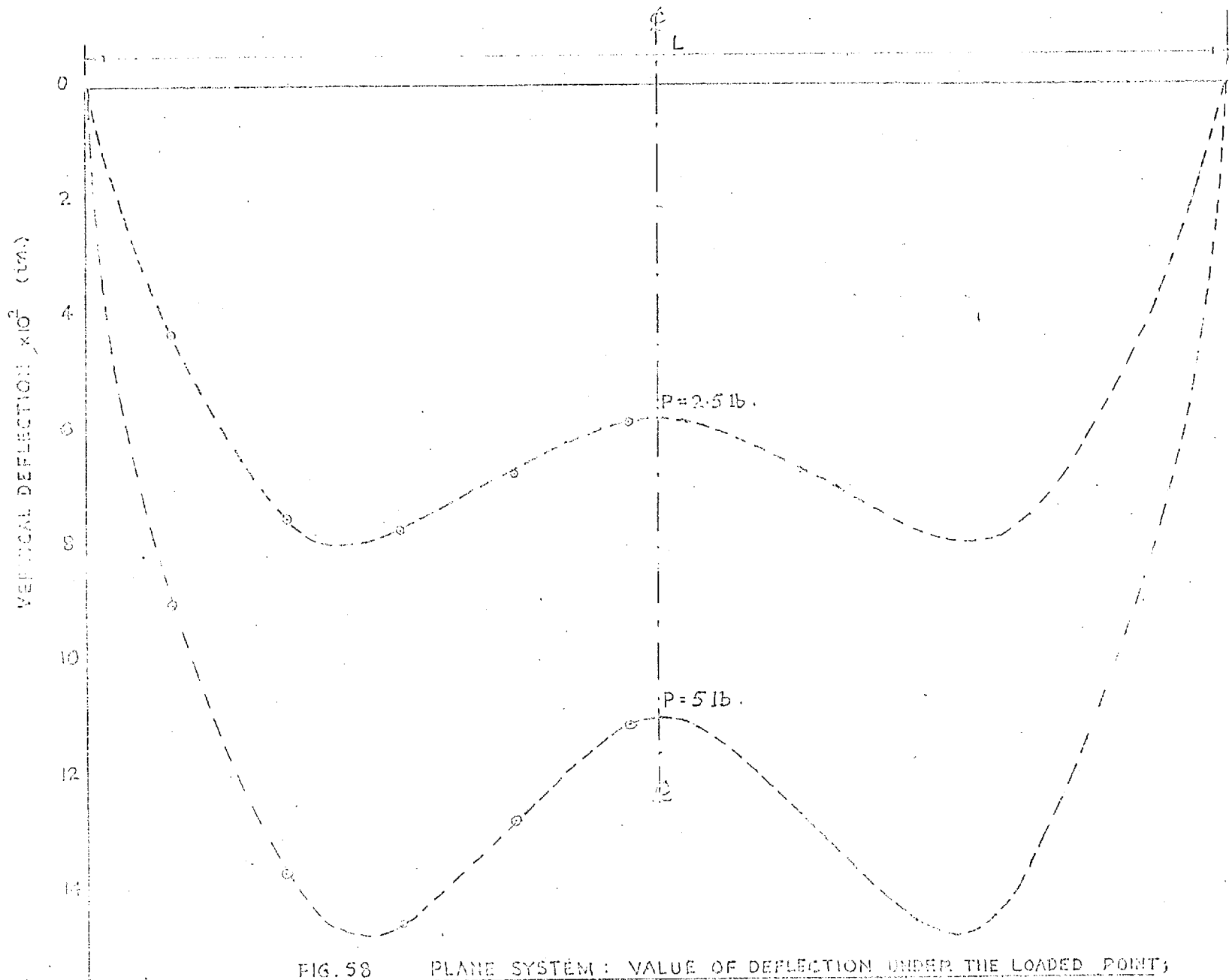FIG. 58   PLANE SYSTEM : VALUE OF DEFLECTION UNDER THE LOADED POINT;
LOAD P APPLIED TO THE UPPER CABLE